Technical Report Documentation Page

1. Report No.	2. Government Accession No.	3. Recipient's Catalog No.
FHWA/TX-07/0-5135-2		

4. Title and Subtitle	5. Report Date
IMPROVING LAB COMPACTION METHODS FOR ROADWAY BASE MATERIALS	October 2006 Published: February 2008
	6. Performing Organization Code
7. Author(s)	8. Performing Organization Report No.
Stephen Sebesta, Pat Harris, and Wenting Liu	Report 0-5135-2
9. Performing Organization Name and Address	10. Work Unit No. (TRAIS)
Texas Transportation Institute The Texas A&M University System College Station, Texas 77843-3135	11. Contract or Grant No. Project 0-5135
12. Sponsoring Agency Name and Address	13. Type of Report and Period Covered
Texas Department of Transportation Research and Technology Implementation Office P. O. Box 5080 Austin, Texas 78763-5080	Technical Report: September 2005-August 2006
	14. Sponsoring Agency Code

15. Supplementary Notes

Project performed in cooperation with the Texas Department of Transportation and the Federal Highway Administration.

Project Title: Improving Correlation between Field Construction of Soils and Bases and Laboratory Sample Construction Techniques

URL: http://tti.tamu.edu/documents/0-5135-2.pdf

16. Abstract

The Texas Department of Transportation (TxDOT) employs the impact hammer method of sample compaction for laboratory preparation of road base and subgrade materials for testing. Experience has shown that this method may not adequately represent the true field performance of the materials. This report describes results investigating how different lab compaction methods influence the laboratory characterization of the materials. As compared to Tex-113-E, Modified compaction improved the performance of a Grade 2 Texas base, but not the Grade 1 material tested. Vibratory compaction resulted in improved performance for both bases tested. Unfortunately, efforts to study the soil fabric to investigate what lab technique best mimics the field structure were unsuccessful. However, future work in this project will utilize four additional Texas base materials, including field sections, in efforts to validate the preliminary findings described in this report.

17. Key Words	18. Distribution Statement
Compaction, Laboratory Compaction, Vibratory Compaction, Tex-113-E, Precision, Computed Axial Tomography, CAT Scan	No restrictions. This document is available to the public through NTIS: National Technical Information Service Springfield, Virginia 22161 http://www.ntis.gov

19. Security Classif.(of this report)	20. Security Classif.(of this page)	21. No. of Pages	22. Price
Unclassified	Unclassified	96	

Form DOT F 1700.7 (8-72) **Reproduction of completed page authorized**

IMPROVING LAB COMPACTION METHODS FOR ROADWAY BASE MATERIALS

by

Stephen Sebesta
Associate Transportation Researcher
Texas Transportation Institute

Pat Harris, P.G.
Associate Research Scientist
Texas Transportation Institute

and

Wenting Liu, P.E.
Assistant Research Scientist
Texas Transportation Institute

Report 0-5135-2
Project 0-5135
Project Title: Improving Correlation between Field Construction of Soils and Bases and Laboratory Sample Construction Techniques

Performed in cooperation with the
Texas Department of Transportation
and the
Federal Highway Administration

October 2006
Published: February 2008

TEXAS TRANSPORTATION INSTITUTE
The Texas A&M University System
College Station, Texas 77843-3135

DISCLAIMER

The contents of this report reflect the views of the authors, who are responsible for the facts and the accuracy of the data presented herein. The contents do not necessarily reflect the official view or policies of the Federal Highway Administration (FHWA) or the Texas Department of Transportation (TxDOT). This report does not constitute a standard, specification, or regulation. The researcher in charge was Stephen Sebesta.

ACKNOWLEDGMENTS

This project was conducted in cooperation with TxDOT and FHWA. The project directors, Mike Arrellano, P.E., and Caroline Herrera, P.E., and program coordinator, Miles Garrison, P.E., provided guidance in the direction of the project, along with the following advisors: Tracy Monds, Glenn Eilert, Chris Starr, Lucio Trujillo, and Mike Young.

TABLE OF CONTENTS

Page

TABLE OF CONTENTS (Continued)

Page

LIST OF FIGURES

Figure **Page**

LIST OF FIGURES (Continued)

Figure **Page**

LIST OF FIGURES (Continued)

Figure **Page**

LIST OF TABLES

Table **Page**

LIST OF TABLES (Continued)

Table **Page**

EXECUTIVE SUMMARY

The Texas Department of Transportation (TxDOT) employs the impact hammer method of sample compaction for laboratory preparation of roadway base and subgrade materials for testing. Experience has shown that this method may not adequately represent the true field performance of the materials. This report describes results investigating how different lab compaction methods influence the laboratory characterization of roadway base materials. First, the impact of increased compactive effort was investigated on flexible base materials. Chapter 1 presents these results, which showed that modified compaction resulted in improved properties for the Groesbeck Grade 2 base as compared to Tex-113-E, but not for the Spicewood Grade 1 material. Next, an interlaboratory study evaluated the precision of several TxDOT Test Methods used for base aggregates. A prototype system for calibrating TxDOT's impact hammer lab compactors also was developed in this stage. Chapter 2 presents this information. Finally, Chapter 3 describes a new vibratory lab compaction procedure that was investigated as an alternative to impact hammer lab compaction for base materials. This vibratory lab compaction resulted in improved properties of both base materials tested as compared to Tex-113-E.

Efforts to study which lab method best mimics the field sample structure are presented in Chapter 4. Unfortunately, no suitable method of preparing the soils was found, and efforts to collect a field sample of one of the flex bases tested were unfruitful. However, the bulk of the work conducted in this project provided interesting findings that warrant further investigation. Chapter 5 summarizes the results to date and the recommendations for future work to validate the findings already observed.

CHAPTER 1

EVALUATION OF INCREASED COMPACTIVE EFFORT FOR BASE MATERIALS

SUMMARY

It has been suggested that TxDOT compaction effort for flexible base materials as defined in Test Method Tex-113-E may be too low, resulting in too easy attainment of field density by contractors, and materials' properties that are not optimized. For this reason, testing was conducted to evaluate in the lab the change in mechanical properties of a Grade 1 and Grade 2 base by using modified compaction instead of 113-E, and a field experiment was conducted to evaluate the correlation of the laboratory compaction curves to field compaction characteristics. The lab results showed no incentive to specify modified compaction for the Grade 1 material; additionally, Tex-113-E curves did not match well with the field compaction characteristics with this material. Lab results in general showed consistent improvement in the properties of the Grade 2 material with modified compaction, and TxDOT could consider specifying higher compaction energy for these materials. However, consideration must be given to attainment of the higher density in the field. While the field optimum moisture essentially matched the Tex-113-E optimum with the Grade 2 material, the highest density achieved was approximately 98 percent of Tex-113-E optimum.

TESTING PROGRAM

To evaluate if Tex-113-E compaction energy is too low for flexible base materials, a laboratory and field investigation was initiated. In the lab, the mechanical properties of two flexible base materials were evaluated both with Tex-113-E and Modified Proctor compaction. Table 1.1 summarizes the laboratory portion of the test program.

Table 1.1. Tests for Evaluating Tex-113-E and Modified Compaction.

Material	Tests Performed
Spicewood Item 247 Flex Base	Tex-110-E Gradation Moisture-Density Relationship* Tex-117-E Triaxial Classification* Tex-144-E Tube Suction Test* Laboratory Seismic Modulus* Tex-110-E Gradation after Testing*
Groesbeck Item 247 Flex Base	

*Performed with specimens prepared both with Tex-113-E and Modified compaction.

In the field, the Texas Transportation Institute (TTI) obtained sufficient material from both flex bases to construct test sites to gauge the compaction energy provided by typical field equipment. To perform this task, the following procedure was followed:

- The contractor mixed small stockpiles of each material to the prescribed moisture contents. These moisture contents represented the range of moisture contents on the Tex-113-E and Modified Proctor curves for the materials.
- For each material, the contractor placed the base on top of a previously prepared cement-treated soil into the prescribed locations as shown in Figure 1.1. The material was placed and compacted in one 6 inch lift.
- For each base, the contractor then rolled the entire section using a pneumatic and vibratory steel wheel roller. For each pass the contractor initiated rolling in the transition zone at one end of the section and rolled completely through the section into the transition zone at the opposite end before changing directions.
- TTI monitored the compaction process using multiple tests with a nuclear density gauge.

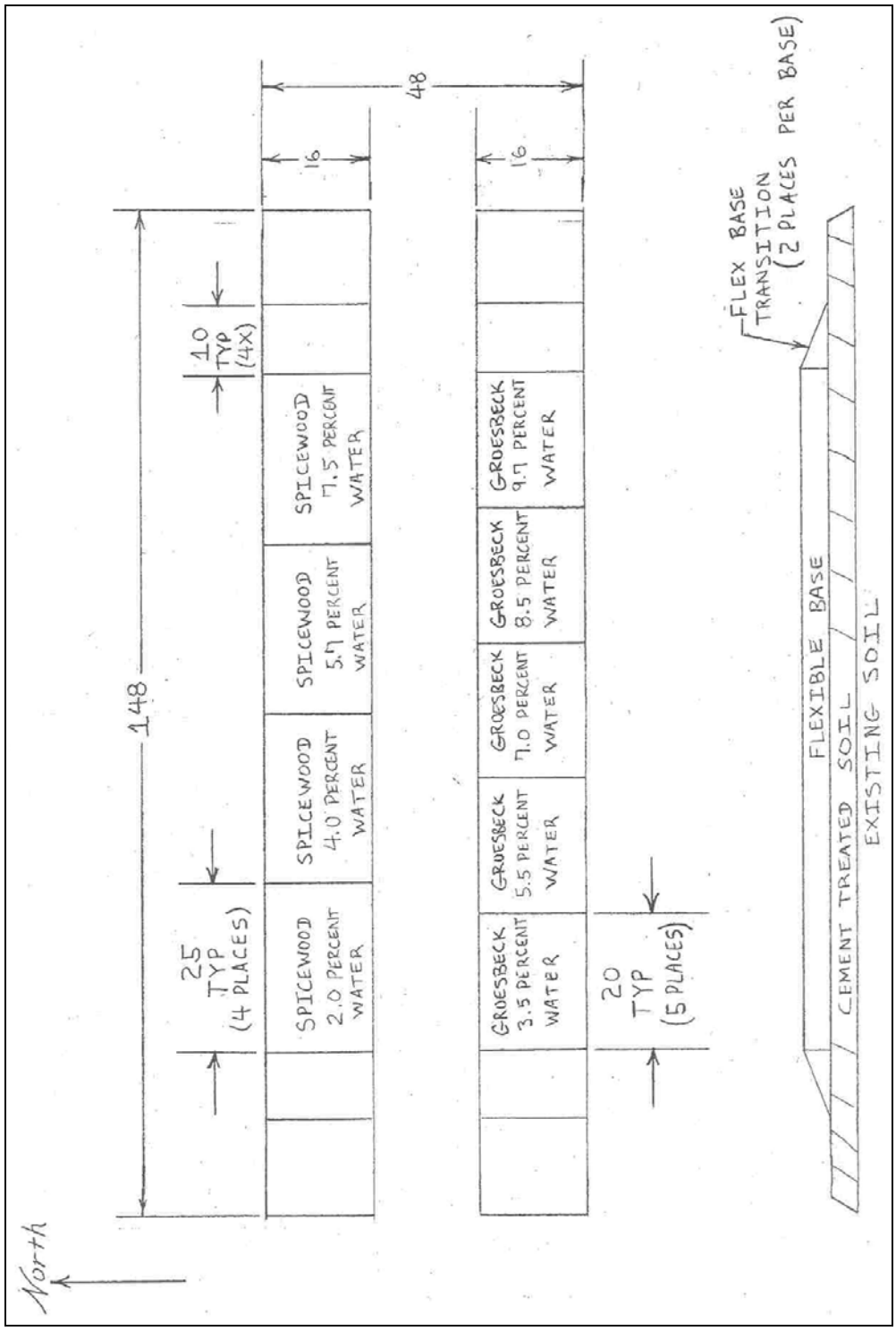

Figure 1.1. Layout of Field Compaction Test Site.

RESULTS FROM LABORATORY TESTING

Table 1.2 shows the bulk fractionation data used for recombining test specimens for each of the base materials. Table 1.3 shows the washed gradation of each flex base tested. Figures 1.2 and 1.3 illustrated the laboratory moisture-density curves for the Spicewood and Groesbeck aggregates, respectively. For the Spicewood aggregate, the liquid limit and plastic index were 18 and 5, respectively. The liquid limit and plastic index were 13 and 4, respectively, for the Groesbeck material.

Table 1.2. Individual Percent Retained for Recombining Flex Bases.

Sieve Size	Spicewood	Groesbeck
1 ¾	0	0
1 ¼	2.6	6.5
7/8	15.1	11.8
5/8	14.1	11.0
3/8	17.2	14.0
#4	16.5	12.5
Passing #4	34.5	44.2

Table 1.3. Wash Gradations of Flex Bases as Percent Passing.

Sieve Size	Spicewood	Groesbeck
1 ¾	100	100
1 ¼	97.2	93.8
7/8	85.6	84.1
5/8	74.6	73.1
3/8	57.8	59.6
#4	43.4	49.0
#10	32.1	43.5
#40	23.8	37.5
#100	20.9	31.4
#200	17.5	12.7

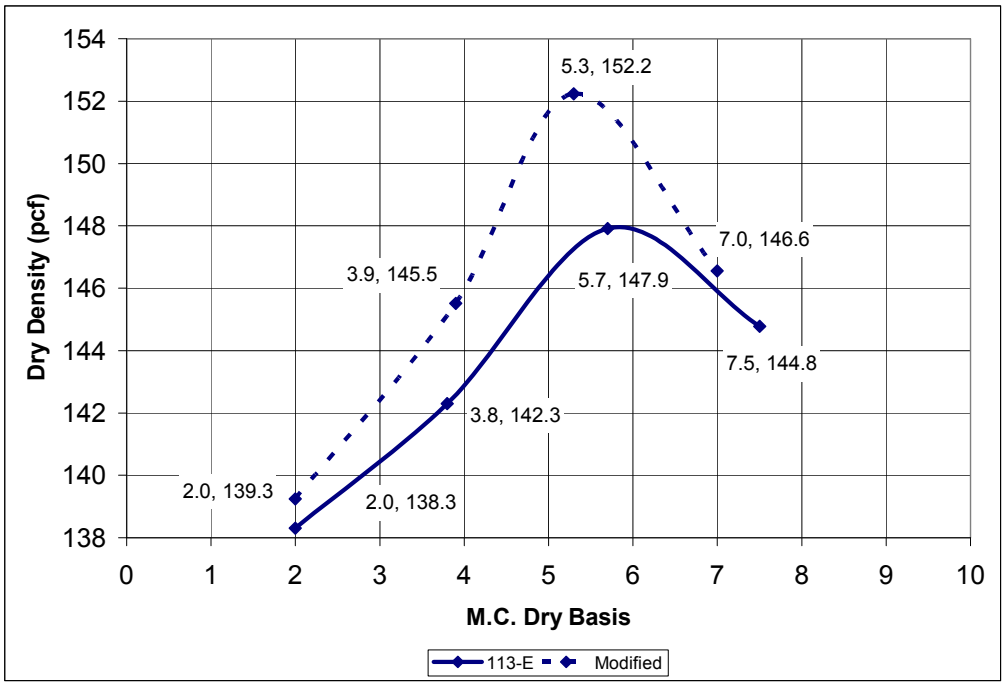

Figure 1.2. Spicewood 113-E and Modified Moisture-Density Curves.

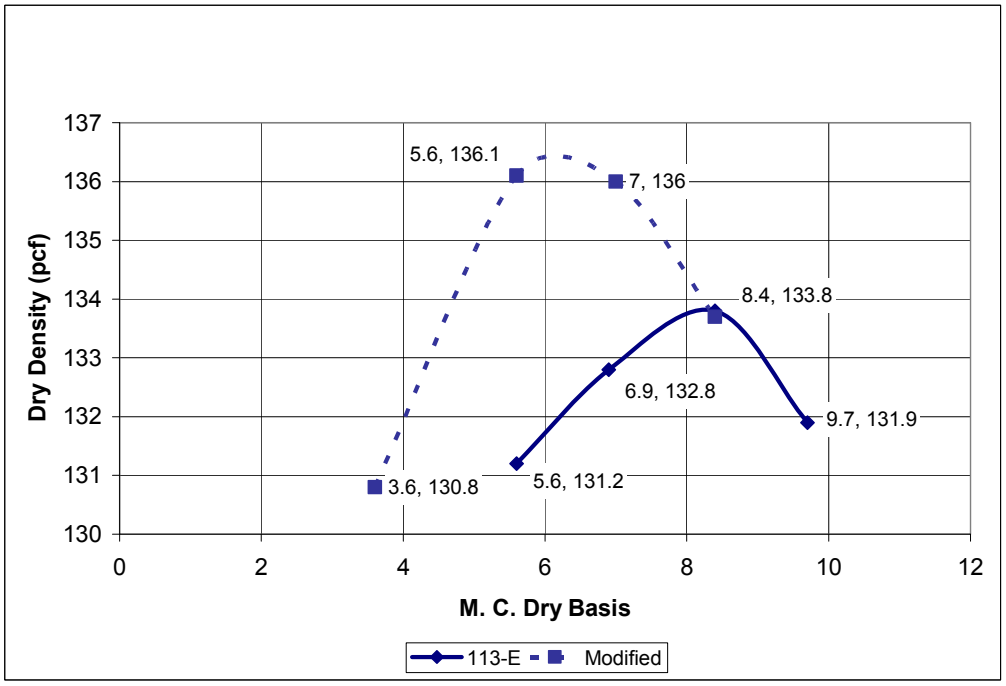

Figure 1.3. Groesbeck 113-E and Modified Moisture-Density Curves.

Triaxial Test Results

Three replicates of the triaxial test were performed with each compaction level. Table 1.4 presents the triaxial test results for the Spicewood aggregate. For both 113-E and Modified

compaction, all three Spicewood replicates classified as Texas Triaxial Class 1.0. Figure 1.4 illustrates the key properties (cohesion and angle of internal friction) from each replicate for the Spicewood material. Table 1.5 presents a statistical analysis revealing that there are no significant differences in the measured cohesion or angle of internal friction between 113-E and Modified compaction energy for the Spicewood aggregate. To perform this analysis, the mean and variance of each data set is first tabulated. Next, Hartley's test is used to determine if the variances are equivalent or not. Finally, the appropriate one-tailed T-test (equal variance or unequal variance, depending on the result from Hartley's test) is used to determine if evidence exists that the means are statistically different. If the tabulated P-value from the T-test is less than the level of significance (typically 0.05), then evidence exists that the sample means statistically differ.

Table 1.4. Spicewood 113-E and Modified Triaxial Results.

Sample ID	Molding Moisture (%)	Dry Density (pcf)	Molded Ht (in)	Moisture after drying (%)	Moisture after capillarity (%)	Confining Pressure (psi)	Total Load (lb)	Extension (in)	Stress (psi)
S113-1	5.8	148.1	7.9	*	4.8	10	7125	0.37	240.2
S113-2	5.7	149.6	7.85	*	4.9	7	7542	0.53	248.8
S113-3	5.7	148.3	7.9	*	4.5	15	9671	0.57	317.4
S113-4	5.6	148.9	7.85	*	4.7	3	5392	0.32	183.0
S113-5	5.9	148.4	7.9	*	4.9	0	967	0.23	33.2
S113-6	5.7	148.1	7.9	*	4.7	5	6604	0.43	220.9
S113-7	6.9	147.0	7.9	*	6.1	0	1115	0.21	38.4
			0					0	
SMOD-1	5.4	150.8	8.05	*	5.2	15	10835	0.42	363.3
SMOD-2	5.3	151.3	8	*	4.9	5	6466	0.36	218.4
SMOD-3	5.4	150.2	8.05	*	4.7	3	4962	0.38	167.2
SMOD-4	5.3	150.5	8.08	*	4.8	0	849	0.21	29.3
SMOD-5	5.7	150.5	8	*	5.2	10	7490	0.47	249.4
SMOD-6	5.4	150.3	8.05	*	4.9	0	1190	0.21	41.0
SMOD-7	5.3	150.5	8.05	*	4.8	7	6328	0.42	212.2
S113-8	5.7	149.1	7.85	3.5	5.0	0	1304	0.22	44.8
S113-10	5.7	149.2	7.9	3.5	5.0	0	1314	0.24	45.1
S113-11	5.7	148.6	7.9	3.7	4.9	3	4689	0.33	158.9
S113-13	5.6	149.3	7.85	3.6	5.0	5	5817	0.36	196.3
S113-14	5.6	147.9	7.85	*	5.0	7	6341	0.31	215.5
S113-12	5.8	148.9	7.9	*	5.2	10	7013	0.38	236.1
S113-9	5.7	149.1	7.9	3.7	5.2	15	7895	0.55	259.8
SMOD-8	5.2	151.0	8	3.3	4.6	0	2025	0.22	69.7
SMOD-10	5.4	150.4	8.05	3.3	4.9	0	1402	0.23	48.2
SMOD-9	5.3	150.8	8	3.4	4.8	3	5875	0.35	198.7
SMOD-12	5.3	151.9	7.95	3.3	4.8	5	6652	0.27	227.3
SMOD-14	5.4	150.2	8.05	3.4	4.9	7	7145	0.3	243.3
SMOD-11	5.3	150.6	8.05	3.3	4.7	10	8019	0.41	269.2
SMOD-13	5.2	152.4	7.9	3.0	4.6	15	10021	0.37	337.9
S113-21	5.7	147.8	7.95	3.7	5.1	10	6327	0.36	213.7
S113-22	5.7	148.1	7.925	3.8	4.9	15	7515	0.31	255.4
S113-23	5.4	147.5	7.9	3.3	4.8	0	1062	0.18	36.7
S113-24	5.7	147.8	7.8	3.9	5.0	7	5837	0.34	197.5
S113-25	5.6	148.1	7.95	3.7	5.1	0	1193	0.18	41.2
S113-26	5.5	148.2	7.95	3.7	4.9	5	5791	0.33	196.3
S113-27	5.5	148.1	7.9	3.4	4.9	3	4121	0.38	138.8
SMOD-21	5.2	150.3	8.075	3.4	4.7	15	9539	0.35	322.8
SMOD-22	5.2	150.5	8.05	3.3	4.7	0	1879	0.2	64.8
SMOD-23	5.2	148.0	8.15	3.4	4.7	10	7073	0.34	239.8
SMOD-24	5.3	149.1	8.1	3.4	4.8	5	6357	0.28	217.1
SMOD-25	5.1	149.6	8.1	3.2	4.7	0	1430	0.18	49.5
SMOD-26	5.0	149.9	8.05	3.3	4.7	3	5401	0.27	184.7
SMOD-27	5.0	150.8	8.05	3.2	4.5	7	6923	0.34	234.5

* Not Measured

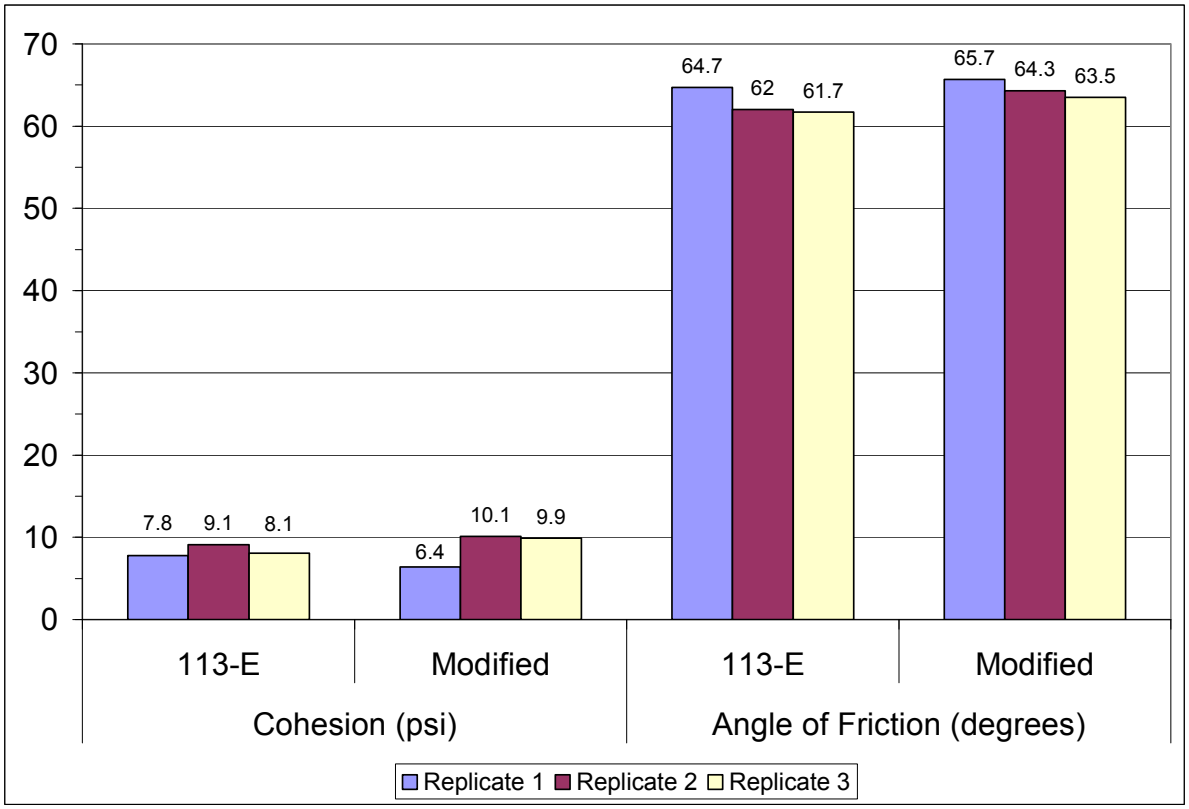

Figure 1.4. Cohesion and Angle of Internal Friction Results for Spicewood from 113-E and Modified Compaction.

Table 1.5. Evaluation of Triaxial Results for Spicewood from 113-E and Modified Compaction.

	Cohesion		Angle of Friction	
	113-E	Modified	113-E	Modified
Replicate 1	7.8	6.4	64.7	65.7
Replicate 2	9.1	10.1	62	64.3
Replicate 3	8.1	9.9	61.7	63.5
Average	8.3	8.8	62.8	64.5
Variance	0.46	4.33	2.73	1.24
Hartley's Test Statistic for Equal Variance	9.35		2.20	
H-critical	39		39	
	Conclude Variances are Equal			
One-tailed t-test P-Value (two sample equal variance)	0.37		0.11	
	Conclude no Difference in Means at 95% Confidence Level			

Table 1.6 presents the results from the triaxial testing with the Groesbeck material. Figure 1.5 presents the cohesion, angle of internal friction, and classification for each of the replicates with the Groesbeck material. A statistical analysis of the data, shown in Table 1.7, indicates that the cohesion is greater, the angle of internal friction is increased, and the triaxial classification is improved, by using Modified compaction with the Groesbeck aggregate.

Table 1.6. Groesbeck 113-E and Modified Triaxial Results.

Sample ID	Molding Moisture (%)	Dry Density (pcf)	Molded Ht (in)	Moisture after drying (%)	Moisture after capillarity (%)	Confining Pressure (psi)	Total Load (lb)	Extension (in)	Stress (psi)
G113-1	8.4	132.4	8	3.7	7.1	3	2251	0.23	77.4
G113-2	8.2	132.4	8.05	4.3	7.0	10	4107	0.28	140.2
G113-3	8.3	133.8	7.95	3.8	7.2	0	573	0.17	19.8
G113-4	8.4	132.4	8.05	3.5	7.1	5	2380	0.28	81.3
G113-5	8.3	133.0	8	3.7	7.1	20	6191	0.45	206.7
G113-6	8.3	132.9	8	4.6	7.1	15	5161	0.35	174.6
G113-7	8.3	133.3	8	3.7	7.4	0	545	0.17	18.9
			0					0	
GMOD-1	6.4	136.7	7.95	2.7	6.4	5	3788	0.15	131.5
GMOD-2	6.3	134.3	8.1	2.7	6.9	0	963	0.16	33.4
GMOD-3	6.7	134.6	8.05	3.2	7.0	0	1147	0.1	40.1
GMOD-4	6.7	135.5	8	3.2	6.9	3	3152	0.16	109.3
GMOD-5	6.2	135.8	8	2.8	6.8	10	4393	0.18	151.9
GMOD-6*	3.6	132.2	8.2	2.2	8.5	7	2078	0.13	72.3
GMOD-7	6.3	135.1	8.05	3.1	6.7	15	6096	0.16	211.4
* Sample botched - molding water not added correctly									
G113-10	8.4	131.9	8.05	6.3	7.7	0	681	0.11	23.8
G113-14	8.4	132.3	8	6.4	7.7	0	729	0.17	25.2
G113-11	8.4	132.4	8	6.4	7.6	3	2471	0.3	84.1
G113-9	8.4	132.3	8	6.4	7.6	5	2907	0.27	99.4
G113-12	8.4	132.1	8	6.2	7.6	7	3229	0.38	108.8
G113-8	8.9	132.8	7.95	6.8	8.1	10	4061	0.31	138.1
G113-13	8.8	131.3	8.1	6.5	8.0	15	5456	0.4	183.5
GMOD-9	6.7	136.2	7.95	4.6	6.8	0	1939	0.12	67.6
GMOD-11	6.5	136.2	7.95	4.6	6.7	0	1540	0.13	53.6
GMOD-12	6.7	135.1	8	4.5	6.8	3	3356	0.23	115.3
GMOD-13	6.5	135.9	8	4.5	6.6	5	5035	0.17	174.3
GMOD-14**	6.6	135.2	8	4.6	6.8	7	4389	0.24	150.6
GMOD-8	6.6	135.4	8	4.4	6.8	10	6027	0.23	207.1
GMOD-10	7.7	134.7	7.95	5.7	8.1	15	8240	0.22	283.4
**Sample damaged in extrusion									
G113-18	8.6	133.3	8.1	6.2	8.0	0	626	0.19	21.6
G113-16	8.1	132.5	8	5.8	8.2	3	2071	0.26	70.9
G113-17	9.8	133.7	7.75	7.3	8.2	5	2024	0.42	67.7
G113-21	8.5	134.0	7.95	6.2	7.7	7	3353	0.36	113.2
G113-19	7.2	131.3	8.15	4.9	8.1	10	4295	0.27	146.9
G113-20	8.3	134.4	7.95	6.1	7.6	15	4096	0.4	137.6
	0.0	0.0	0	0.0	0.0	0	5	0	0.0
GMOD-15	6.6	135.9	7.9	3.9	7.2	0	1139	0.15	39.5
GMOD-16	6.4	137.5	7.85	4.4	7.2	0	1166	0.12	40.6
GMOD-21	6.3	135.1	8.05	3.0	7.0	3	2727	0.15	94.7
GMOD-20	6.5	135.2	8.1	5.6	7.0	5	3668	0.17	127.0
GMOD-17	6.5	134.9	8.05	5.0	7.1	7	3517	0.25	120.5
GMOD-18	6.5	134.6	8	3.6	7.1	10	4936	0.17	170.9
GMOD-19	6.4	135.3	8.05	4.2	7.0	15	6095	0.17	211.0

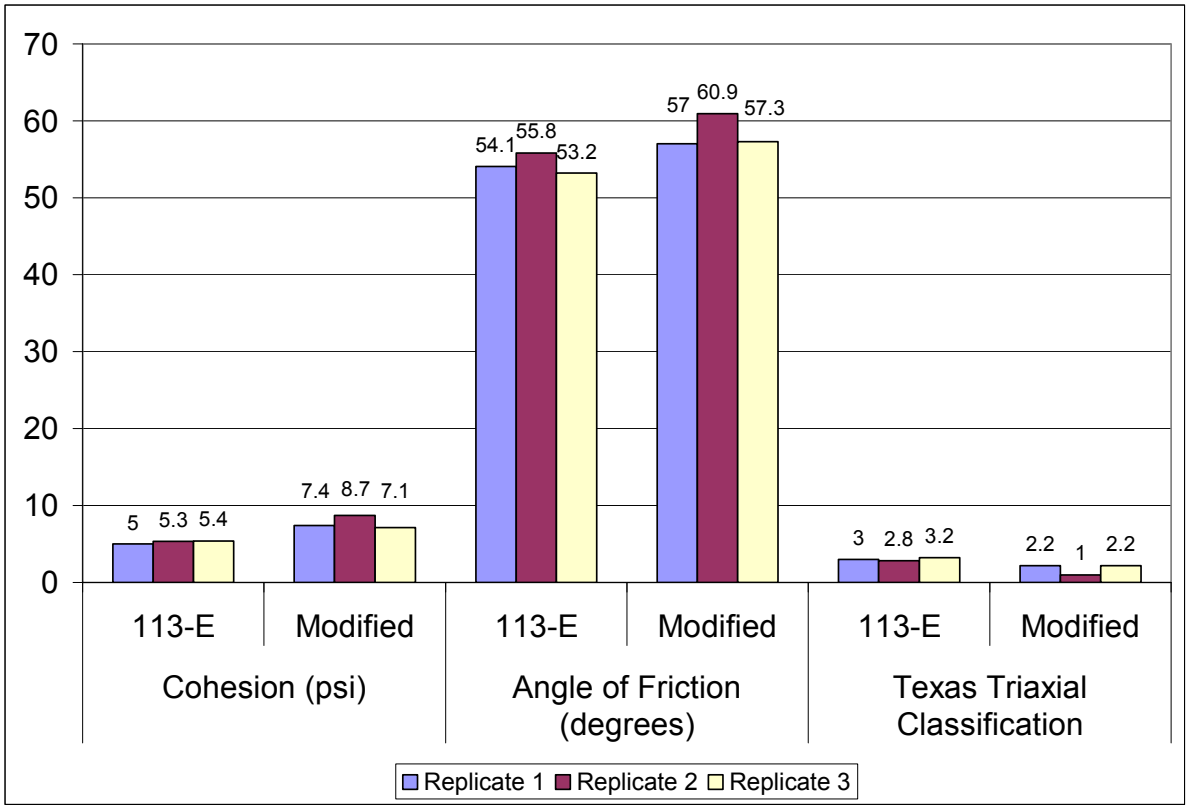

Figure 1.5. Cohesion, Angle of Internal Friction, and Texas Triaxial Classification Results for Groesbeck from 113-E and Modified Compaction.

Table 1.7. Evaluation of Triaxial Results for Groesbeck from 113-E and Modified Compaction.

	Cohesion (psi)		Angle of Friction (degrees)		Texas Triaxial Classification	
	113-E	Modified	113-E	Modified	113-E	Modified
Replicate 1	5	7.4	54.1	57	3	2.2
Replicate 2	5.3	8.7	55.8	60.9	2.8	1
Replicate 3	5.4	7.1	53.2	57.3	3.2	2.2
Average	5.2	7.7	54.4	58.4	3.0	1.8
Variance	0.04	0.72	1.74	4.71	0.04	0.48
Hartley's Test Statistic for Equal Variance	16.69		2.70		12.00	
H-critical	39		39		40	
	Conclude Variances are Equal					
One-tailed t-test P-Value (two sample equal variance)	0.00		0.03		0.02	
	Conclude Difference in Means Exists at the 95 % Confidence Level					

Tube Suction Test Results

The Tube Suction Test (Test Method Tex-144-E) evaluates base materials' moisture susceptibility by using the surface dielectric of the material during a 10 day capillary soak, along with the moisture content gain of the specimen during the capillary soaking. For each aggregate, TTI tested six specimens prepared with both compaction energies. As evidenced in Figure 1.6, one clear outlier exists in each data set for the Spicewood aggregate. This outlier was excluded from further analysis. Table 1.8 presents an analysis of the results for the Spicewood aggregate. The results show that for this material:

- Modified compaction resulted in a slightly higher final average dielectric value.
- No difference existed in the initial moisture content after drying.
- Modified compaction resulted in reduced gravimetric moisture content after soaking.
- Modified compaction resulted in a decrease in both percent moisture loss during drying and percent moisture gain during soaking.

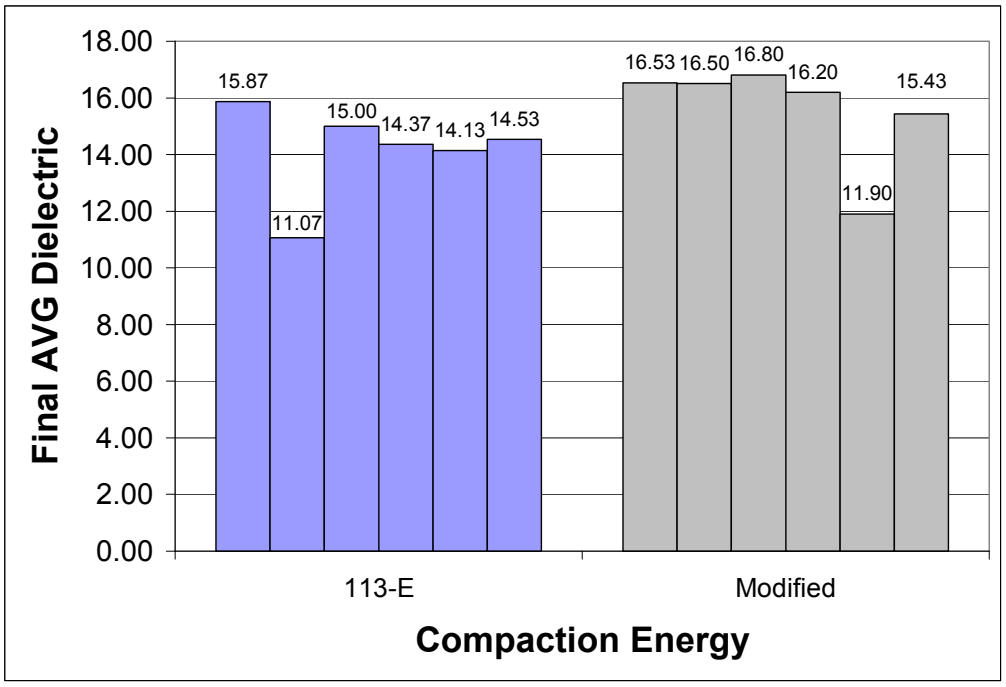

Figure 1.6. Dielectric Results from Spicewood with 113-E and Modified Compaction.

Table 1.8. Spicewood Tex-144-E Results from 113-E and Modified Compaction.

Replicate	AVG Dielectric		Initial M.C. after Drying		Final M.C. after Capillary Soak		M.C. Loss During Drying		M.C. Gain During Soak	
	113-E	Modified	113-E	Modified	113-E	Modified	113-E	Modified	113-E	Modified
1	15.87	16.53	0.43	0.52	4.71	4.46	5.17	4.74	4.27	3.94
2	15.00	16.50	0.49	0.55	4.75	4.45	5.19	4.73	4.26	3.90
3	14.37	16.80	0.46	1.33	4.80	4.47	5.25	4.72	4.34	3.14
4	14.13	16.20	0.82	0.90	4.77	4.54	5.16	4.77	3.96	3.63
5	14.53	15.43	0.46	0.56	4.85	4.43	5.30	4.56	4.39	3.87
Mean	14.78	16.29	0.53	0.77	4.78	4.47	5.21	4.70	4.24	3.70
Variance	0.47	0.28	0.03	0.12	0.00	0.00	0.00	0.01	0.03	0.11
Hartley's Test	1.69		4.65		1.74		1.91		3.90	
H-Critical (95% Confidence)	7.15		7.15		7.15		7.15		7.15	
Decision	*Conclude Variances are Equal*									
P-Value one-tail T-test	0.002		0.099		0.000		0.000		0.005	
Decision	*Conclude means differ*		*Conclude means are equal*		*Conclude means differ*		*Conclude means differ*		*Conclude means differ*	

In general, similar observations were made with the Groesbeck material in Tex-144-E. Figure 1.7 illustrates the final dielectric results. Modified compaction resulted in an increase of the final average dielectric value and a decrease in the level of moisture content changes during the drying and capillary wetting phases of the test. Table 1.9 presents all of the results for the Groesbeck material.

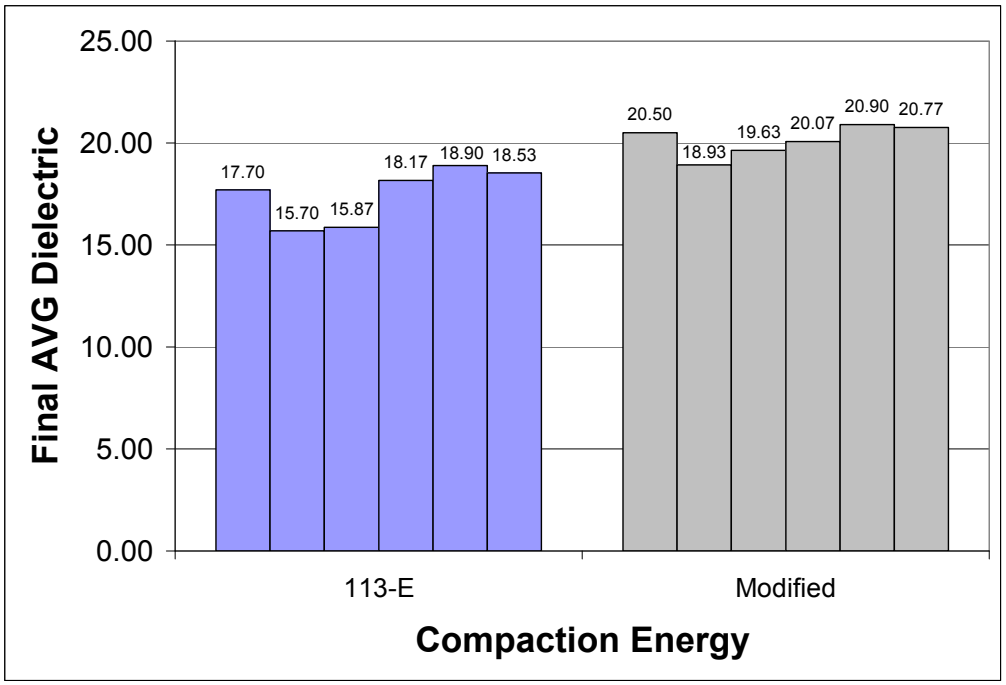

Figure 1.7. Dielectric Results from Groesbeck with 113-E and Modified Compaction.

Table 1.9. Groesbeck Tex-144-E Results from 113-E and Modified Compaction.

Replicate	Avg Dielectric		Initial M.C. After Drying		Final M.C. after Capillary Soak		M.C. Loss During Drying		M.C. Gain During Soak	
	113-E	Modified	113-E	Modified	113-E	Modified	113-E	Modified	113-E	Modified
1	17.70	20.50	1.02	0.79	7.25	6.28	7.41	5.34	6.23	5.49
2	15.70	18.93	0.96	1.22	6.70	6.15	7.18	4.85	5.73	4.93
3	15.87	19.63	1.00	0.87	6.62	6.22	7.12	5.26	5.62	5.36
4	18.17	20.07	1.03	1.09	7.52	6.36	7.37	5.12	6.50	5.27
5	18.90	20.90	0.97	0.92	7.59	6.56	7.41	5.24	6.62	5.63
6	18.53	20.77	0.99	1.01	7.32	6.36	7.47	5.24	6.33	5.35
Mean	17.48	20.13	1.00	0.98	7.17	6.32	7.33	5.17	6.17	5.34
Variance	1.88	0.56	0.00	0.02	0.17	0.02	0.02	0.03	0.17	0.06
Hartley's Test	3.34		38.97		8.64		1.41		2.93	
H-Critical (95% Confidence)	7.15		7.15		7.15		7.15		7.15	
Decision	*equal variance*		*unequal variance*		*unequal variance*		*equal variance*		*equal variance*	
P-Value one-tail T-test	0.00		0.43		0.00		0.00		0.00	
Decision	*conclude means differ*		*conclude means equal*		*conclude means differ*		*conclude means differ*		*conclude means differ*	

Given the consistency of the results in Tex-144-E from both bases, it appears increased compaction effort will reduce the moisture susceptibility ranking of the material. The higher dielectric value in the Modified specimens indicates that water is occupying a higher percentage of the available pore space in these samples. It is hypothesized that at least one contributing factor to this occurrence could be increased suction from reduced radius of capillaries in specimens prepared with Modified compaction.

Laboratory Seismic Results

The laboratory seismic modulus was measured on the Tex-144-E specimens at three stages of the test: after molding (at optimum moisture content), after 48 hours drying, and after the 10 days of capillary soaking. For the Spicewood aggregate, the only statistically verifiable difference in the seismic modulus was after the drying phase of the test. Both at optimal and after the capillary soak, no difference in the laboratory seismic modulus existed for the Spicewood material. Figure 1.8 illustrates the average results from the Spicewood specimens.

Unlike the Spicewood material, Modified compaction of the Groesbeck base resulted in a statistically verifiable higher mean seismic modulus at all three stages of moisture conditioning. Figure 1.9 presents the results for the Groesbeck material.

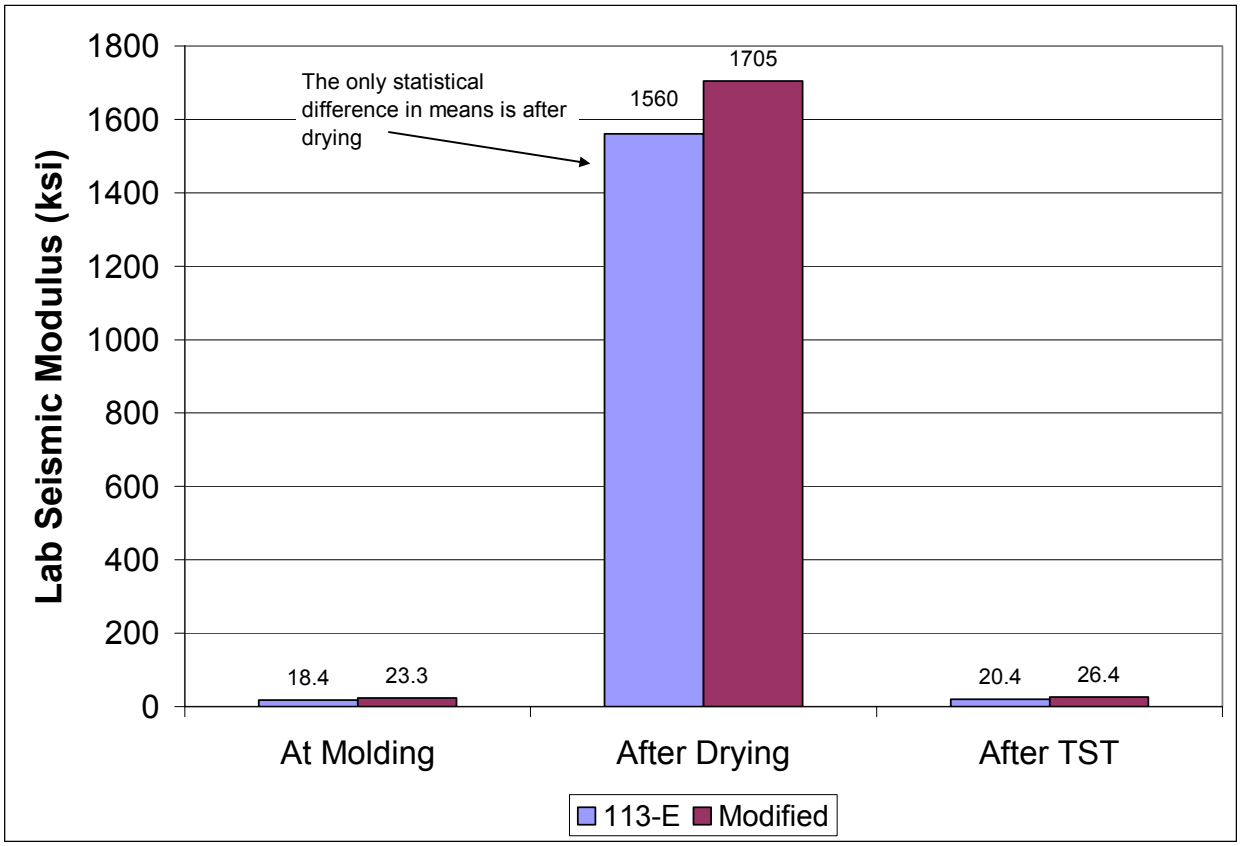

Figure 1.8. Lab Seismic Modulus of Spicewood from 113-E and Modified Compaction.

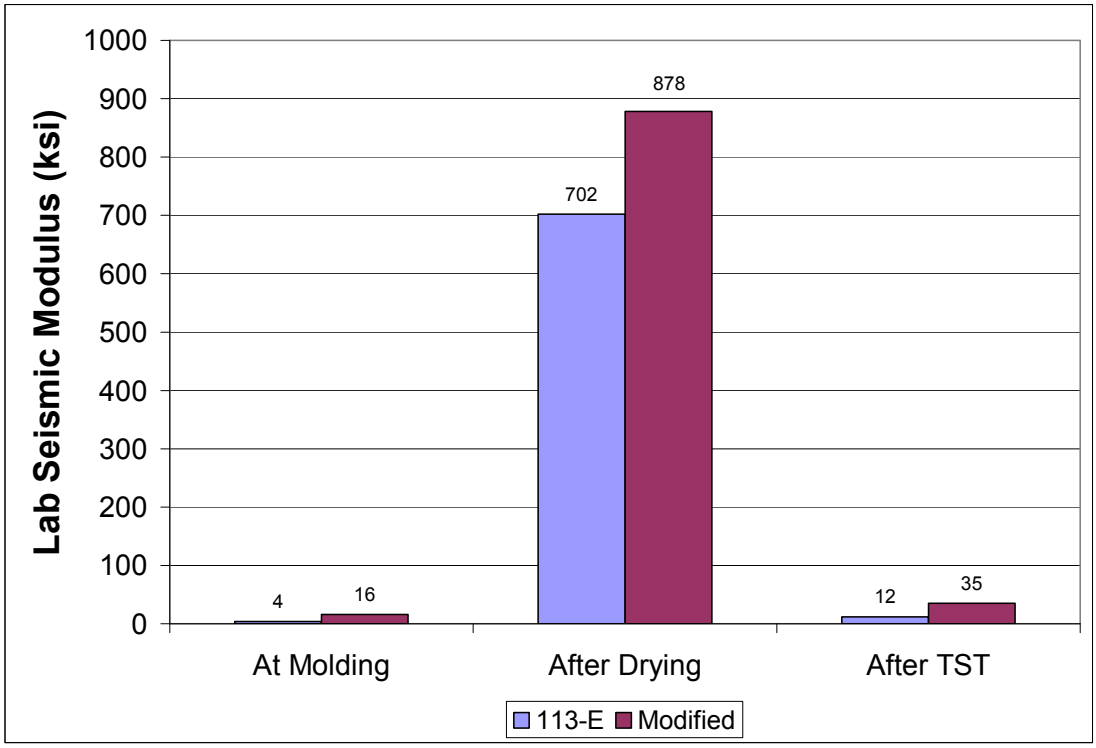

Figure 1.9. Lab Seismic Modulus of Groesbeck from 113-E and Modified Compaction.

Aggregate Breakdown from Increased Compaction Energy

In efforts to help explain some of the lab behavior of the Spicewood and Groesbeck specimens prepared and tested with both Tex-113-E and Modified compaction, random specimens were saved after testing and washed gradations through the #4 sieve conducted. Specimens were only sieved through the #4 since that is the smallest sieve size used for bulk recombination of specimens during sample preparation. A minimum of 10 tests were conducted on each material with each compaction method.

With the Spicewood aggregate, no significant particle breakdown occurred by using Modified instead of Tex-113-E compaction. Figure 1.10 shows the data. For Groesbeck, a slight increase in the amount of material passing the #4 sieve was generated by using Modified compaction. This additional passing #4 material was generated primarily by breakdown of material from the 3/8 inch sieve size, as Figure 1.11 shows.

Based upon the observed lab results already presented and the gradation data presented below, it is hypothesized that the primary factor for any observed differences with the Spicewood material (the higher dielectric value in Tex-144-E and the higher seismic modulus when dry) are due to the increased density of the specimens. The slightly increased amount of passing #4 material generated by the additional compaction effort with the Groesbeck material was minimal, and higher density likely is also the driving factor in the observed changes in the Groesbeck performance. Lab results showed neither of the materials powdered with the additional compaction effort.

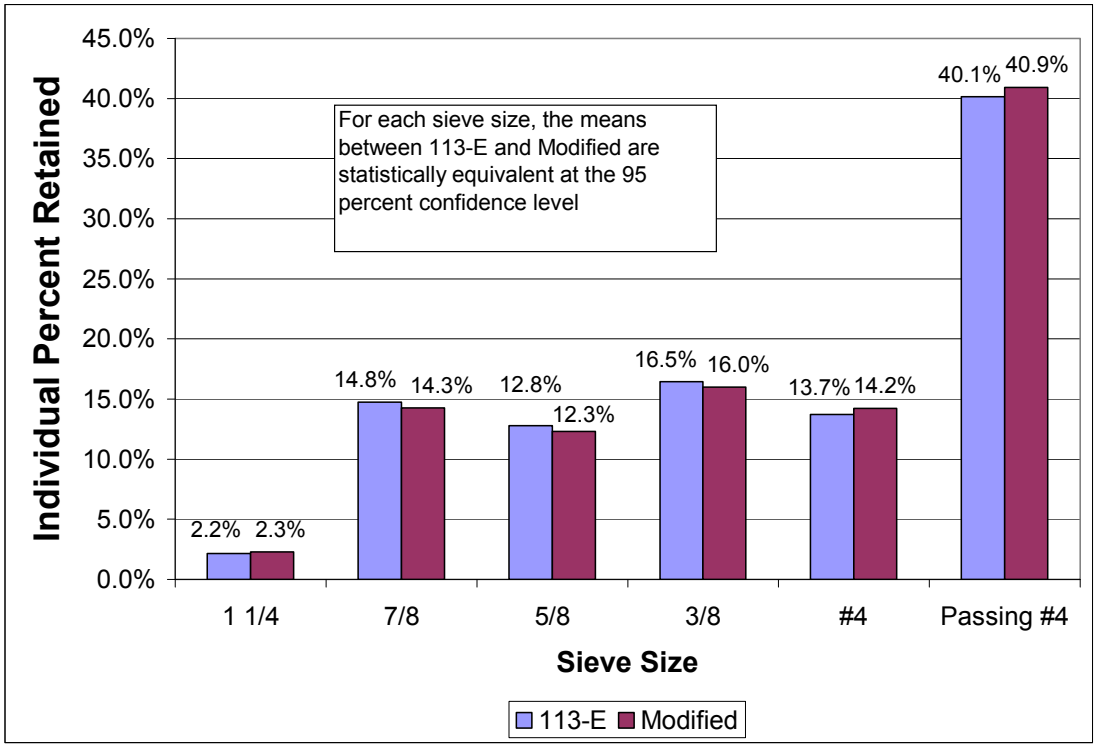

Figure 1.10. Average Individual Percent Retained of Spicewood 113-E and Modifed Specimens after Testing.

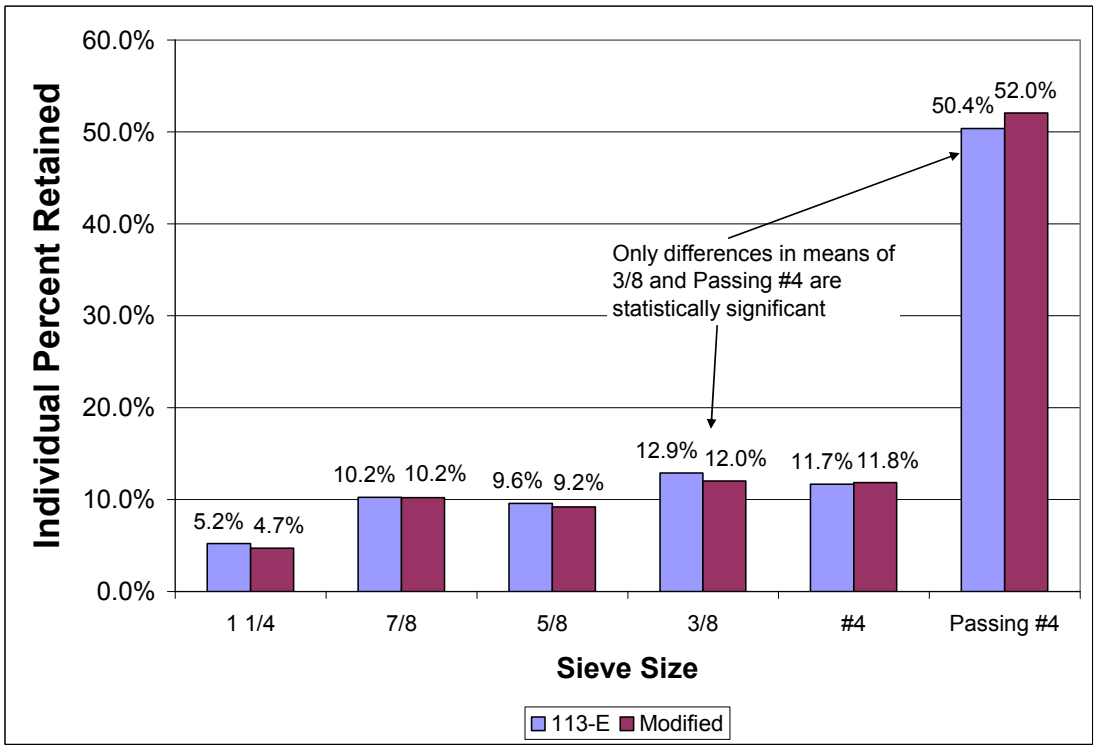

Figure 1.11. Average Individual Percent Retained of Groesbeck 113-E and Modifed Specimens after Testing.

RESULTS FROM FIELD TESTING

At the time of placing the Spicewood base, the contractor's only roller available was a Cat PS-150B. The roller was fully ballasted with water, and based on the manufacturer's charts, produced a ground contact pressure of approximately 52 psi. The contractor also used a Dynapac CA 251 steel wheel vibratory roller. After placing and spreading the Spicewood base, as illustrated in Figure 1.12, the contractor performed rolling in the order outlined in Table 1.10. After each rolling sequence, TTI checked the density and moisture content of the sections with a nuclear gauge. Figure 1.13 shows the rolling operations. Figure 1.14 shows the resulting compaction curves produced from each sequence. Figure 1.15 shows the two field curves that most nearly achieved Tex-113-E density, which were after rolling sequences 3 and 5. Although the maximum density approached 113-E maximum, the highest level of field compaction achieved was 98 percent of Tex-113-E density, and that density was at moisture contents between 6.8 and 7.2 percent.

Figure 1.12. Spreading Spicewood Base at Test Site.

Table 1.10. Rolling Sequences on Spicewood Field Test Site.

Rolling Sequence	Rolling Conducted
1	2 passes pneumatic followed by 1 pass steel wheel (vibrate down; static return)
2	5 passes pneumatic
3	4 passes pneumatic
4	2 passes steel wheel (vibrating)
5	2 passes steel wheel (vibrating)
6	2 passes pneumatic
7	4 passes pneumatic

Note: one pass is down and back

Figure 1.13. Rolling at Spicewood Test Site.

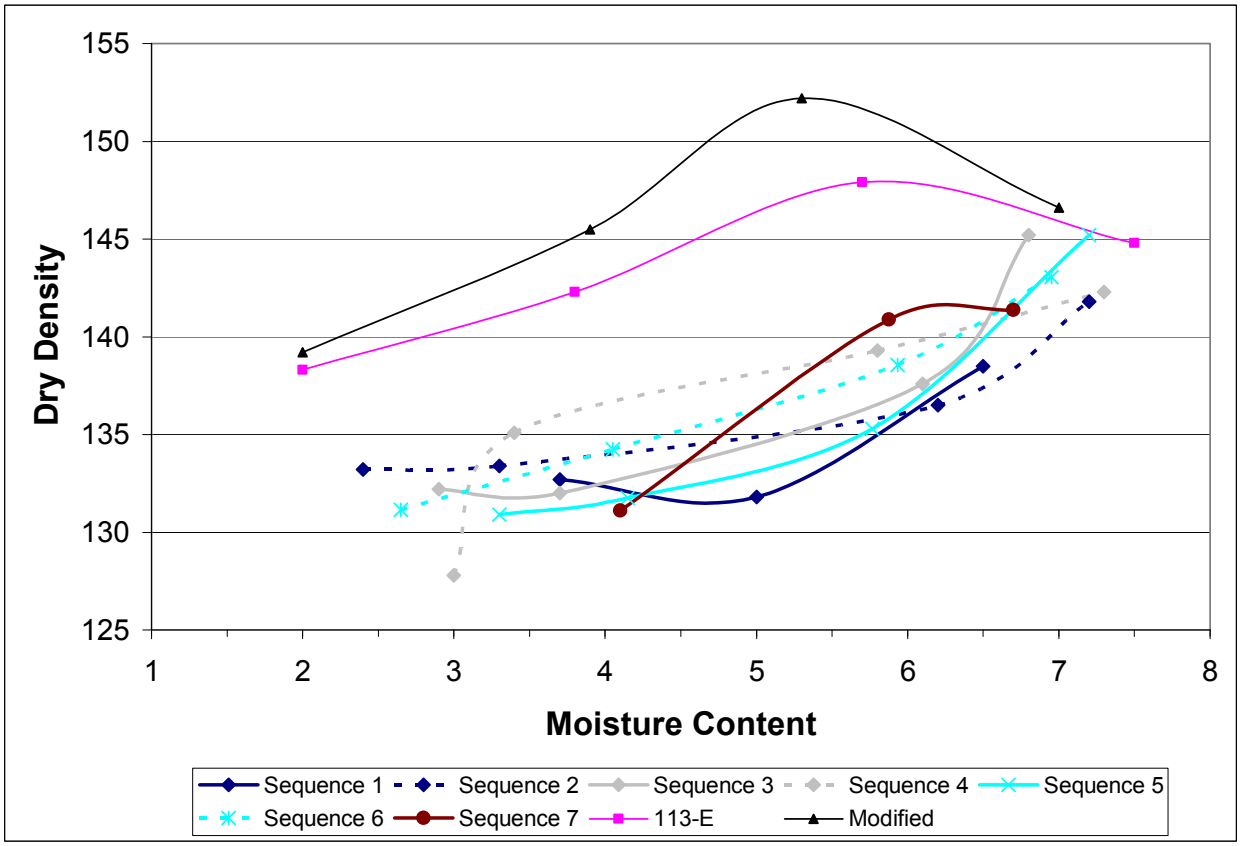

Figure 1.14. Spicewood Field Compaction Results.

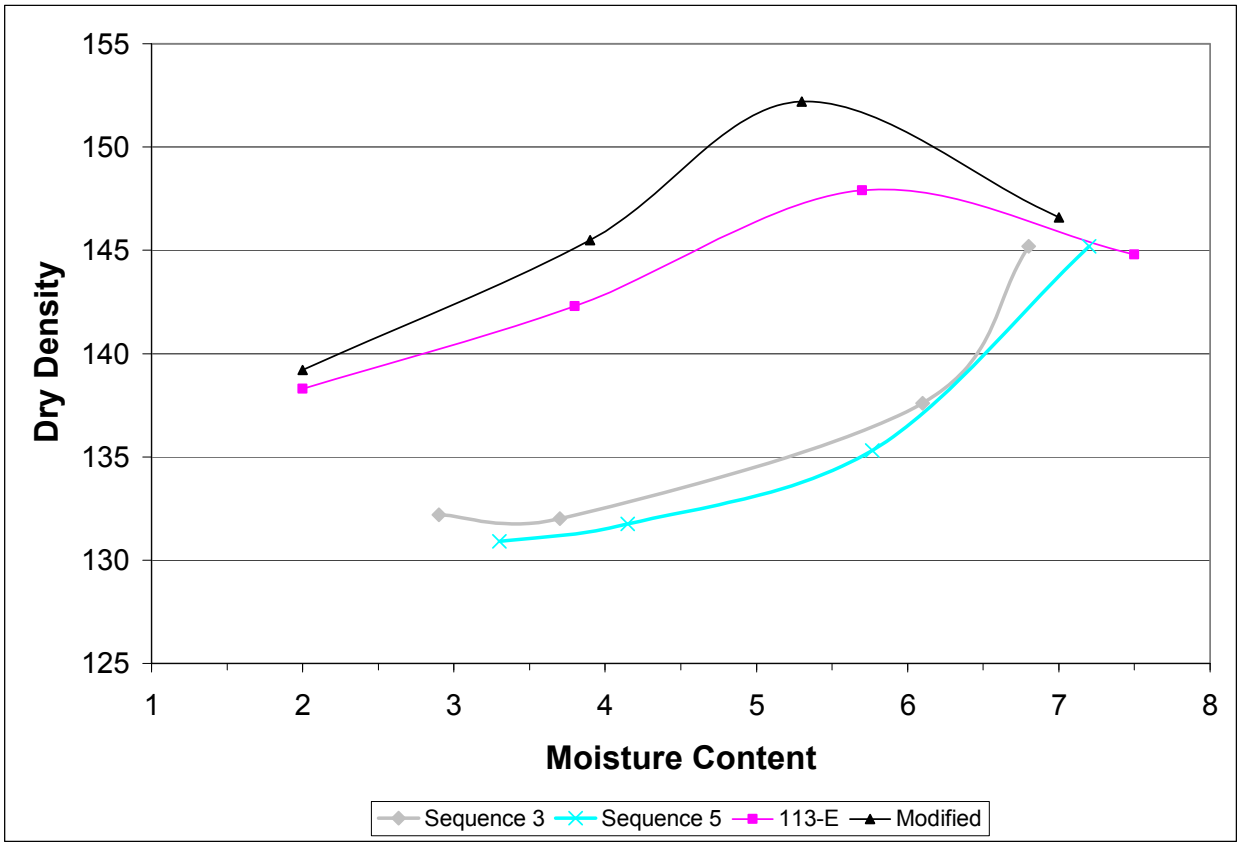

Figure 1.15. Spicewood Field Compaction Results from Rolling Sequences That Most Nearly Achieved Tex-113-E Density.

Four rolling sequences were conducted on the Groesbeck field test site, as described in Table 1.11. For this test site, the contractor was able to secure use of an Ingram 11-5400 pneumatic roller, which they ballasted with water and adjusted the tire inflation pressures to provide a ground contact pressure of 80 psi. Figure 1.16 shows the Ingram roller. The same Dynapac vibratory roller previously shown was also used on the Groesbeck material. Figure 1.17 shows the results from the Groesbeck field test. Although the field density rapidly approached 98 percent of Tex-113-E maximum density, as with the Spicewood material, 100 percent of Tex-113-E was not achieved. The highest achieved field density was 98 percent of Tex-113-E.

Table 1.11. Rolling Sequences on Groesbeck Field Test Site.

Rolling Sequence	Rolling Conducted
1	2 passes pneumatic followed by 1 pass steel wheel (vibrate down; static return)
2	5 passes pneumatic
3	3 passes pneumatic
4	2 passes vibratory steel wheel

Figure 1.16. Rolling with the Pneumatic on the Groesbeck Test Site.

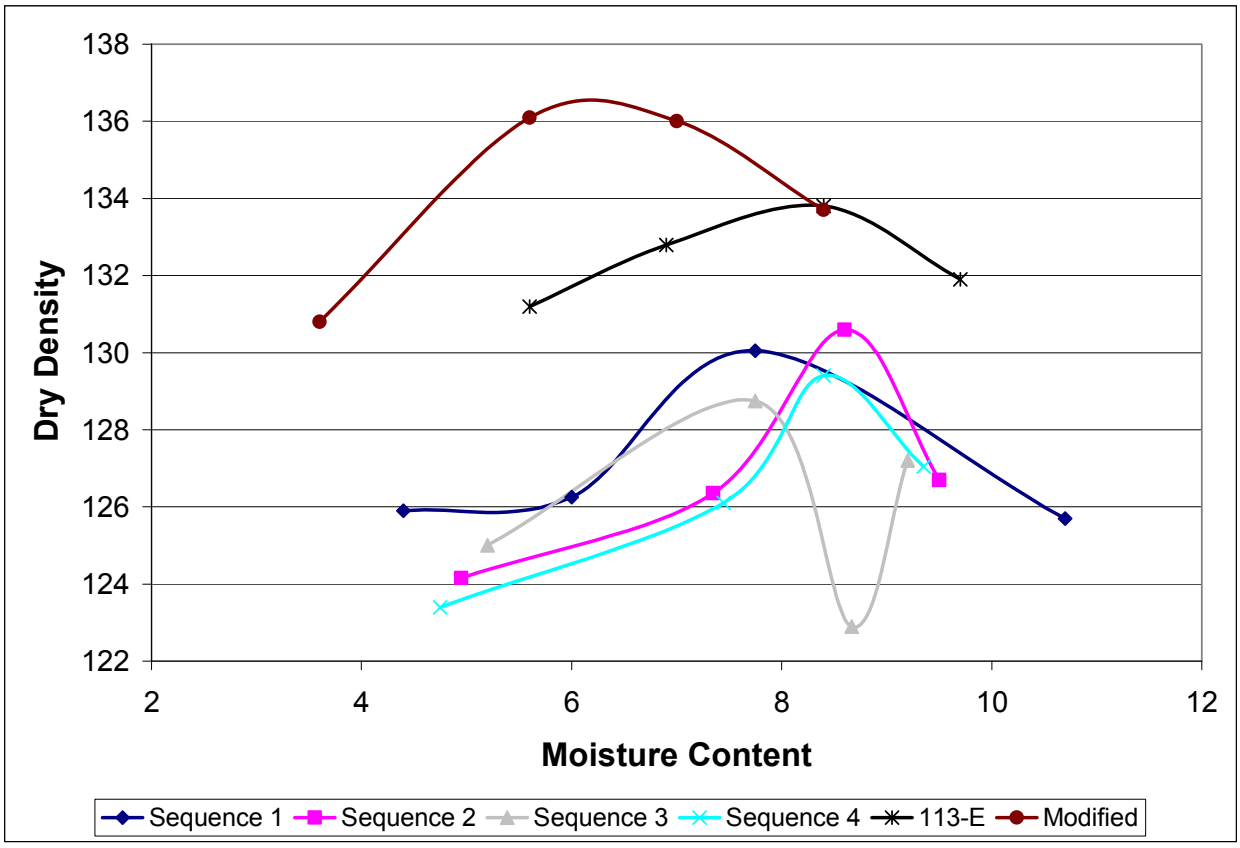

Figure 1.17. Groesbeck Field Compaction Results.

From the test sections to gauge compaction energy of typical field equipment, the following observations were made:

- With the base lift thickness (6 inches) and equipment used, Tex-113-E maximum density was not achieved in the field. With the Spicewood aggregate, the field moisture contents were not wet enough to make the field curve break over.
- Successful compaction in the field appears much more sensitive to water content than in the lab. The slope of the field curves when approaching the maximum field density is significantly greater than the laboratory curves. For example, with the Groesbeck material, the data points on the laboratory 113-E curve ranged from 5.6 to 9.7 percent, spanning a water content range of 4.1 percent, and none of the resultant densities fell below 98 percent of the lab maximum. In contrast, the field curve suggests a water content requirement between 7.9 and 9.2 percent in order to achieve at least 98 percent of the maximum field density. This acceptable field water content range of this material is only 1.3 percent, far less than the 4.1 percent range observed in the lab.
- The correlation between field compaction and the lab compaction characteristics appear at least partially dependent upon the material. For example, the Spicewood data clearly suggests the laboratory optimal water content is too dry for the field equipment used. In contrast, the optimal water content for the Groesbeck material in the field essentially matched the Tex-113-E optimum. It should be pointed out that, after conducting the experiment described, discussions with Vulcan materials revealed that very high ground contact pressures are required to compact the Spicewood material. The Vulcan representative interviewed recommended that the best way to compact the Spicewood material is with a fully loaded, single-axle water truck, and their next preferred method was to roll the base with a fully loaded dirt scraper.

CONCLUSIONS

Specification of laboratory compaction energy requires balancing materials' properties in the lab with consideration of constructability in the field. Lab testing performed indicated mixed results when utilizing higher compaction energy. With the Spicewood Grade 1 material, modified compaction did little to improve the performance. Additionally, in the field, Tex-113-E compaction could not be achieved. With the Groesbeck Grade 2 material, modified compaction did improve the materials' resistance to shear failure, as measured by triaxial tests, and also resulted in increased modulus. However, the highest level of compaction achieved in the field with the Grade 2 material was approximately 98 percent of Tex-113-E.

Given these observations, the data suggest specification of higher lab compaction energy is not warranted for Grade 1 flexible bases. The observed improvement of properties with the Grade 2 material by using modified compaction suggest TxDOT could consider specifying higher compaction energy for these materials. However, consideration must also be given to field constructability. With the methods used in this project, Tex-113-E density was not achievable in the field. However, contractors have reported success in meeting higher density requirements by using other construction techniques such as reduced lift thickness, placing the base with base pavers, and performing rolling with equipment that produces higher contact pressures.

CHAPTER 2

INTERLABORATORY STUDY WITH CURRENT TXDOT TEST METHODS

SUMMARY

To develop a performance baseline of the materials tested and develop estimates of precision of the test methods using impact hammer compaction, an interlaboratory study was conducted with the current TxDOT Test Methods using the Spicewood and Groesbeck flex bases. This chapter presents the results and resultant precision statistics. Additionally, as part of these efforts, the research team tested a prototype system for calibrating the energy of the impact hammer lab compactors. The results indicate that with further refinement, this system should be able to satisfy TxDOT's calibration needs for a majority of its lab impact hammer compactors.

TESTING PROGRAM

Five materials laboratories performed testing. These labs were: Austin M&P, Waco, Tyler, and Atlanta TxDOT District labs, and TTI Materials Laboratory. Due to time and labor constraints, the project monitoring committee chose to limit the number of materials tested to the two bases previously mentioned. Table 2.1 summarizes the testing plan.

Table 2.1. Testing Plan for Interlaboratory Study.

Test	General Procedure Followed
Moisture Density Relationship	Test Method Tex-113-E. Each lab performed one test per material.
Triaxial Characterization	Tex-117-E conditioning followed. Each base tested in triplicate with confining pressures of 0 and 15 psi.
Tube Suction Test	Test Method Tex-144-E

TEST RESULTS

The base materials used were the same Spicewood and Groesbeck flexible bases described in Chapter 1. Tables 2.2 and 2.3 contain the key test results from Spicewood and Groesbeck materials, respectively.

Table 2.2. Results from Spicewood Interlaboratory Tests.

Testing Laboratory			TTI	Austin M&P	Waco	Tyler	Atlanta
113-E	Max Density		147.9	148.5	141.9	147.1	148.2
	Optimum Water (%)		5.7	5.2	5.9	5.8	5.9
117-E Unconfined	Peak Stress (psi)	Test 1	38.4	62.6	35.5	37.7	24
		Test 2	44.8	58.1	43.1	41.3	34.6
		Test 3	41.2	66	44.4	46.6	44.7
	Dry Density (pcf)	Test 1	147	146.2	Not recorded	149.1	146.6
		Test 2	149.1	145.7		148.5	146.8
		Test 3	148.1	145.8		148.8	148.5
117-E with 15 psi Confining	Peak Stress (psi)	Test 1	317.4	239.8	265	217.6	241
		Test 2	259.8	201.6	276.7	238.3	220.7
		Test 3	255.4	236.5	280.8	246.9	227.1
	Dry Density (pcf)	Test 1	148.3	145.2	Not recorded	148.4	148.1
		Test 2	149.1	145.1		148.5	146.1
		Test 3	148.1	144.3		147.9	146.4
144-E Tube Suction	Dry Density (pcf)	Test 1	150.8	144.2	147.6	148	Not Tested
		Test 2	148.7	142.9	148.5	148.8	
		Test 3	148.2	142.9	148.1	148.7	
	Initial Moisture	Test 1	5.6	4.9	4.9	5.8	
		Test 2	5.7	4.9	5.1	5.8	
		Test 3	5.7	4.9	5.1	5.8	
	MC after Drying	Test 1	0.4	0.2	0.4	0.1	
		Test 2	0.5	0.2	0.5	0.2	
		Test 3	0.5	0.2	0.3	0.3	
	Final MC	Test 1	4.7	4.8	5	4.8	
		Test 2	4.8	4.8	5.2	4.7	
		Test 3	4.8	4.6	5.2	4.8	
	MC Gain	Test 1	4.3	4.6	4.6	4.7	
		Test 2	4.3	4.6	4.7	4.5	
		Test 3	4.3	4.4	4.9	4.5	
	Final Dielectric	Test 1	15.9	10.1	10.8	16	
		Test 2	14.4	10	11.3	16	
		Test 3	15	8.9	12	17	
	UCS (psi)	Test 1	Not Tested	46.3	42.1	32.4	
		Test 2		49	25	38.2	
		Test 3		43.2	27.8	43.2	

Table 2.3. Results from Groesbeck Interlaboratory Tests.

Testing Laboratory			TTI	Austin M&P	Waco	Tyler	Atlanta
113-E	Max Density		133.6	134.8	131.9	132.4	135.4
	Optimum Water (%)		7.9	6.8	7.3	7.1	6.7
117-E Uncofined	Peak Stress (psi)	Test 1	19.8	46.6	31	38.7	40
		Test 2	23.8	46	30.9	36.5	47.9
		Test 3	21.6	39.5	36.8	36.3	33.2
	Dry Density (pcf)	Test 1	133.8	133.4	Not Recorded	132.8	135.3
		Test 2	131.9	132.9		133	135.9
		Test 3	133.3	132.7		132.9	134.9
117-E with 15 psi Confining	Peak Stress (psi)	Test 1	174.6	193.8	192.2	173.4	181
		Test 2	183.5	187.2	178.9	178	193.1
		Test 3	137.6	183.1	167.1	164.3	204
	Dry Density (pcf)	Test 1	132.9	132.5	Not Recorded	132.9	134
		Test 2	131.3	132.3		132.8	135.4
		Test 3	134.4	132.2		132.7	134.9
144-E Tube Suction	Dry Density (pcf)	Test 1	133	130.9	132	133.8	Not Tested
		Test 2	133.7	131.7	133.8	133.3	
		Test 3	134.8	131.6	132.7	133.3	
	Initial Moisture	Test 1	8.4	7	6.8	7	
		Test 2	8.1	6.5	6.8	7	
		Test 3	8.1	6.5	6.7	7	
	MC after Drying	Test 1	1	0.6	0.8	0.5	
		Test 2	1	0.6	1	0.6	
		Test 3	1	0.7	1.4	0.7	
	Final MC	Test 1	7.2	7.5	7.8	7	
		Test 2	6.7	7.6	7.8	7.5	
		Test 3	6.6	7.5	7.6	7.7	
	MC Gain	Test 1	6.2	6.9	7	6.5	
		Test 2	5.7	7	6.8	6.9	
		Test 3	5.6	6.8	6.2	7	
	Final Dielectric	Test 1	17.7	16	19.4	20	
		Test 2	15.7	16.9	18.3	19.9	
		Test 3	15.9	15.9	19.4	20.2	
	UCS (psi)	Test 1	Not Tested	19.9	16.1	18	
		Test 2		24.1	21.6	22.8	
		Test 3		22.1	18.3	18.2	

PRECISION STATISTICS OF TEST RESULTS

Using the data processing procedures from ASTM E 691, the precision statistics were tabulated for the following parameters for the flex bases:

- Molded dry density (Table 2.4)
- UCS after Tex-117-E (Table 2.5)
- Compressive strength with 15 psi confining pressure after Tex-117-E (Table 2.6)
- Final dielectric value after Tex-144-E (Table 2.7)
- UCS after Tex-144-E (Table 2.8)

Table 2.4. Dry Density from Tex 113-E Compaction at Optimum Moisture – Precision Statistics.

Material	X bar	S_r	S_R	r	R
Groesbeck	133.3	0.8	1.3	2.2	3.6
Spicewood	147.4	0.9	1.8	2.5	5.0

Table 2.5. UCS after Tex-117-E – Precision Statistics.

Material	X bar	S_r	S_R	r	R
Groesbeck	35.2	4.2	9.4	11.8	26.3
Spicewood	44.2	5.9	11.8	16.5	33.0

Table 2.6. Compressive Strength with 15 psi Confining Pressure after Tex-117-E – Precision Statistics.

Material	X bar	S_r	S_R	r	R
Groesbeck	179.5	13.9	16.8	38.9	47.0
Spicewood	248.3	20.2	31.1	56.6	87.1

Table 2.7. Final Dielectric Value after Tex-144-E – Precision Statistics.

Material	X bar	S_r	S_R	r	R
Spicewood	13.1	0.7	3.2	1.8	8.9
Groesbeck	18.2	0.8	1.8	2.2	5.0

Table 2.8. UCS after Tex-144-E – Precision Statistics.

Material	X bar	S_r	S_R	r	R
Groesbeck	20.1	2.6	2.7	7.3	7.6
Spicewood	38.6	6.4	9.0	17.9	25.2

IMPACT HAMMER CALIBRATION RESULTS

To evaluate one potential source of variation in compaction among the different laboratories, efforts were made to develop a technique to calibrate the impact hammer used for Tex-113-E compaction. Most of TxDOT's impact hammers are the Rainhart model, where the hammer-tamping foot rotates within the soil specimen. Because of this rotation, the load is not centered in the cylinder mold, and therefore it is difficult to measure the load of each hammer drop at the different point of impact locations. Also, the load is related to the stiffness of the soil specimen, so normally each drop will create a different compaction load. Due to these factors, directly calibrating based on load is not a good way to calibrate the compaction hammer.

For calibration, TTI tried an accelerometer device to measure the movement of the hammer. These efforts focused on measuring the velocity of the hammer since the velocity determines the energy the hammer will transfer to the soil specimen. By determining a detailed displacement and velocity curve, all the important information about the compaction hammer device is obtained. Furthermore, the hammers are currently calibrated based on drop height (displacement).

Hardware Setup

Figure 2.1 shows the hardware setup for calibrating the compaction hammer. The accelerometer is glued to the top of the hammer, and a conditioning amplifier is used for signal conditioning. Signal conditioning includes the following to process the signal:

- Amplify the signal for easy to read and processing.
- Integrate the acceleration signal to get the velocity signal.
- Filter the signal.

The filtered signal is sent to a connection box, then a cable sends the signal to a computer through a high-speed data acquisition card.

Because the compaction hammer working frequency is low, a special accelerometer is used. In this research TTI used a Brüel & Kjær model 4370v. This accelerometer has a very low frequency measurement range from 0.1Hz to 4800Hz, and the accelerometer weighs 1.9 oz. For data acquisition researchers used a National Instrument DAQ card 6062E, which has a maximum data acquisition rate of 500K samples per second. Data resolution is 12 bit for a 20 voltage range. TTI coded special data acquisition software to collect the test data. Normally, 10 or more cycles (or drops) are collected.

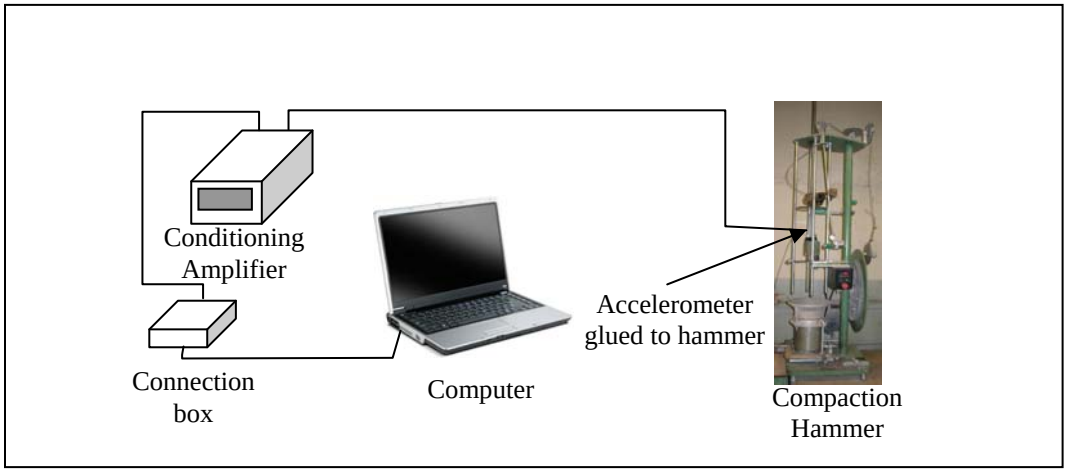

Figure 2.1. Hardware Setup for Impact Hammer Calibration.

Data Analysis

Figure 2.2 shows typical test results from one cycle of the hammer. Velocity was recorded through the output of the signal conditioner and the displacement obtained by integration of the velocity data. This figure shows the following information:

- Velocity when hammer touches the soil sample.
- Hammer drop height.
- Period or the time for one cycle of hammer drop.

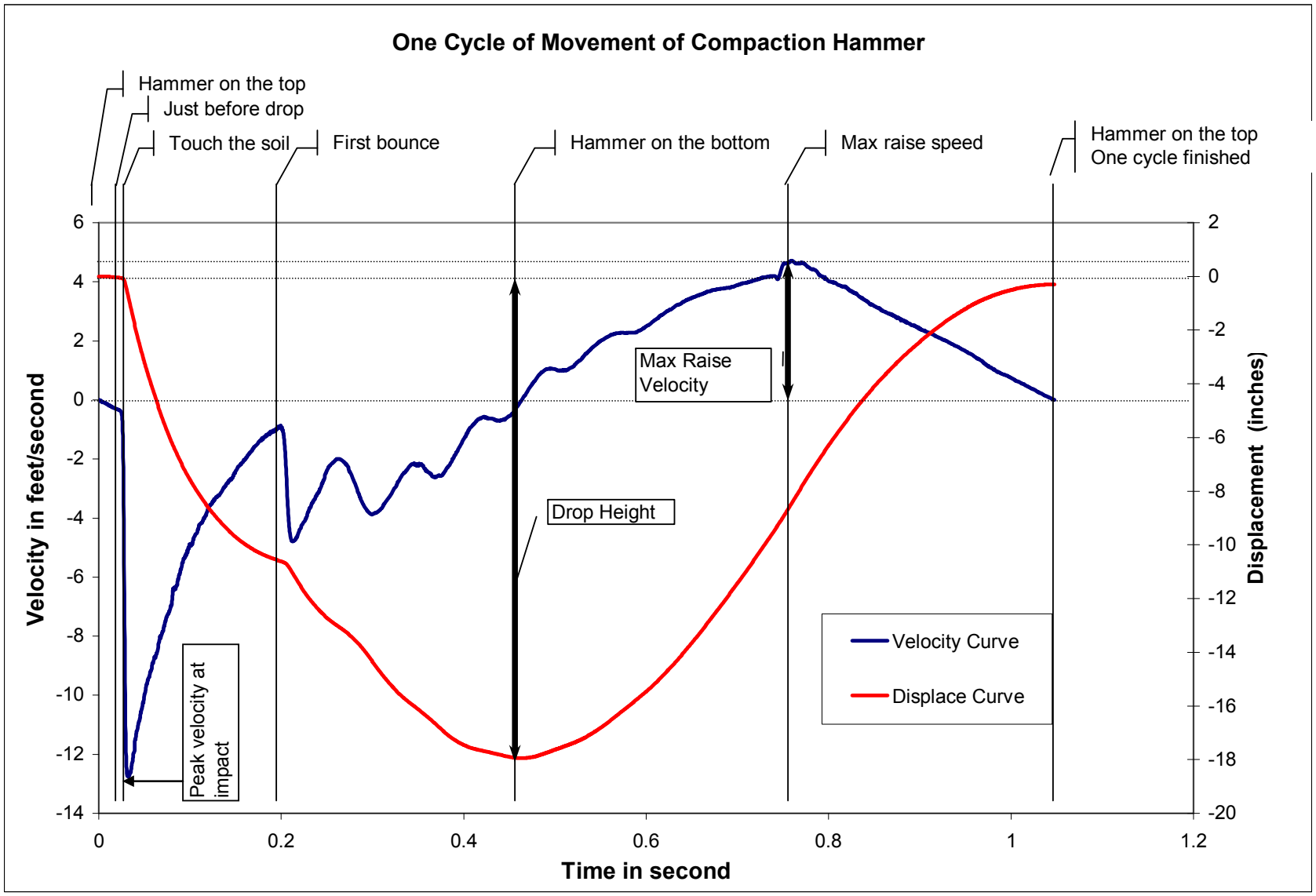

Figure 2.2. Typical Compaction Hammer Movement Curve.

Test Summary

On February 27, 2006, TTI tested compaction hammers at the Austin M&P lab, and the Waco, Atlanta, and Tyler District labs. The Austin lab was the first hammer tested, and the accelerometer's conditioning amplifier was set too sensitive resulting in the test data being beyond the limits of the system. Therefore, these data are not presented here.

Waco Lab Results

Waco uses a Ploog compaction hammer as shown in Figure 2.3. The accelerometer was glued to the side of the hammer shaft. Figure 2.4 shows the measured hammer velocity and displacement from nine consecutive drops. For displacement, the reference location is at the top. When the hammer drops to the specimen, the displacement becomes negative.

Figure 2.3. Impact Hammer at Waco District Lab.

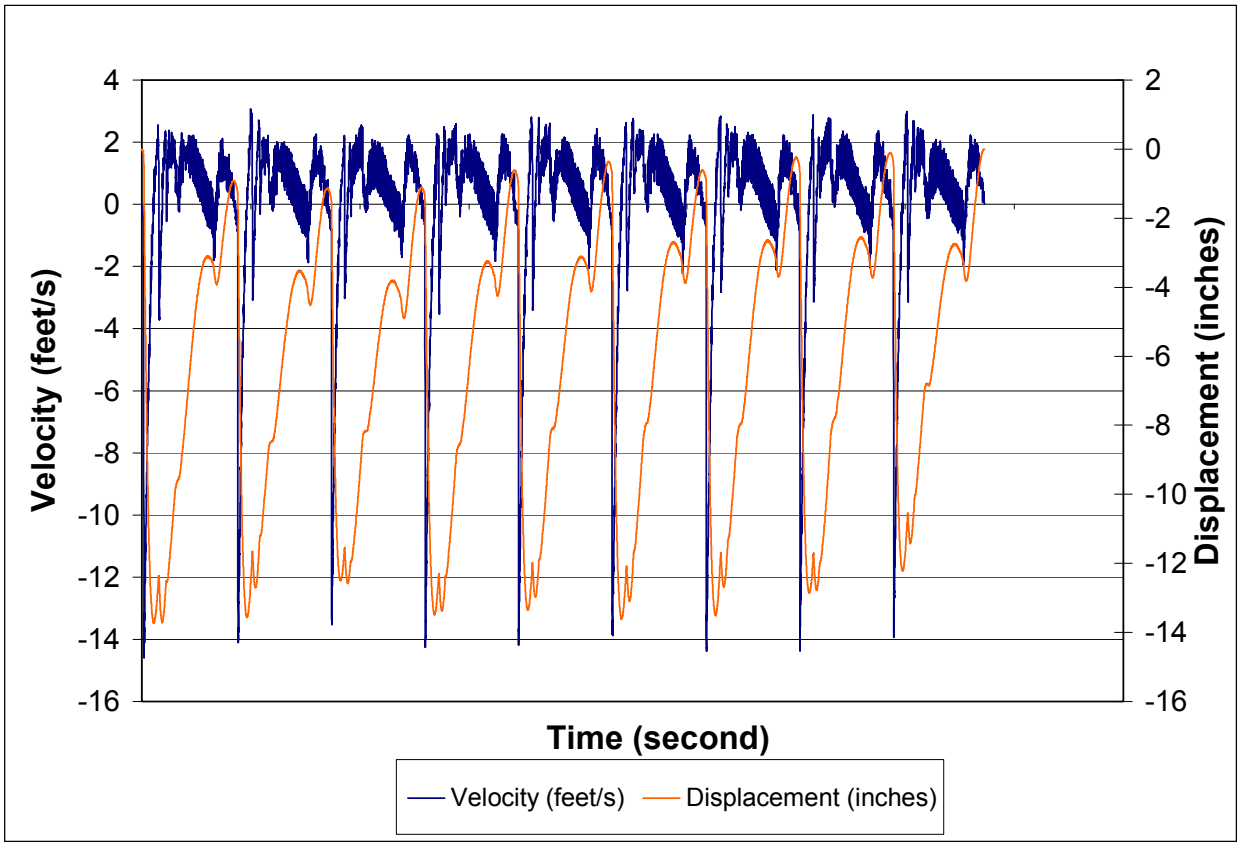

Figure 2.4. Results from Waco District Lab.

Table 2.9 presents the key results from Figure 2.4. The velocity presented is the value just before the hammer impacts the material, and this velocity is the maximum velocity in each cycle. From this table, researchers noticed that the drop heights are related to the velocity; also the velocity value does not vary as much as displacement (velocity variation is 2.2 percent and the drop height variation is 6.2 percent). When the test was performed, the drop height was set to 18 inches, but the average drop height measured by the sensor is only 12 inches. This difference may be due to the fact that the hammer's frequency range is not covered by the sensor's frequency range.

Table 2.9. Results from Waco Compaction Hammer Testing.

Drop #	Velocity (feet/s)	Drop Height (inches)
1	14.56201	13.19291
2	14.00131	12.00394
3	13.52067	10.57087
4	14.19357	11.75197
5	14.17749	11.95276
6	13.87303	12.57441
7	14.32152	12.39173
8	14.35367	11.95669
9	13.88911	11.3815
σ	0.312846	0.740905
Average	14.09915	11.9752
σ/Average (%)	2.22%	6.19%

Atlanta Lab Results

Atlanta uses the Rainhart compaction hammer as shown in Figure 2.1. The accelerometer was directly glued to the top of the hammer as Figure 2.5 shows. Figure 2.6 presents the recorded velocity and displacement curve from eight consecutive drops. Table 2.10 lists the analysis results. Table 2.10 also presents the period for one cycle of hammer movement, which averages 1031.7 milliseconds. The average measured drop height was 18.960 inches, and the average maximum velocity was 12.837 feet/s. Because the tamper apparatus releases the hammer from the top location, the hammer will drop to the specimen by the earth's gravity. Because the drop height is 18.96 inches, the theoretical velocity at the end of the drop (or just before the hammer touches the soil specimen) can be calculated by the following equation:

$$v = \sqrt{2sg}$$

In this equation, s is the drop height of 1.58 feet, and g is the earth's gravity acceleration. The calculated velocity is about 10.1 feet/s, and this value is close to the measured value of 12.837 feet/s. As Table 2.10 shows, the variation of the drop height is about 11.8 percent, much larger than the test result from Waco which was about 6.2 percent.

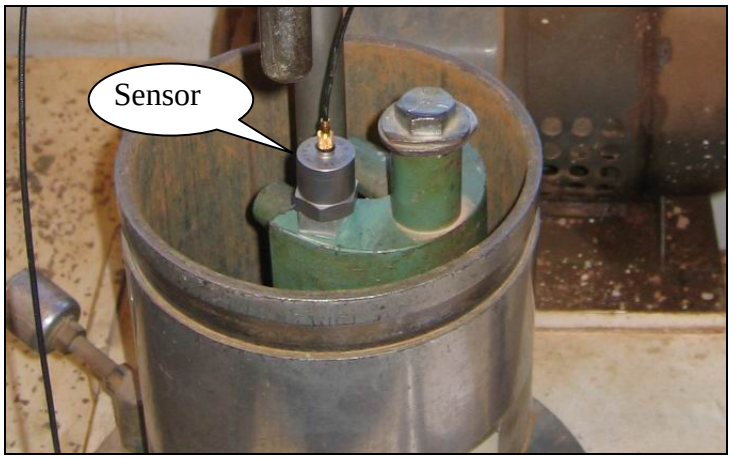

Figure 2.5. Accelerometer Attached to Top of Rainhart Impact Hammer.

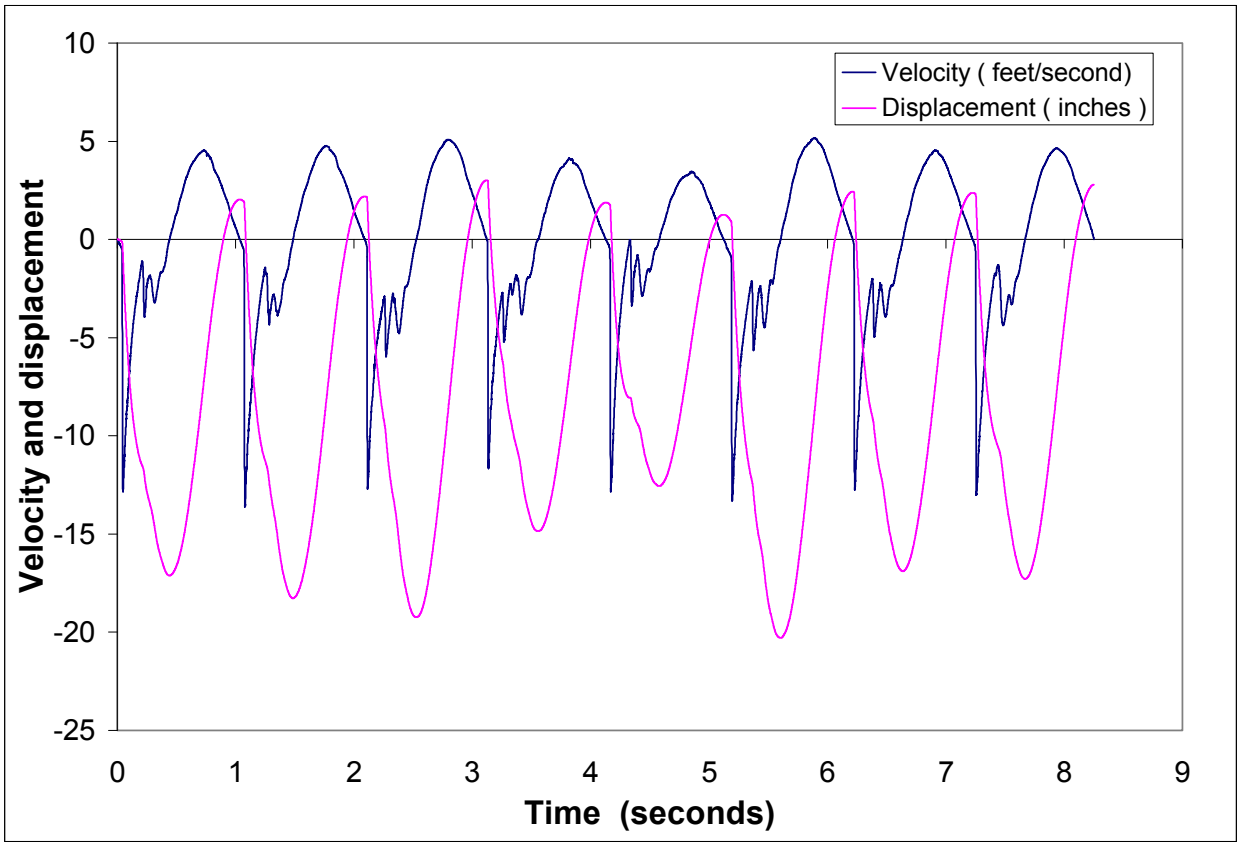

Figure 2.6. Results from Atlanta District Lab.

Table 2.10. Results from Atlanta Compaction Hammer Testing.

Drop #	Period (ms)	Velocity (feet/s)	Drop Height (inches)
1	1035.0	12.837	17.114
2	1055.5	13.633	20.307
3	1031.5	12.704	21.425
4	1005.0	11.599	17.862
5	996.0	12.852	14.437
6	1091.0	13.309	21.547
7	1012.0	12.748	19.331
8	1027.5	13.014	19.657
Average	1031.7	12.837	18.960
σ	28.5	0.553	2.244
σ/Average (%)	2.76	4.31	11.83

Tyler Lab Results

Tyler also uses the Rainhart compaction hammer and the accelerometer was glued directly to the top of the hammer (Figure 2.5). TTI performed the same tests as in Atlanta and recorded eight drops of hammer velocity. The drop height was obtained by integrating the velocity data. Figure 2.7 presents the data from the Tyler apparatus. Table 2.11 presents the results for each drop cycle. The average drop height of Tyler's compaction hammer was close to 18 inches (19.124 inches), and the drop height was more consistent than Atlanta (Tyler has a drop height variation of 3.1 percent and Atlanta's was 11.8 percent). The average maximum drop velocity is 13.1 feet/s. The period is around 1 second, and the period data has very small variation (0.5 percent).

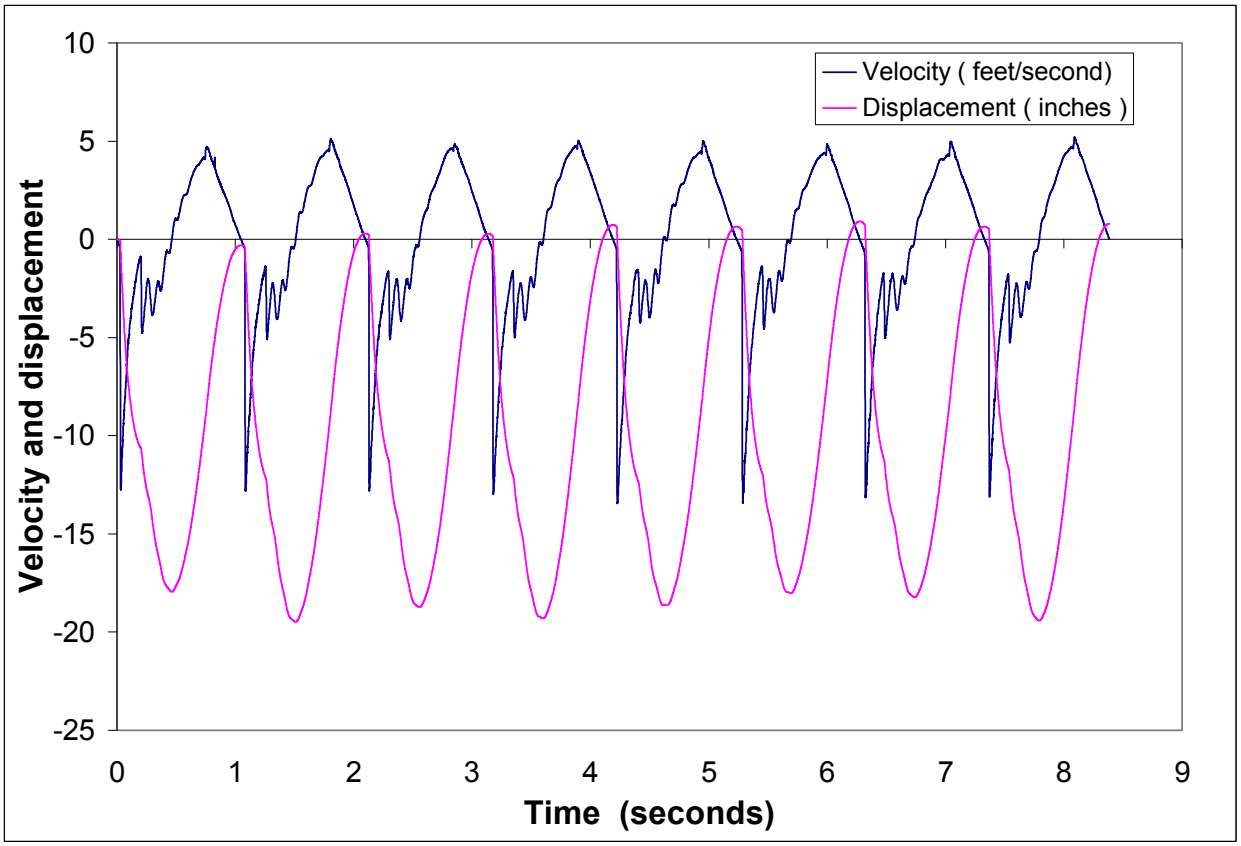

Figure 2.7. Results from Tyler District Lab.

Table 2.11. Results from Tyler Compaction Hammer Testing.

	Period	Velocity	Drop Height
Drop #	(ms)	(feet/s)	(inches)
1	1047.5	12.763	17.945
2	1051.0	12.808	19.189
3	1041.0	12.793	19.035
4	1050.5	12.970	19.579
5	1044.5	13.441	19.366
6	1041.0	13.412	18.657
7	1053.0	13.117	19.146
8	1056.5	13.117	20.075
Average	1048.1	13.053	19.124
σ	5.278	0.252	0.591
σ/Average (%)	0.504	1.928	3.088

Comparison of Three Systems

Tables 2.12 and 2.13 compare results from the Waco, Atlanta, and Tyler compaction hammers. Figure 2.8 illustrates each hammer's variation result. These data indicate Tyler's hammer is performing the best because it has the lowest variation in both drop height and velocity at point of impact.

Table 2.12. Comparison of Max Velocity Results.

		Waco	Atlanta	Tyler
Average	ft/s	13.88911	12.837	13.053
σ	ft/s	0.312846	0.553	0.252
σ/Average	%	14.09915	4.31	1.928

Table 2.13. Comparison of Drop Height Results.

		Waco	Atlanta	Tyler
Average	ft/s	11.3815	18.960	19.124
σ	ft/s	0.740905	2.244	0.591
σ/Average	%	11.9752	11.83	3.088

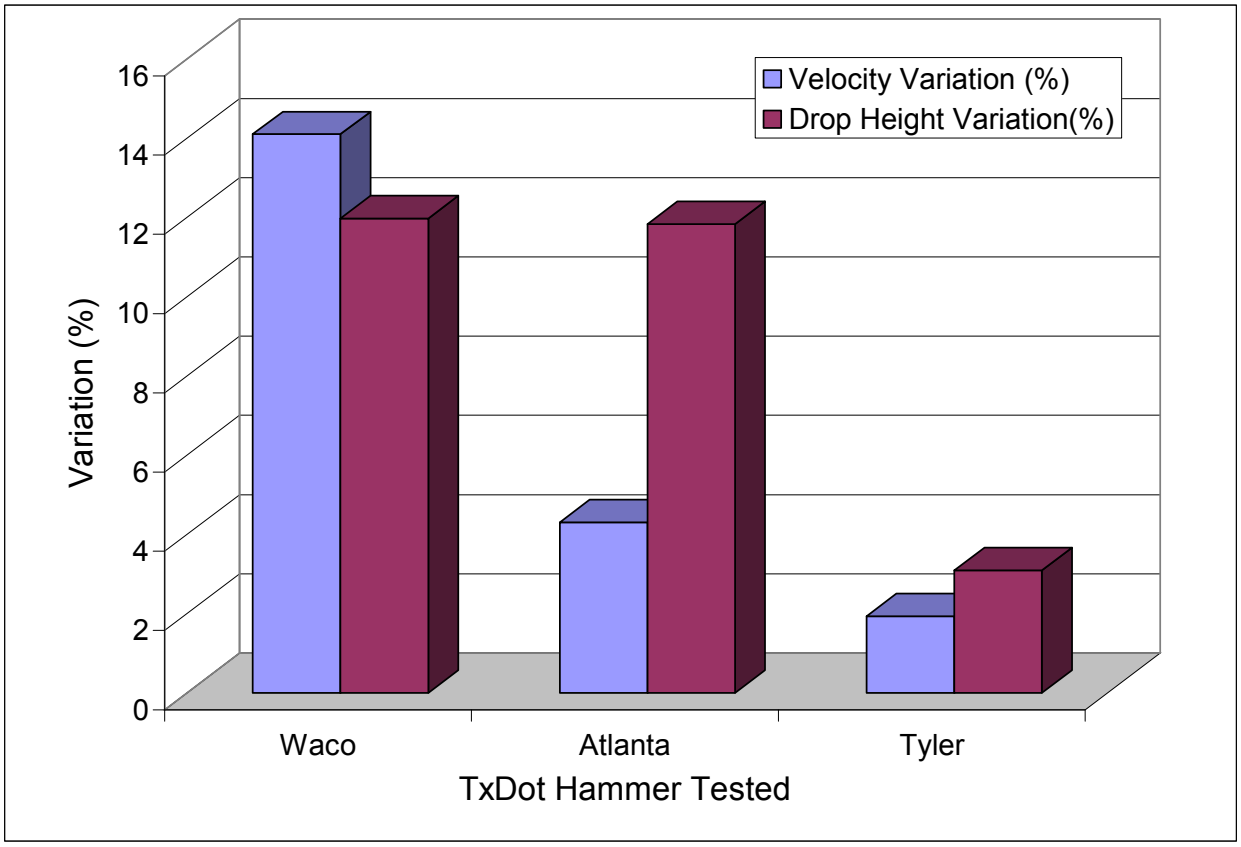

Figure 2.8. Variation Results for Each Impact Hammer Tested.

Figure 2.9 presents a bar chart of each hammer's velocity and drop height. Normally these three hammers are all set to 18 inches drop height. Errors result in measurement because the accelerometer system employed for these pilot tests does not have static measurement capability. This topic will be discussed further in the next section.

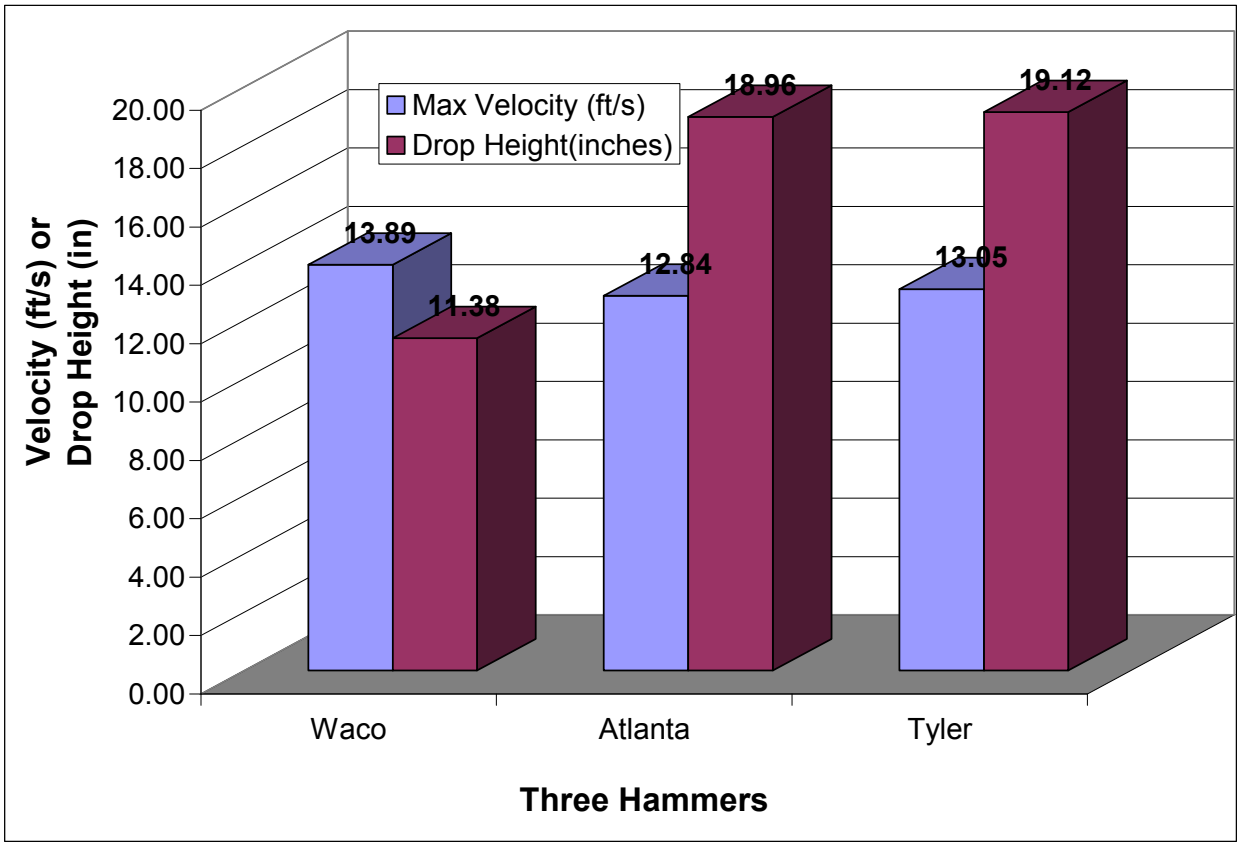

Figure 2.9. Comparison of Each Hammer's Velocity and Drop Height.

Discussion of Impact Hammer Calibration Results

The Brüel & Kjær accelerometer model 4370v used in these tests measures low frequencies in the range from 0.1Hz to 4800Hz. However, in the operation of the impact hammers, two instances occur where the hammer is static. The hammer is static at its highest point when its direction of travel is changing, and the hammer is static after it impacts the specimen and awaits the catch mechanism to lift it again. The accelerometer used in these pilot tests cannot measure static movement. Due to this reason, this calibration system is not a very accurate system. It can only roughly calibrate the compaction hammer. While it is believed the velocity at point of impact is reasonable, the system is not believed adequate for checking drop height. This problem is very apparent with the Ploog tamper used at the Waco District lab.

To improve the utility of this calibration system, TTI proposes investigation of the following options:

- Use of a static accelerometer to capture the static vibration.

- Use of a load cell to directly measure the load. The load time history will be related to the compaction condition of the specimen, so a standard material which can not be compacted must be used as a specimen for calibrating purpose.
- Use of laser or other techniques to make a non-contact measurement of hammer movement. However at present, this type of equipment is still expensive.
- For improved consistency in the test environment, a special high damping rubber is needed to simulate a specimen. This rubber can not be compacted but has damping properties that prevent the hammer from bouncing excessively.

CONCLUSIONS

The interlaboratory tests conducted provide numerical quantification as to the current level of variability in test results from several common TxDOT methods used for base materials. A first step in obtaining more precise test specimens is more precise calibration of the impact hammer compactors used to prepare samples. The concept system tested in this project, with further refinement, should be able to provide the improved calibration method. Further work in this project should develop this system into an implementable form for TxDOT use.

CHAPTER 3

EVALUATION OF ALTERNATIVE LAB COMPACTION PROCEDURES

SUMMARY

In efforts to improve the relationship between laboratory compaction and field compaction, prototype lab preparation methods were studied. The potential need for different lab preparation methods arises due to the potential impact on lab-measured properties from the spatial variability and soil fabric that the particular lab compaction technique produces. A review of alternative lab compaction methods for both bases and soils was undertaken and is described in this chapter. With the input of the project director, this project then focused on evaluating laboratory vibratory compaction with base materials. Results showed that for both bases evaluated, vibratory lab compaction resulted in improved triaxial strength properties as measured in Tex-117-E, improved moisture susceptibility rankings as measured by Tex-144-E, and improved rutting characteristics as measured with the VESYS pavement performance model.

ALTERNATIVES TO IMPACT HAMMER LAB COMPACTION

Several alternative lab compaction methods exist. These methods include: static, vibratory, gyratory, and kneading. The reason other lab methods may be more appropriate is because laboratory impact hammer compaction may not adequately replicate the spatial variability of particles and the soil fabric of field compaction.

Spatial Variability

TxDOT test specimens are compacted in lifts of approximately 1.5 in. for soils and 2 in. for base. Field construction rarely involves such thin layers. Although diligent scarification between layers in the lab is employed, unrealistic inter-layer barriers can result, particularly with clayey soils. For example, Figure 3.1 shows a soil (PI = 24; 77% passing #200) specimen after triaxial testing. During compressive loading, each lift failed separately in a progression from top to bottom, clearly not the intended result of the test.

Figure 3.1. Soil Specimen after Triaxial Testing.

TxDOT recently initiated efforts to evaluate the moisture susceptibility of materials through the Tube Suction Test, Tex-144-E. Lift interfaces resultant from traditional compaction methods can impede the hydraulic contact between lifts to the extent that results from tests involving capillary soak conditions may not represent expected field performance with some materials. Sebesta, et al. (2004) showed instances where layer interfaces from impact hammer compaction impeded the ability of laboratory swell tests to replicate expected field performance. Figure 3.2 shows how specimens prepared with impact hammer compaction separated at the lowest lift boundary, resulting in extensive swell in the bottom lift and virtually no swell in the top lifts.

Figure 3.2. Layer Separation in Swell Test of Specimen Compacted in Lifts with Impact Hammer Compaction (Sebesta, et al. 2004).

Impact hammer compaction can clearly impart inter-layer barriers within test specimens, but evidence also exists that variations exist within layers. It is well understood that building test specimens by impact compaction in lifts results in density variations even within each lift (Witczak 2004, Holtz and Kovacs 1981). Witzak (2004) notes that these within-lift density variations can influence the results of modulus testing.

Soil Fabric

In addition to spatial variability within samples, the soil fabric can significantly influence the engineering properties of the soil. Mitchell (1993) states that remolding or compacting a soil will affect the pre-existing fabric at constant water content by breaking down flocculated aggregations, destroying shear planes, eliminating large pores, and producing a more homogeneous fabric (on a macroscopic scale). He also states that compaction technique can impart a preferred orientation to platy soil particles.

Kirkpatrick and Rennie (1973) remolded samples of kaolin using various molding techniques and studied the resulting fabrics. They determined that molding water content and method of remolding greatly affected soil fabric. They also state there is no advantage in using methods of preparation unless the structure of the sample can be related clearly to the structure of the soil in the field. Hoeg, et. al. (2000) similarly concluded that when reconstituting specimens, simply satisfying correct density and particle size distribution is not sufficient: the soil fabric must be reproduced or analyses based on results of reconstituted specimens may be misleading. More recent investigations attributed poor correlations between field behavior and lab specimen performance to differences in particle orientation as a result of laboratory molding techniques (Weibiao and Hoeg 2002).

Potential new Lab Compaction Methods

Since the literature indicates alternative lab compaction techniques may be needed to better relate the lab to the field, a review of alternative methods was conducted. Four alternative methods exist: static compression, vibratory, gyratory, and California kneading. Static compression was eliminated because it does not simulate any commonly used field construction compaction techniques. The kneading compactor is thought to simulate sheepsfoot and pneumatic rollers and has been recommended for use on soils. However, based on availability of equipment in Texas and the input of the project monitoring committee, this project evaluated the use of a laboratory vibratory compactor for bases. Figure 3.3 shows the prototype lab vibratory compactor.

Figure 3.3. Prototype Lab Vibratory Compactor.

TESTING PROGRAM

The primary focal point of the research work with alternative lab compaction was on the flex bases. The same Spicewood and Groesbeck flex bases described in Chapter 1 were used for evaluating the vibratory compaction method. In the vibratory compactor, specimens were mixed and placed in four lifts just as in the drop hammer method. On each lift, the vibrating motor was operated for 10 seconds. For each base and for each compaction method, the following data

were collected to evaluate the results from the vibratory compaction technique as opposed to Tex-113-E:

- Moisture-density relationship
- Texas Triaxial Class with Tex-117-E conditioning
- Tube Suction Test (TST) (Tex-144-E)
- Laboratory Seismic Modulus (at optimum, after drying, and after capillary wetting stages of Tex-144-E)
- Permanent Deformation at optimum moisture content (OMC)

RESULTS FROM TESTING

Moisture-Density Relationship

Figures 3.4 and 3.5 illustrate the moisture-density relationships of the Tex-113-E curves and the vibratory curves for the Spicewood and Groesbeck material, respectively. With the lab vibratory technique used, the maximum density for Spicewood was 151.0 pcf at 5.3 percent water. For Groesbeck, these values were 133.7 pcf at 8.0 percent water. Some observations from these data are:

- The vibratory curve most nearly matches the modified compaction curve with the Spicewood aggregate.
- With the Groesbeck material, the vibratory curve produced a maximum density and optimum water content essentially identical to Tex-113-E.
- The data appear to indicate that the shape of the vibratory curve may better replicate the shape of the field curve. For example, Figure 3.5 illustrates that when dry of optimum, the dry density achieved with laboratory vibratory compaction declines rapidly, similar to the field curve. Although still not as sensitive to moisture content as the field, the lab vibratory curve is less forgiving than the 113-E curve with respect to water content.

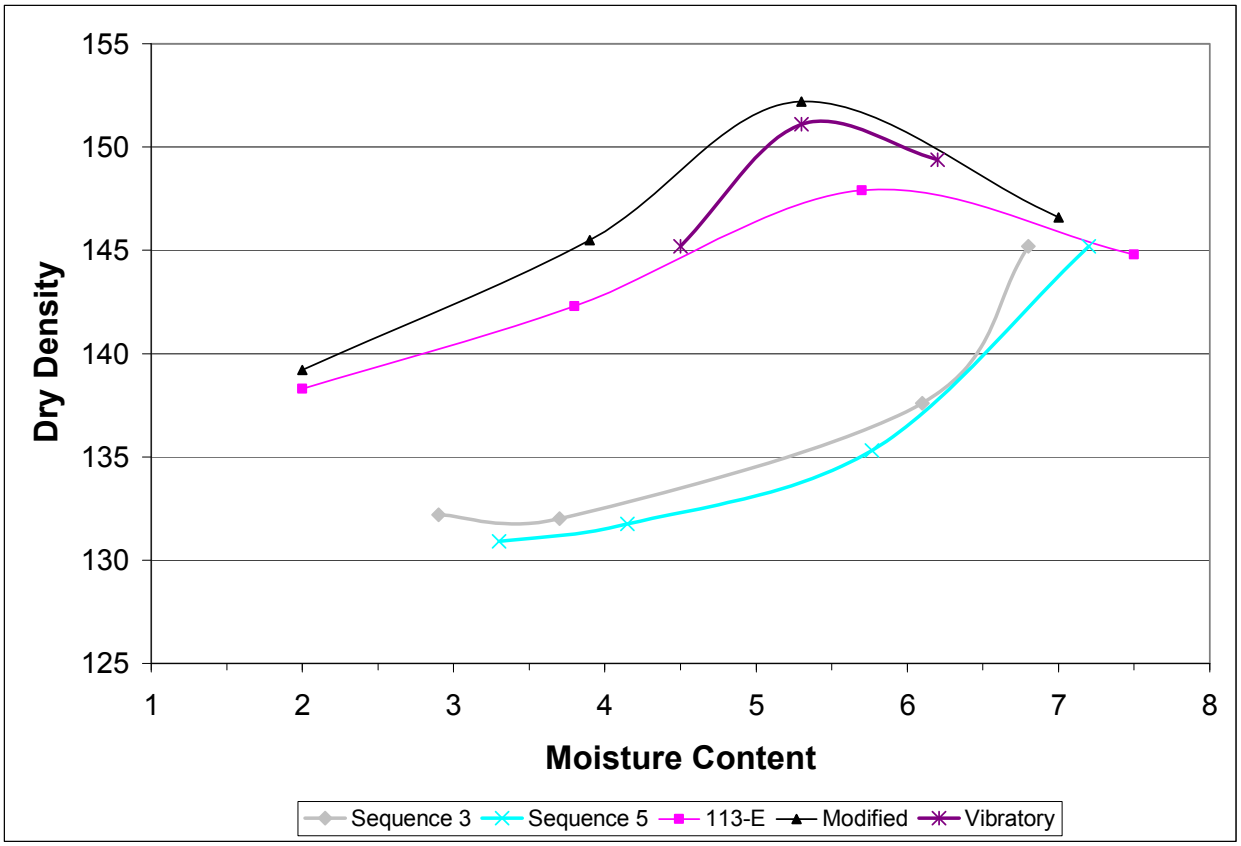

Figure 3.4. Spicewood Moisture-Density Relationships.
Note: Sequence 3 and Sequence 5 are field curves presented in Chapter 1.

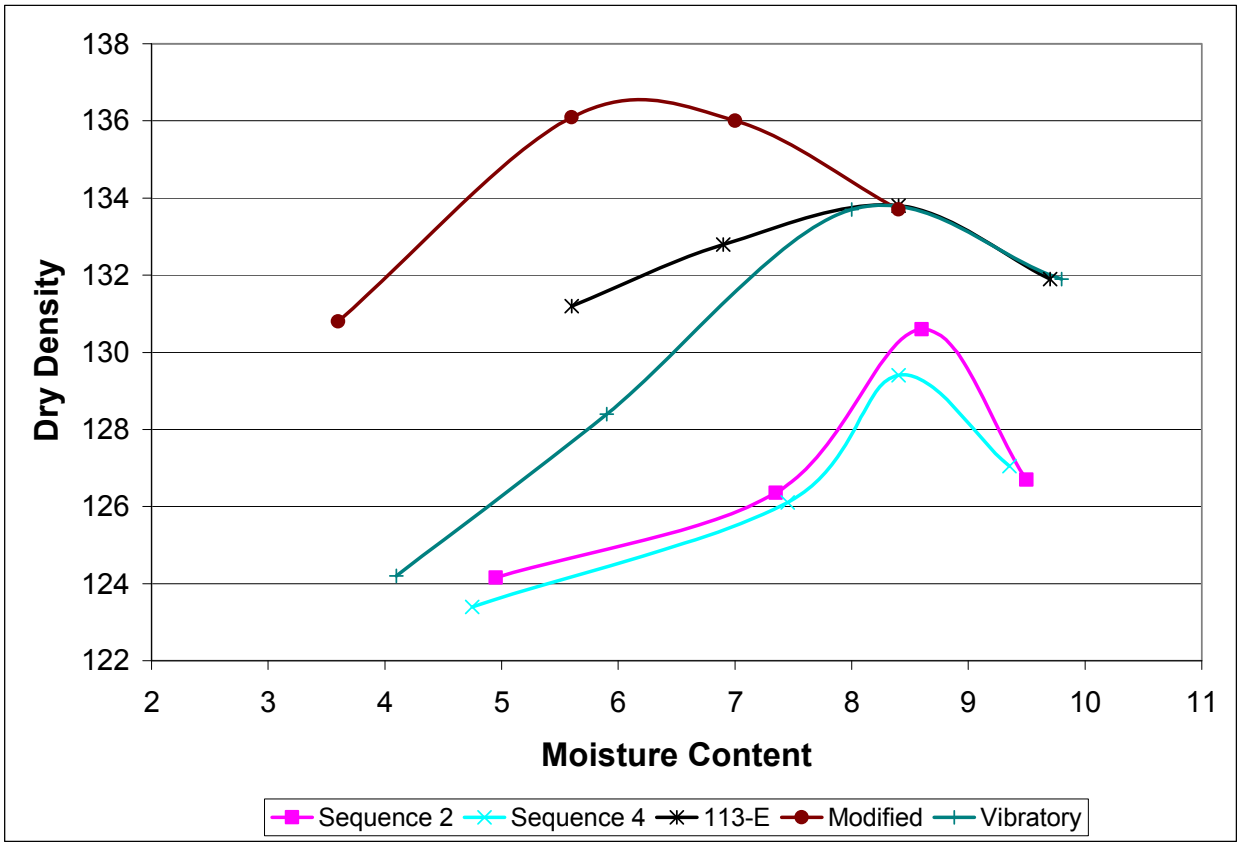

Figure 3.5. Groesbeck Moisture-Density Relationships.
Note: Sequence 2 and Sequence 4 are field curves presented in Chapter 1.

Triaxial Test Results

The research team performed triaxial tests in triplicate for both 113-E and vibratory lab compaction methods. For the Spicewood material, Table 3.1 summarizes the results from the vibratory specimens, and Table 2.2 contains the results from all the specimens prepared with Tex-113-E. The results of all three Spicewood replicates are classified as Texas Triaxial Class 1. Figure 3.6 shows the measured cohesion and angle of internal friction of the vibratory results in comparison with the 113-E results for Spicewood. Statistical tests revealed that at the 95 percent confidence level, specimens prepared with vibratory compaction had higher cohesion. No significant difference in the angle of internal friction existed among the two compaction techniques with this material.

Table 3.1. Spicewood Triaxial Results from Specimens Compacted with Vibratory.

Sample ID	Molding Moisture (%)	Dry Density (pcf)	Molded Ht (in)	Moisture after drying (%)	Moisture after capillarity (%)	Confining Pressure (psi)	Total Load (lb)	Extension (in)	UCS (psi)
SV 1	5.3	149.3	7.95	2.5	4.7	0	2235	0.16	77.5
SV 2	5.3	147.5	8.05	2.7	4.8	7	5554	0.21	191.3
SV 3	6.2	146.9	8	3.7	5.6	0	1149	0.13	40.0
SV 4	5.4	149.5	7.95	2.3	4.7	5	6041	0.35	204.3
SV 5	5.6	151.6	8.05	2.9	4.7	3	5729	0.36	193.6
SV 6	5.3	148.4	8	2.8	4.7	15	8451	0.31	287.4
SV 7	8.1	145.1	8	5.4	7.4	10	6408	0.51	212.2
SV-14	5.2	148.6	8.025	1.9	4.4	0	3161	0.13	110.0
SV-15	5.3	148.7	8	2.1	4.5	3	4559	0.15	158.2
SV-16	5.4	149.5	7.95	2.1	4.7	0	1965	0.13	68.4
SV-17	5.5	149.7	7.95	2.3	4.8	10	7210	0.22	248.0
SV-18	5.4	150.0	7.95	2.1	4.6	15	8824	0.26	301.9
SV-19	5.5	149.6	7.975	2.2	4.7	7	5237	0.22	180.1
SV-20	5.4	149.8	7.95	2.0	4.7	5	5056	0.29	172.3
SV-21	5.4	150.2	7.95	2.1	4.7	0	2689	0.17	93.1
SV-22	5.5	149.9	7.95	2.2	4.8	5	5751	0.28	196.3
SV-23	5.4	149.8	8	1.9	4.6	3	4365	0.2	150.5
SV-24	5.4	149.9	8	2.1	4.8	7	6086	0.3	207.2
SV-25	5.4	149.6	8	0.0	4.7	10	7730	0.26	264.5
SV-26	5.4	149.6	8	0.0	4.7	15	8803	0.33	298.5
SV-27	5.3	149.5	8.05	2.0	4.7	0	1595	0.12	55.6

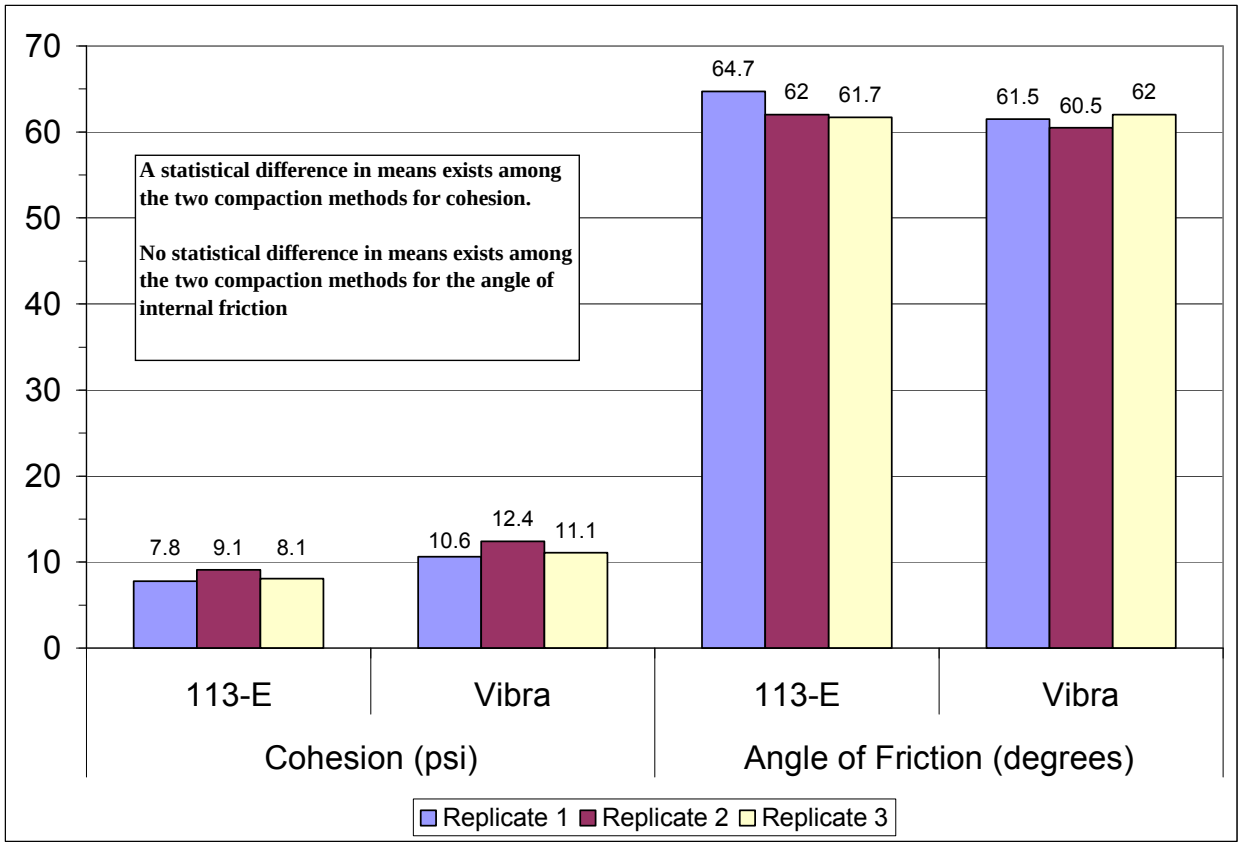

Figure 3.6. Cohesion and Angle of Internal Friction for Spicewood with 113-E and Vibratory Compaction.

Table 3.2 presents the results of the triaxial test specimens prepared with the prototype vibratory compactor for the Groesbeck material. Table 2.3 contains the 113-E results for this material. Figure 3.7 shows the cohesion, angle of internal friction, and Texas triaxial classification results for the Groesbeck specimens. At the 95 percent confidence level, statistical tests show that vibratory compaction of this material resulted in higher cohesion and improved Texas triaxial class.

Table 3.2. Groesbeck Triaxial Results from Specimens Compacted with Vibratory.

Sample ID	Molding Moisture (%)	Dry Density (pcf)	Molded Ht (in)	Moisture after drying (%)	Moisture after capillarity (%)	Confining Pressure (psi)	Total Load (lb)	Extension (in)	UCS (psi)
GV-1	8.5	132.6	8.05	6.1	7.4	0	946	0.15	32.8
GV-2	8.5	133.7	8	6.3	7.5	0	990	0.12	34.5
GV-3	8.4	132.6	8.05	5.8	7.2	3	2197	0.23	75.5
GV-4	8.5	133.3	8	6.2	7.7	5	2544	0.21	87.6
GV-5	8.6	134.1	7.95	6.4	7.5	7	3149	0.26	107.7
GV-6	8.3	133.6	8	6.2	7.3	10	3797	0.24	130.3
GV-7	8.4	133.7	7.95	6.1	7.5	15	4821	0.37	162.6
			0					0	
GV-8	8.3	133.4	8.05	6.4	7.4	0	941	0.12	32.8
GV-9	8.3	134.0	7.95	6.2	7.4	0	875	0.13	30.4
GV-10	8.4	133.5	7.975	6.0	7.3	3	1920	0.2	66.2
GV-11	8.3	134.4	7.95	6.3	7.2	5	2532	0.21	87.2
GV-12	8.3	134.4	7.975	5.9	8.1	7	3000	0.32	101.9
GV-13	8.4	133.6	8	5.8	7.4	10	3785	0.29	129.0
GV-14	8.4	133.5	8	5.9	7.1	15	4807	0.32	163.2
GV-15	8.4	134.0	8	5.6	6.8	0	741	0.17	25.7
GV-16	8.4	133.9	8	5.3	6.6	0	867	0.5	28.8
GV-17	8.3	134.4	8	5.7	6.8	3	2138	0.25	73.3
GV-18	8.7	133.4	8	6.0	7.1	5	2404	0.32	81.6
GV-19	8.4	134.0	8	5.9	6.9	10	3728	0.32	126.6
GV-20	8.4	134.1	8	5.8	6.9	15	4366	0.31	148.5
GV-21	8.4	134.2	8	5.8	7.5	7	3014	0.38	101.6

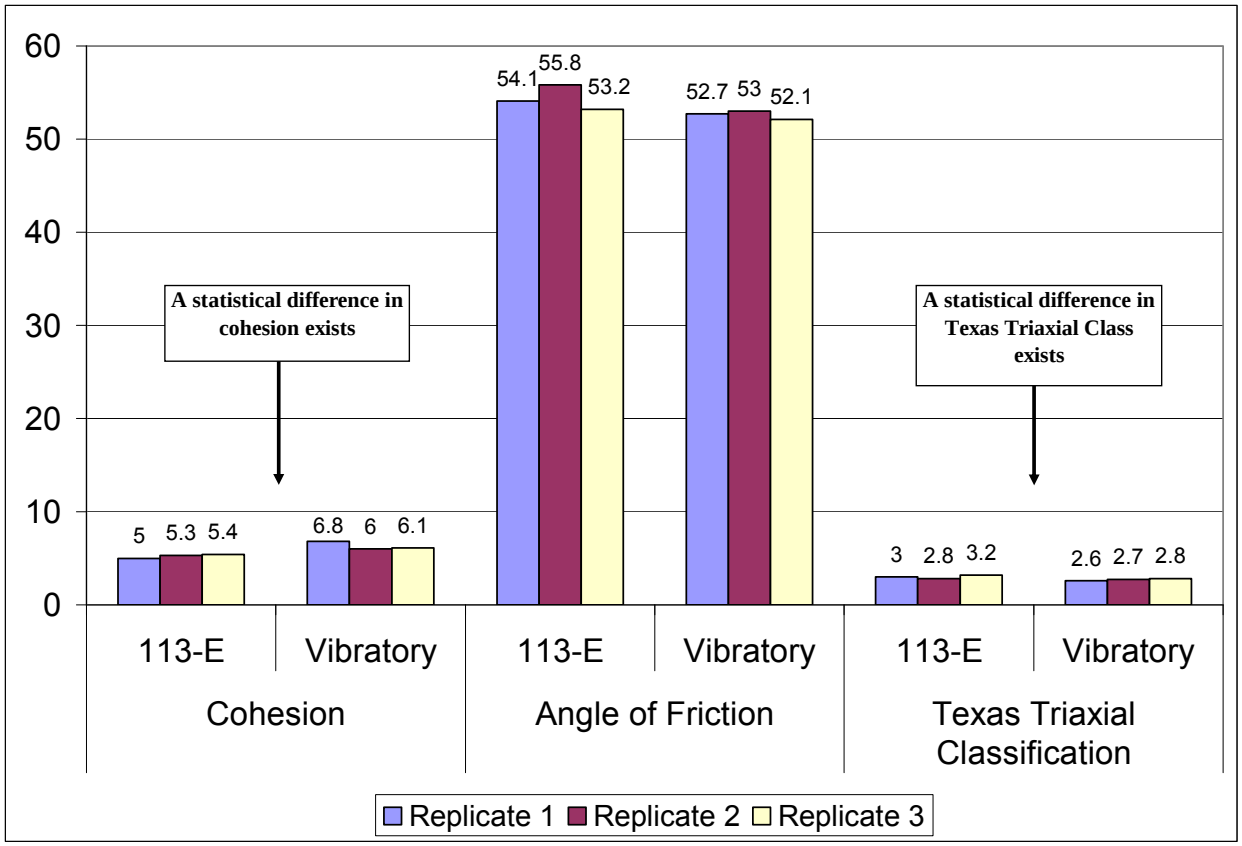

Figure 3.7. Cohesion, Angle of Internal Friction, and Texas Triaxial Classification for Groesbeck with 113-E and Vibratory Compaction.

Tube Suction Test Results

With each base material, six specimens were tested in the capillary rise conditions of Tex-144-E using both compaction techniques. Figure 3.8 shows the dielectric results from the Spicewood aggregate. There is a clear outlier in each data set, which was eliminated from further analysis. Table 3.3 presents the key test results from Tex-144-E for the Spicewood material. The results show a reduction in the final dielectric value when vibratory compaction is used.

Figure 3.9 shows the results from the Groesbeck material. Table 3.4 presents key test results, which show that vibratory compaction with this material resulted in reduced final water content and a lower final dielectric value.

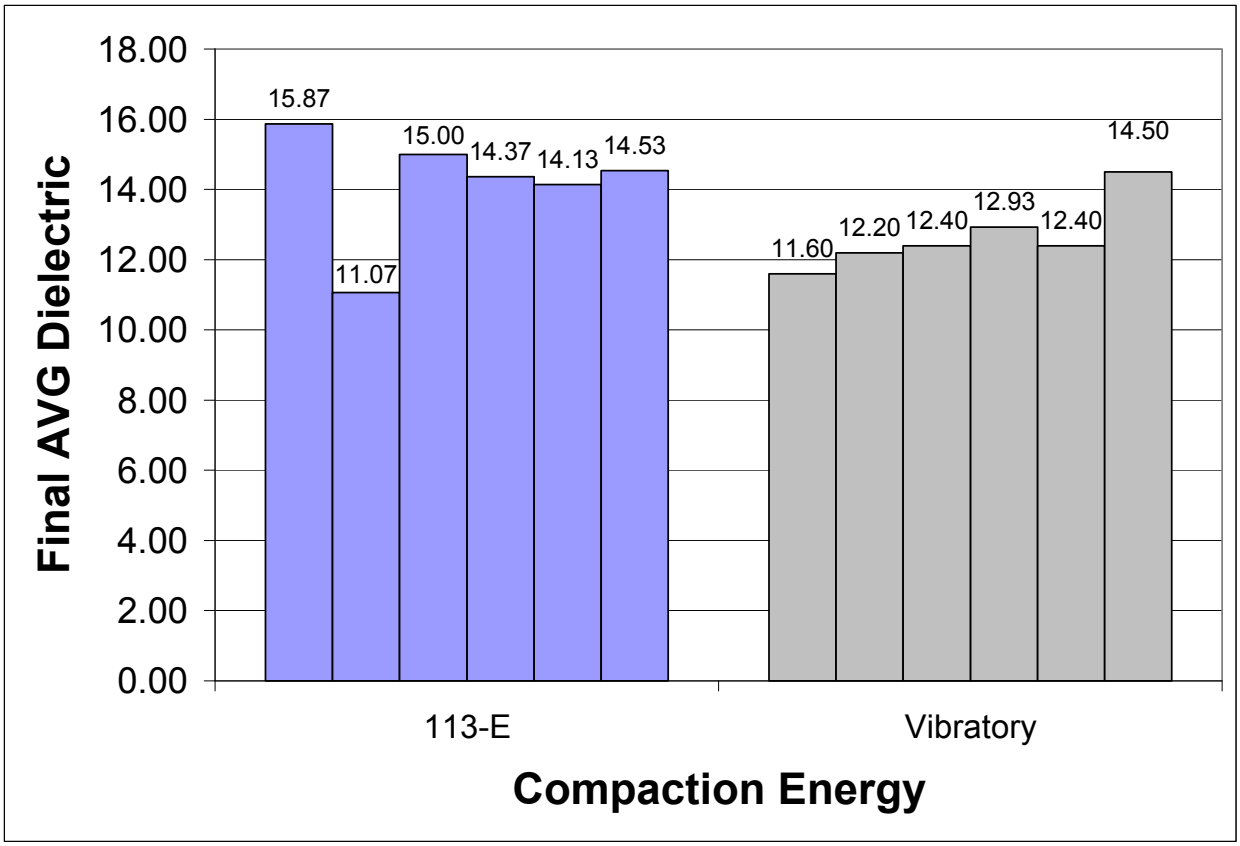

Figure 3.8. Final Dielectric Values for Spicewood 113-E and Vibratory Samples.

Table 3.3. Spicewood Tex-144-E Results for 113-E and Vibratory Compaction.

Replicate	AVG Dielectric		Initial M.C. after Drying		Final M.C. after Capillary Soak		M.C. Loss During Drying		M.C. Gain During Soak	
	113-E	Vibratory	113-E	Vibratory	113-E	Vibratory	113-E	Vibratory	113-E	Vibratory
1	15.87	11.60	0.43	1.42	4.71	4.45	5.17	5.09	4.27	3.02
2	15.00	12.20	0.49	0.42	4.75	4.48	5.19	4.89	4.26	4.06
3	14.37	12.40	0.46	0.40	4.80	4.10	5.25	4.86	4.34	3.70
4	14.13	12.93	0.82	0.41	4.77	4.55	5.16	5.01	3.96	4.14
5	14.53	12.40	0.46	0.45	4.85	4.56	5.30	5.00	4.39	4.11
Mean	14.78	12.31	0.53	0.62	4.78	4.43	5.21	4.97	4.24	3.81
Variance	0.47	0.23	0.03	0.20	0.00	0.04	0.00	0.01	0.03	0.22
Hartley's Test	2.04		7.73		12.47		2.46		7.96	
H-Critical (95% Confidence)	7.15		7.15		7.15		7.15		7.15	
Decision	*Conclude equal variance*		*Conclude unequal variance*				*Conclude equal variance*		*Conclude unequal variance*	
P-Value one-tail T-test	0.000		0.350		0.006		0.001		0.054	
Decision	*Conclude means differ*		*Conclude means are equal*		*Conclude means differ*		*Conclude means differ*		*Conclude means are equal*	

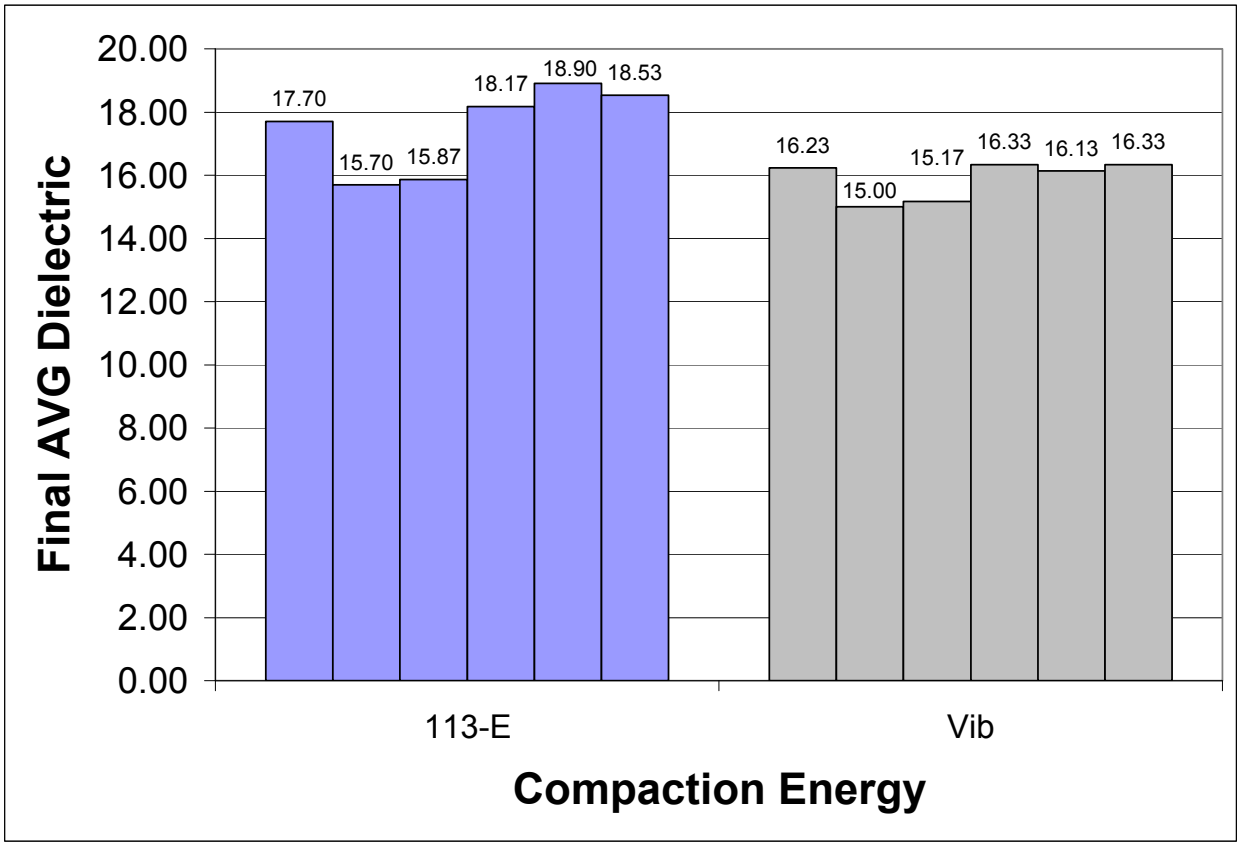

Figure 3.9. Final Dielectric Values for Groesbeck 113-E and Vibratory Samples.

Table 3.4. Groesbeck Tex-144-E Results for 113-E and Vibratory Compaction.

Replicate	Avg Dielectric		Initial M.C. After Drying		Final M.C. after Capillary Soak		M.C. Loss During Drying		M.C. Gain During Soak	
	113-E	Vib	113-E	Vib	113-E	Vib	113-E	Vib	113-E	Vib
1	17.70	16.23	1.02	1.23	7.25	6.14	7.41	7.26	6.23	4.91
2	15.70	15.00	0.96	1.09	6.70	6.16	7.18	7.41	5.73	5.07
3	15.87	15.17	1.00	1.03	6.62	6.39	7.12	7.40	5.62	5.36
4	18.17	16.33	1.03	1.09	7.52	6.65	7.37	7.36	6.50	5.56
5	18.90	16.13	0.97	1.18	7.59	6.80	7.41	7.35	6.62	5.62
6	18.53	16.33	0.99	1.13	7.32	6.84	7.47	7.41	6.33	5.71
Mean	17.48	15.87	1.00	1.12	7.17	6.50	7.33	7.37	6.17	5.37
Variance	1.88	0.38	0.00	0.01	0.17	0.10	0.02	0.00	0.17	0.10
Hartley's Test	5.00		8.18		1.74		6.72		1.60	
H-Critical (95% Confidence)	7.15		7.15		7.15		7.15		7.15	
Decision	*Conclude equal variance*		*conclude unequal variance*		*conclude equal variance*					
P-Value one-tail T-test	0.01		0.00		0.01		0.27		0.00	
Decision	*conclude means differ*		*conclude means differ*		*conclude means differ*		*conclude means equal*		*conclude means differ*	

Laboratory Seismic Modulus Results

Figures 3.10 and 3.11 present the average seismic modulus values for the Spicewood and Groesbeck materials, respectively. With the Spicewood aggregate, specimens compacted in the lab with vibratory compaction exhibited a higher seismic modulus value both after drying and after conditioning in Tex-144-E. With the Groesbeck material, lab vibratory compaction resulted in a higher seismic modulus value at all moisture states tested.

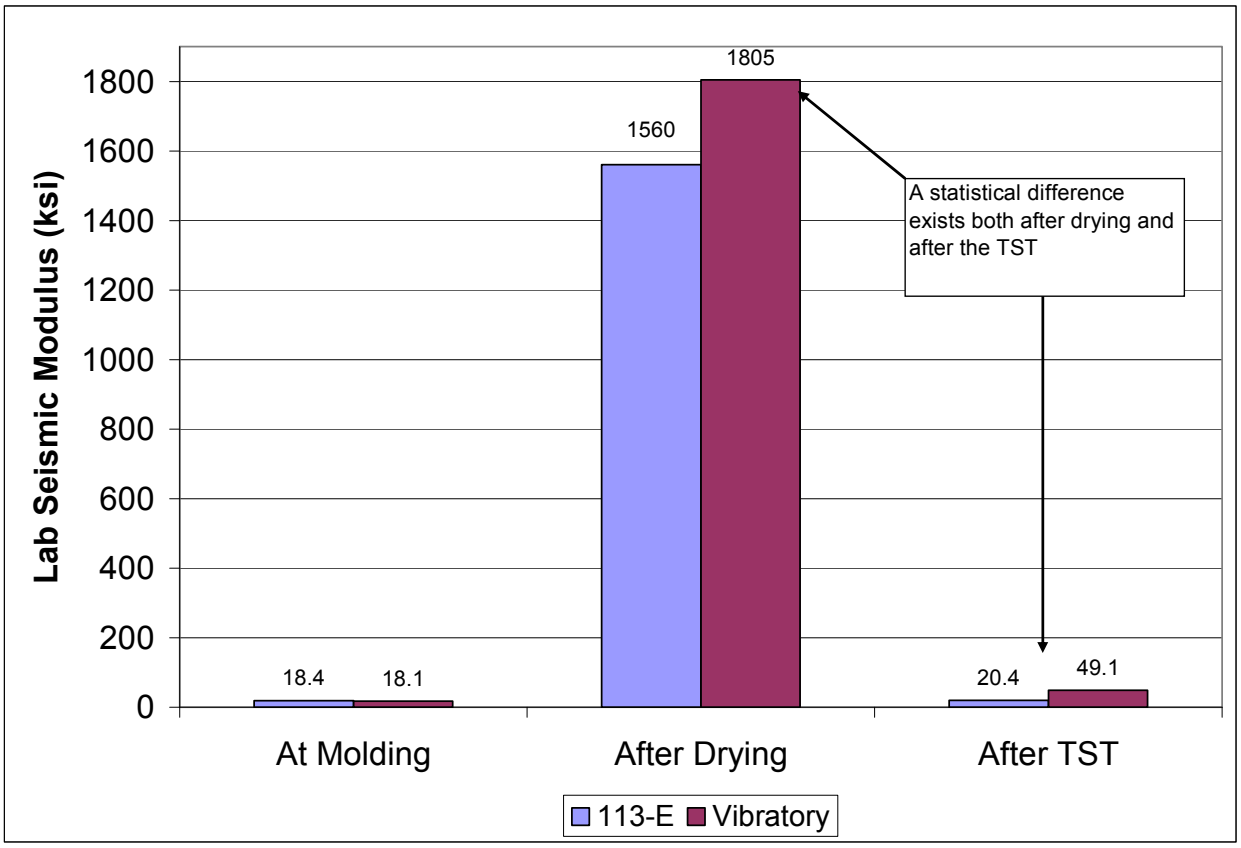

Figure 3.10. Lab Seismic Modulus of Spicewood from 113-E and Vibratory Compaction.

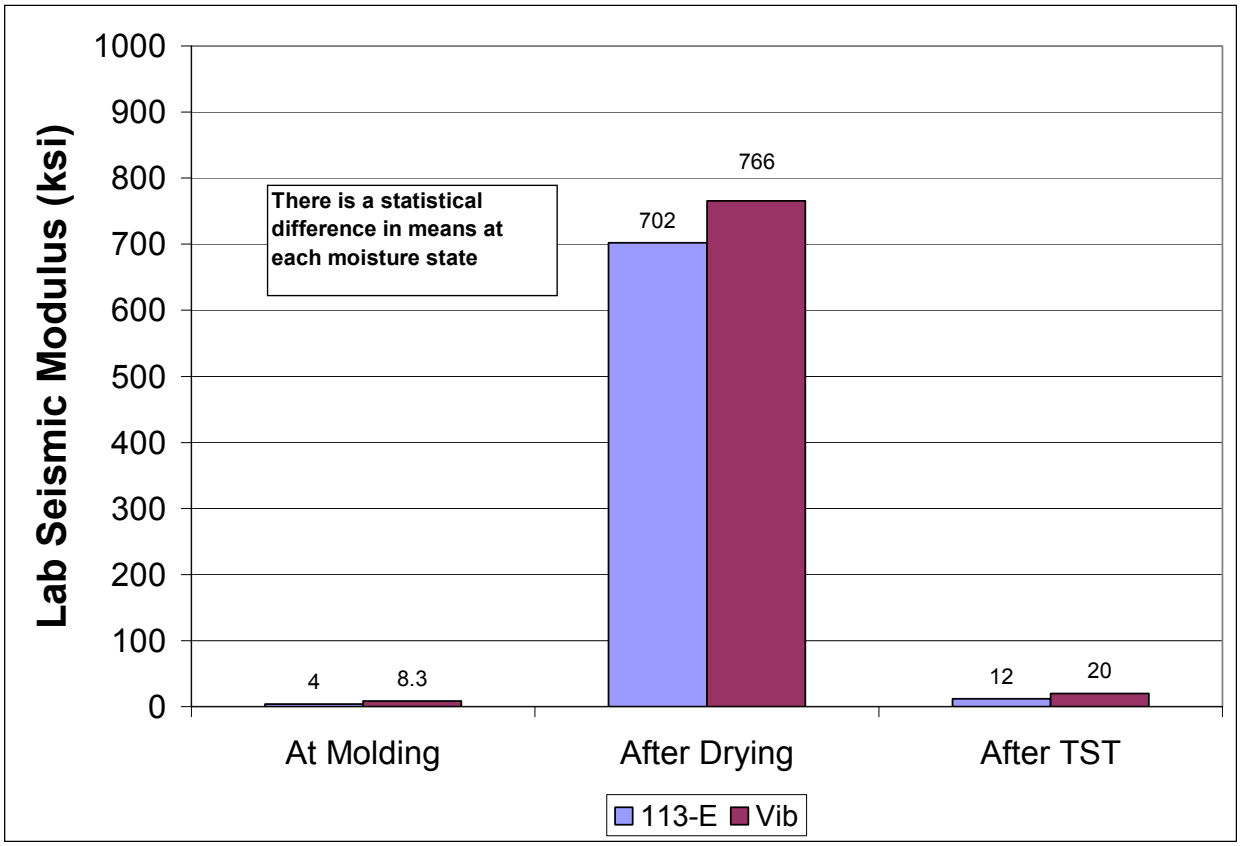

Figure 3.11. Lab Seismic Modulus of Groesbeck from 113-E and Vibratory Compaction.

Permanent Deformation Results

Because of the current interest in mechanistic-empirical pavement design methods, testing sequences to determine rutting parameters necessary for inputs in the VESYS pavement analysis program were performed in triplicate using both vibratory and impact hammer compaction on both the Spicewood and Groesbeck flex bases. Huang (1993) provides a summary of how the rutting parameters are developed, and Zhou and Scullion (2004) describe in detail the laboratory procedure used to develop these rutting parameters.

Figure 3.12 illustrates representative permanent deformation test results for the Spicewood aggregate. With the Groesbeck material, two of the 113-E specimens quickly accumulated permanent deformation, resulting in the measurement LVDTs reaching their measurement limit of approximately 3 percent strain extremely early in the test. Figure 3.13 contrasts results from a representative vibratory and 113-E- prepared Groesbeck specimen. Tables 3.5 and 3.6 summarize the permanent deformation test results for all specimens tested. Most notable is the fact that vibratory compaction resulted in a reduction in the μ parameter of more than 50 percent for both bases tested. This would have the effect of reducing the predicted amount of rutting by more than 50 percent at any given load repetition.

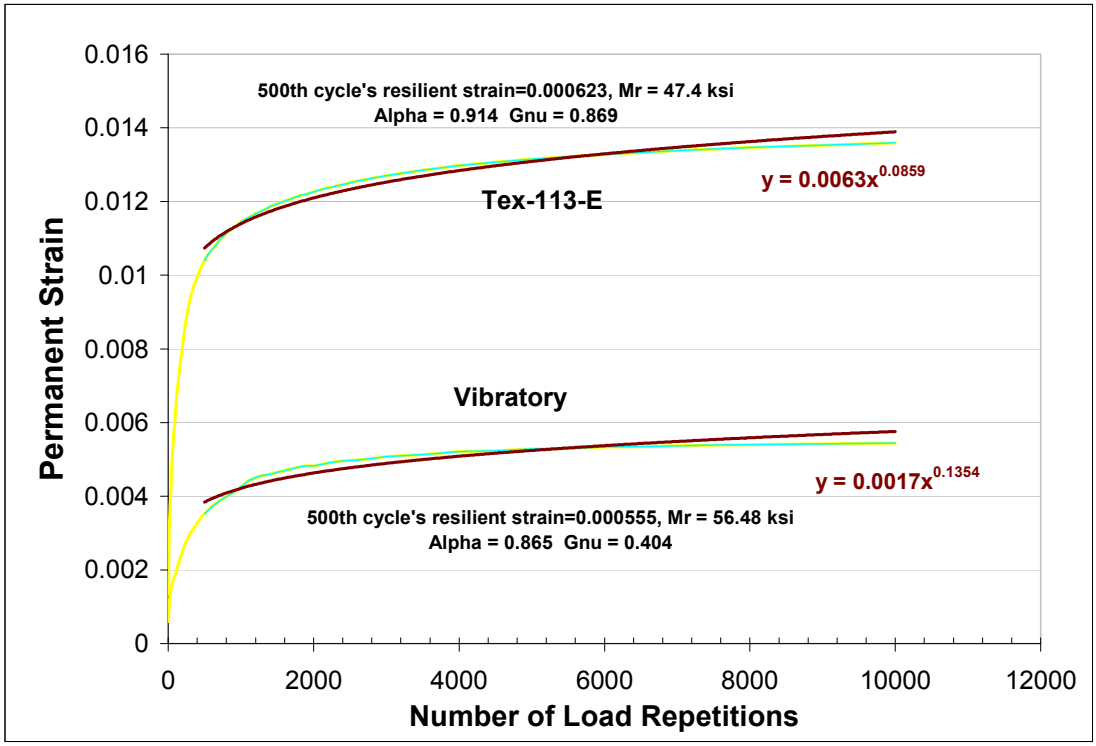

Figure 3.12. Example Permanent Deformation Results for Spicewood Base at Optimal Moisture Content.

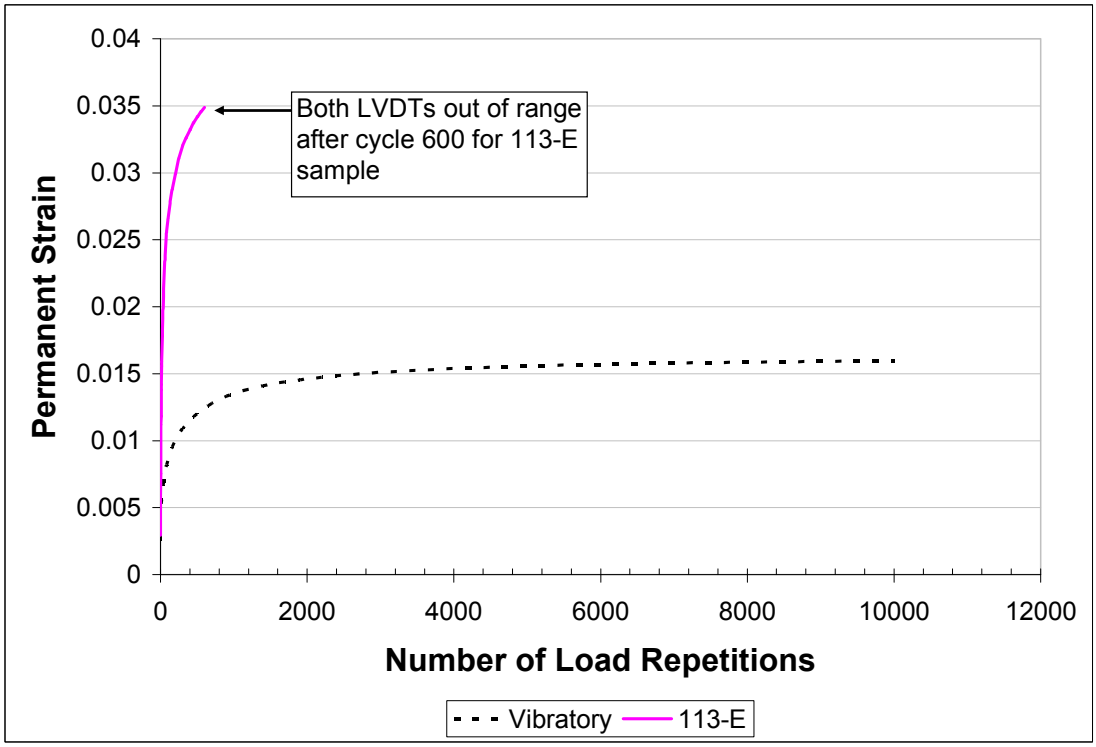

Figure 3.13. Representative Data from Groesbeck Permanent Deformation Tests.

Table 3.5. Permanent Deformation Results at Optimal for Spicewood Base.

Specimen	500th Cycle Resilient Strain	Resilient Modulus (ksi)	Rutting Parameter α	Rutting Parameter μ
113-E #1	0.000573	52.6	0.924	1.186
113-E #2	0.000776	38.8	0.875	1.005
113-E #3	0.000623	47.4	0.914	0.869
Vibratory #1	0.000555	56.5	0.865	0.404
Vibratory #2	0.000429	66.5	0.899	0.476
Vibratory #3	0.000629	48.4	0.895	0.535
AVG 113-E	**0.000657**	**46.3**	**0.904**	**1.020**
AVG Vibratory	**0.000538**	**57.1**	**0.886**	**0.472**

Table 3.6. Permanent Deformation Results at Optimal for Groesbeck Base.

Specimen	500th Cycle Resilient Strain	Resilient Modulus (ksi)	Rutting Parameter α	Rutting Parameter μ
113-E #1*				
113-E #2	0.000565	55.8	0.943	1.724
113-E #3**	0.000528	58.3	0.859	3.80
Vibratory #1	0.000592	52.3	0.911	1.026
Vibratory #2	0.000617	52.3	0.911	1.047
Vibratory #3	0.000580	51.4	0.936	0.484
AVG 113-E	**0.000547**	**55.6**	**0.901**	**2.76**
AVG Vibratory	**0.000596**	**52.0**	**0.919**	**0.852**

* No reasonable result available because LVDT 1 reached measurement limit of ~ 3 percent strain after 118 cycles and LVDT 2 reached measurement limit at 229 cycles.
** Results obtained from cycle 200 through 600 because after cycle 600 both LVDTs reached their maximum measurement range of ~ 3 percent strain.

To more thoroughly illustrate the difference in permanent deformation properties obtained from the different compaction methods, VESYS 5W was used to compare pavement performance predictions for a "dummy" pavement. To investigate the base layer performance, the pavement layers used were 0.5 inches of Type D HMA over 10 inches of granular base on a sandy subgrade. The default materials properties were used for the HMA and the subgrade. For the Spicewood base, t-tests showed no significant difference in means among the compaction methods for the base resilient modulus or the alpha rutting parameter. Therefore, these values were set by averaging the average values from each compaction technique, resulting in a resilient modulus value of 51.7 ksi and the alpha rutting parameter of 0.895. Statistical tests did reveal a significant difference in means for the μ rutting parameter; therefore the respective average value from each compaction method was used when performing the analysis. Using a simple repeated load input of an 18 kip single axle, VESYS 5W produced rutting predictions for the bases as illustrated in Figure 3.14. The predicted rutting in the base layer with the 113-E lab results is approximately double the predicted rutting using the results from lab vibratory compaction.

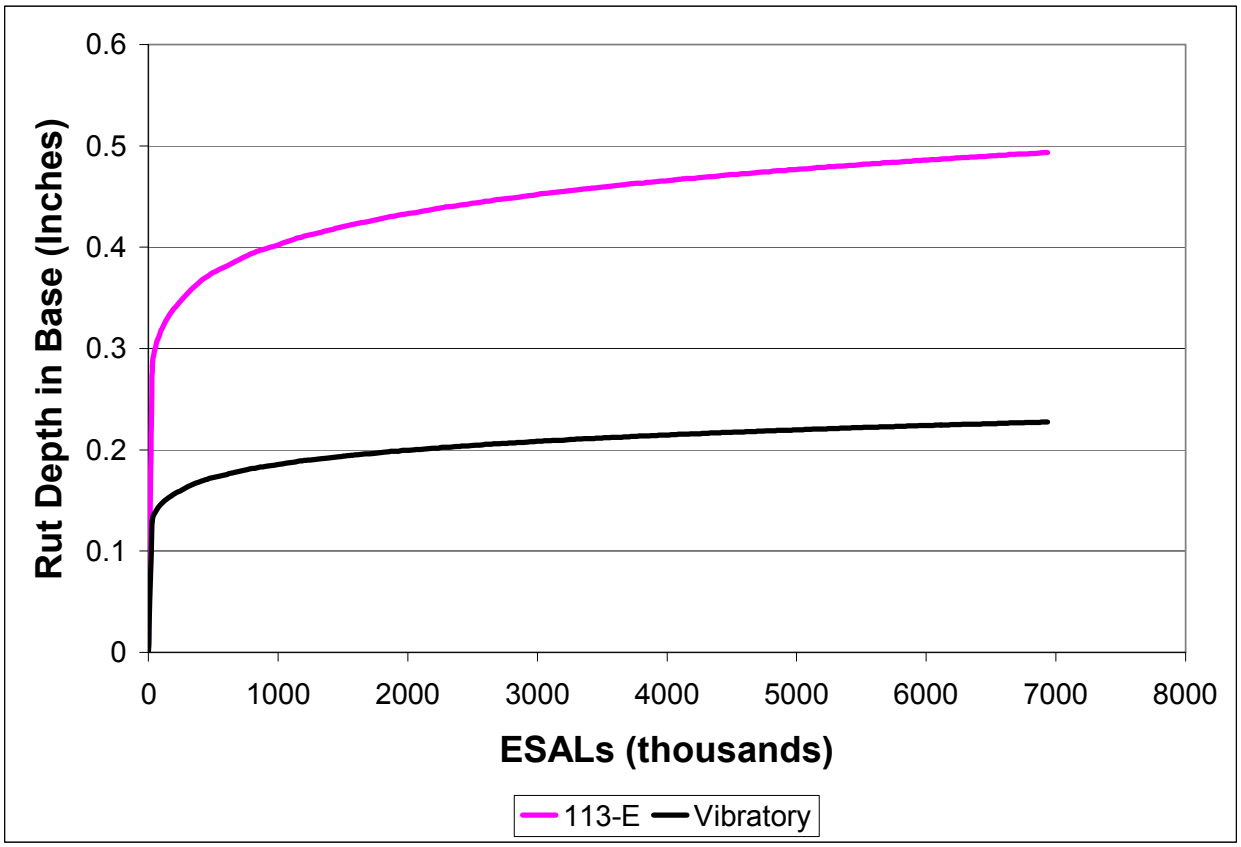

Figure 3.14. Predicted Base Rutting from VESYS Rut Parameters Obtained with 113-E and Vibratory Lab Compaction for Spicewood Base.

With the Groesbeck base, the average resilient modulus value of 53.8 ksi and the average alpha parameter of 0.912 were used in VESYS 5W along with the appropriate μ parameter for the compaction method being investigated. The same "dummy" pavement as described previously was employed for the other inputs. Figure 3.15 shows the VESYS predicted base rutting from the parameters measured with the two compaction methods for the Groesbeck base.

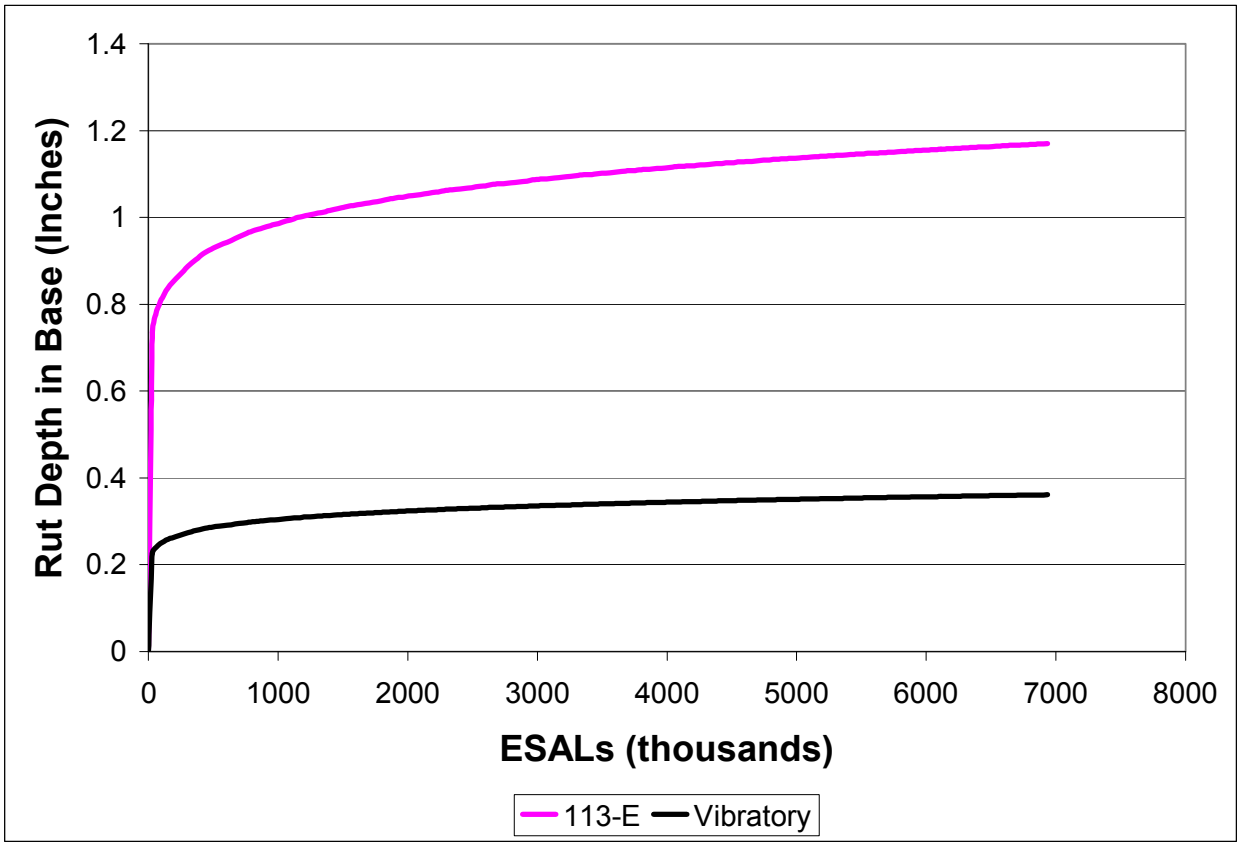

Figure 3.15. Predicted Base Rutting from VESYS Rut Parameters Obtained with 113-E and Vibratory Lab Compaction for Groesbeck Base.

Aggregate Breakdown from Vibratory Lab Compaction

To investigate if a significant difference in gradation after compaction exists among the 113-E and vibratory compaction, random specimens of both bases were saved after testing and washed gradations were performed down through the #4 sieve. The smallest sieve size used was the #4 because that is the smallest sieve size used for recombination of specimens when preparing them for molding. Figure 3.16 shows the results from the Spicewood material, and Figure 3.17 shows the results from the Groesbeck aggregate. With the Spicewood base, the results show a verifiable difference in the 7/8, 3/8, and passing #4 size fractions. The most significant difference is in the reduced amount of the passing #4 sieve by using vibratory compaction. With the Groesbeck material, differences exist in the 7/8 and passing #4 size fractions. Essentially the data seem to indicate that impact hammer compaction causes more particle breakdown than vibratory, as indicated by the amounts passing the #4 sieve.

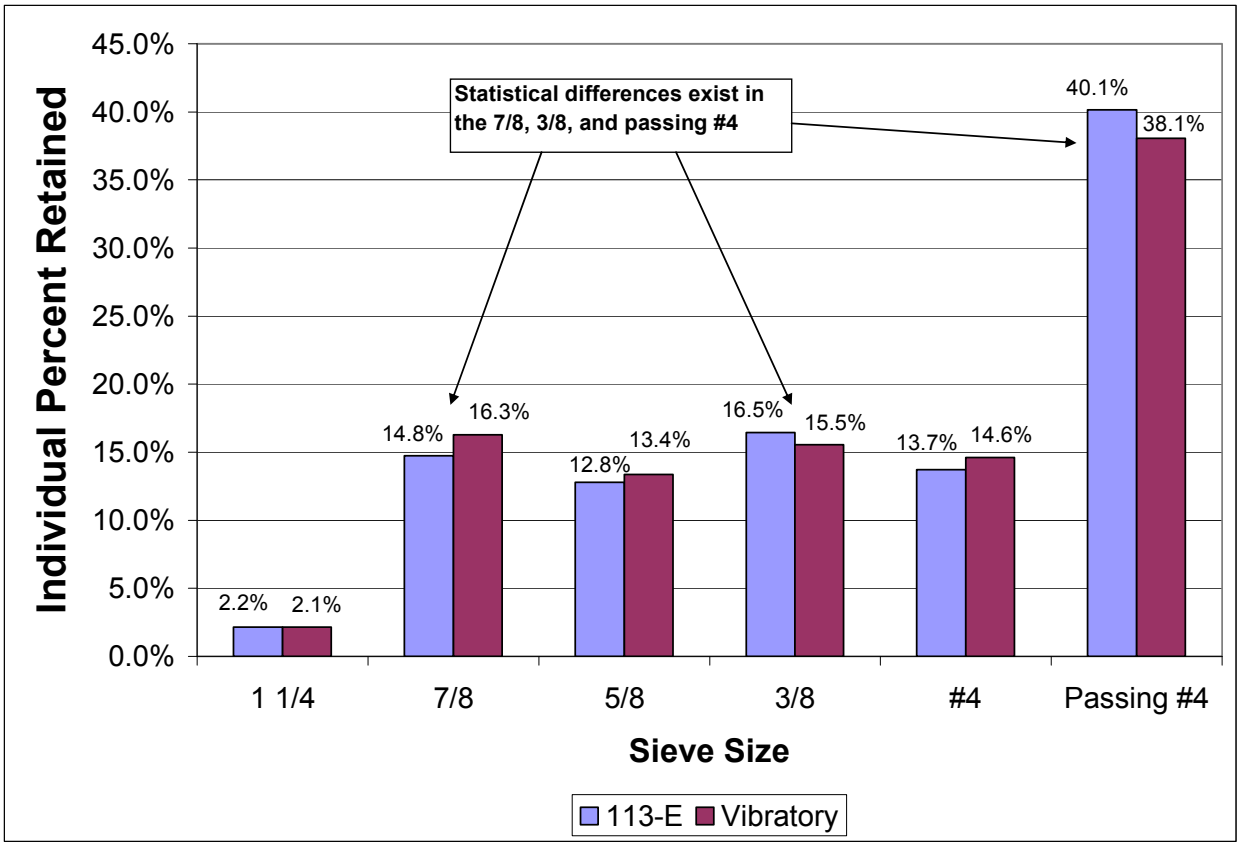

Figure 3.16. Gradation Results for Spicewood from 113-E and Vibratory Compaction.

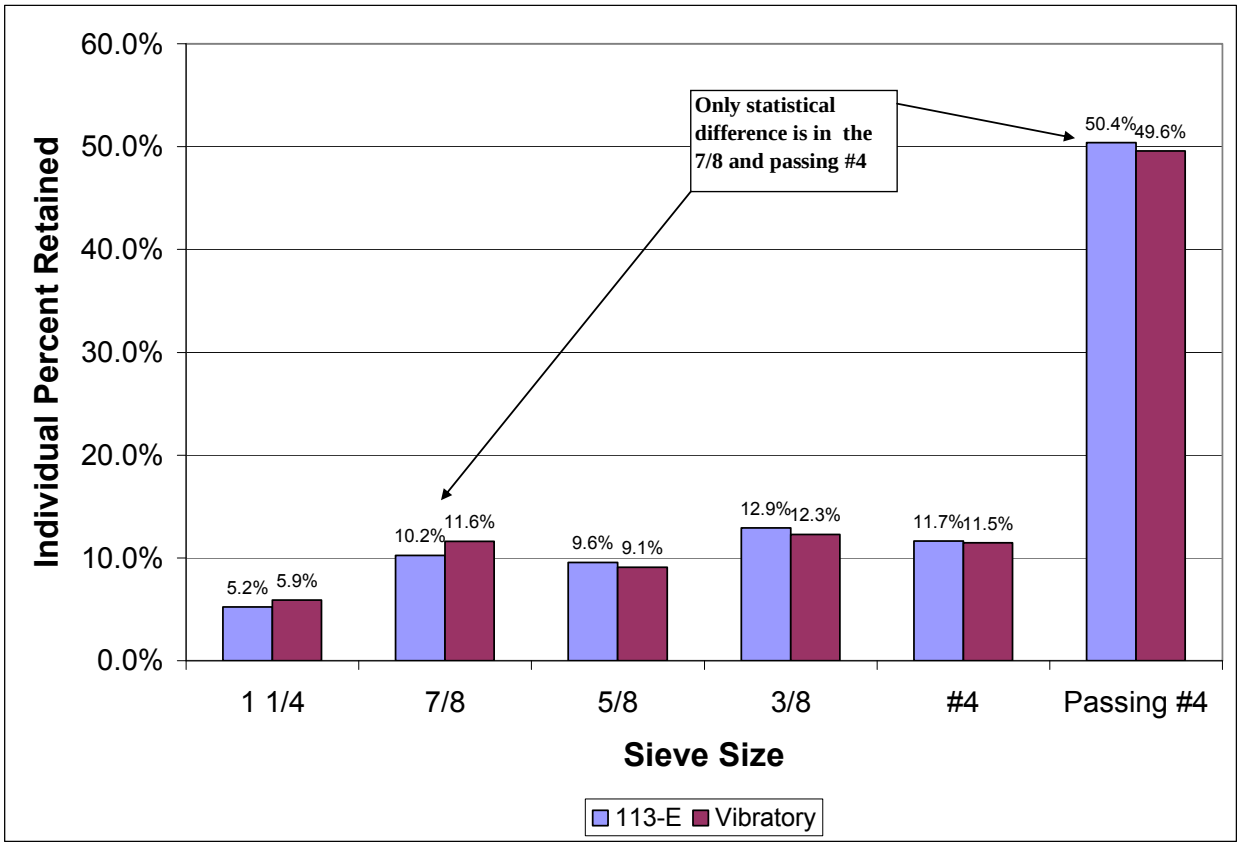

Figure 3.17. Gradation Results for Groesbeck from 113-E and Vibratory Compaction.

Precision of Sample Dry Density from Vibratory Compaction

With the large number of test specimens produced in the course of this project, the data were analyzed to evaluate how the precision of specimen dry density from lab vibratory compaction compared to the precision from Tex-113-E. Figure 3.18 shows the within-lab repeatability standard deviation of specimen dry density. If each material is analyzed individually, the data indicate that vibratory compaction was more precise for Groesbeck, but not for the Spicewood material. However, ASTM D 4855 outlines procedures for comparing test precision among alternative test methods when more than one level of material is used. Table 3.7 presents the data necessary to use the ASTM analysis procedure. Only TTI data were used to generate the data in Table 3.7 because no interlab results exist with the vibratory lab compaction method.

Analysis of the data revealed that for vibratory compaction, the variance was not constant with the level of material. Therefore, the variance could not be used to evaluate precision. Following the ASTM procedure, further analysis revealed that for both compaction methods, the coefficient of variation was constant with the level of material. Therefore, the pooled coefficient of variation for each test method was used as the measure of precision. Figure 3.19 shows the pooled coefficient of variation values. Statistical tests as outlined in ASTM D 4855 reveal that, with the lab methods and materials used, no difference in precision of sample dry density existed

between Tex-113-E and vibratory lab compaction. It should also be noted that with the number of materials tested and number of replicate tests performed, this analysis procedure would detect a difference in precision of 60 percent or greater.

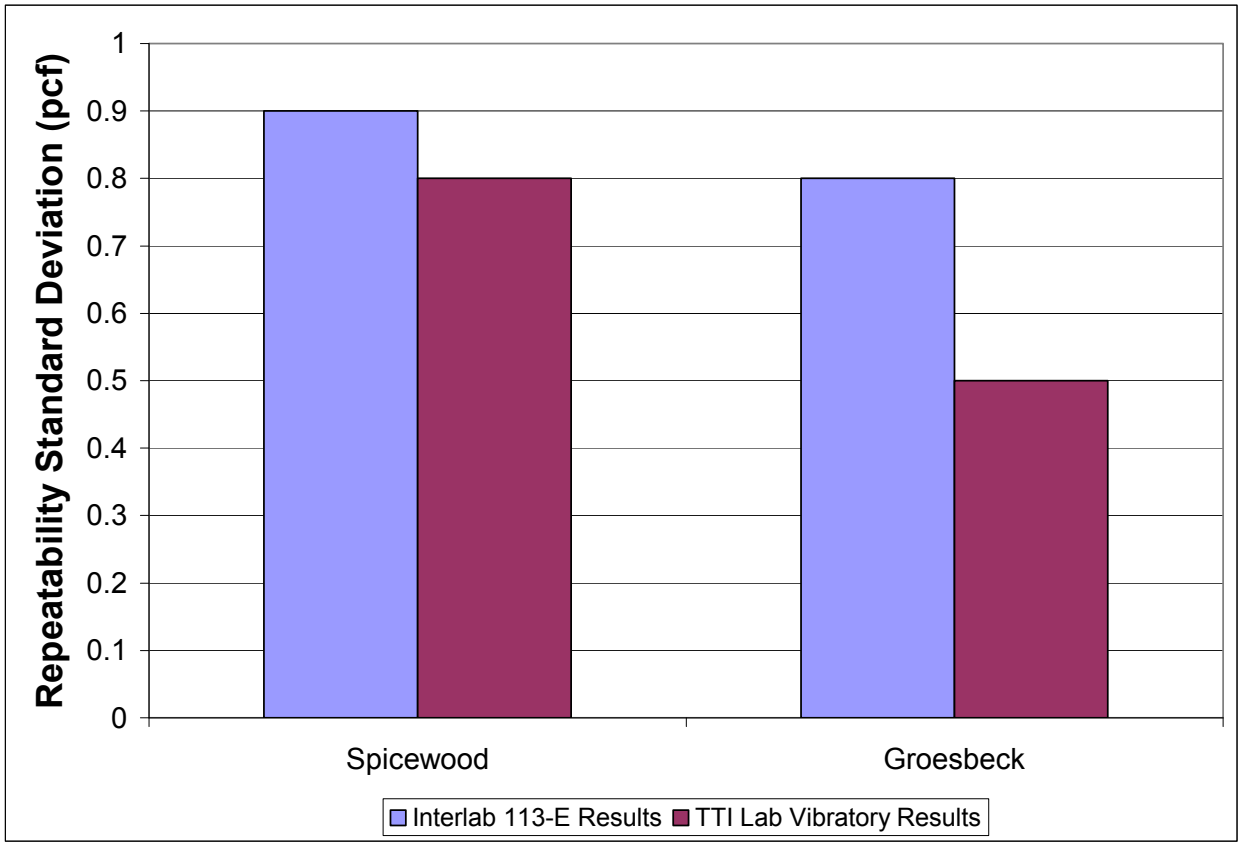

Figure 3.18. Repeatability Standard Deviation of Sample Dry Density from 113-E and Vibratory Compaction.

Table 3.7. Key Data to Compare Precision of 113-E and Vibratory Lab Compaction.

		Test Method					
		113-E			Vibratory		
Level	Material	AVG (pcf)	s (pcf)	d.f.*	AVG (pcf)	s (pcf)	d.f.*
1	Groesbeck	132.8	0.861	25	133.8	0.476	26
2	Spicewood	148.6	0.789	26	149.5	0.758	23

*d.f. is degrees of freedom

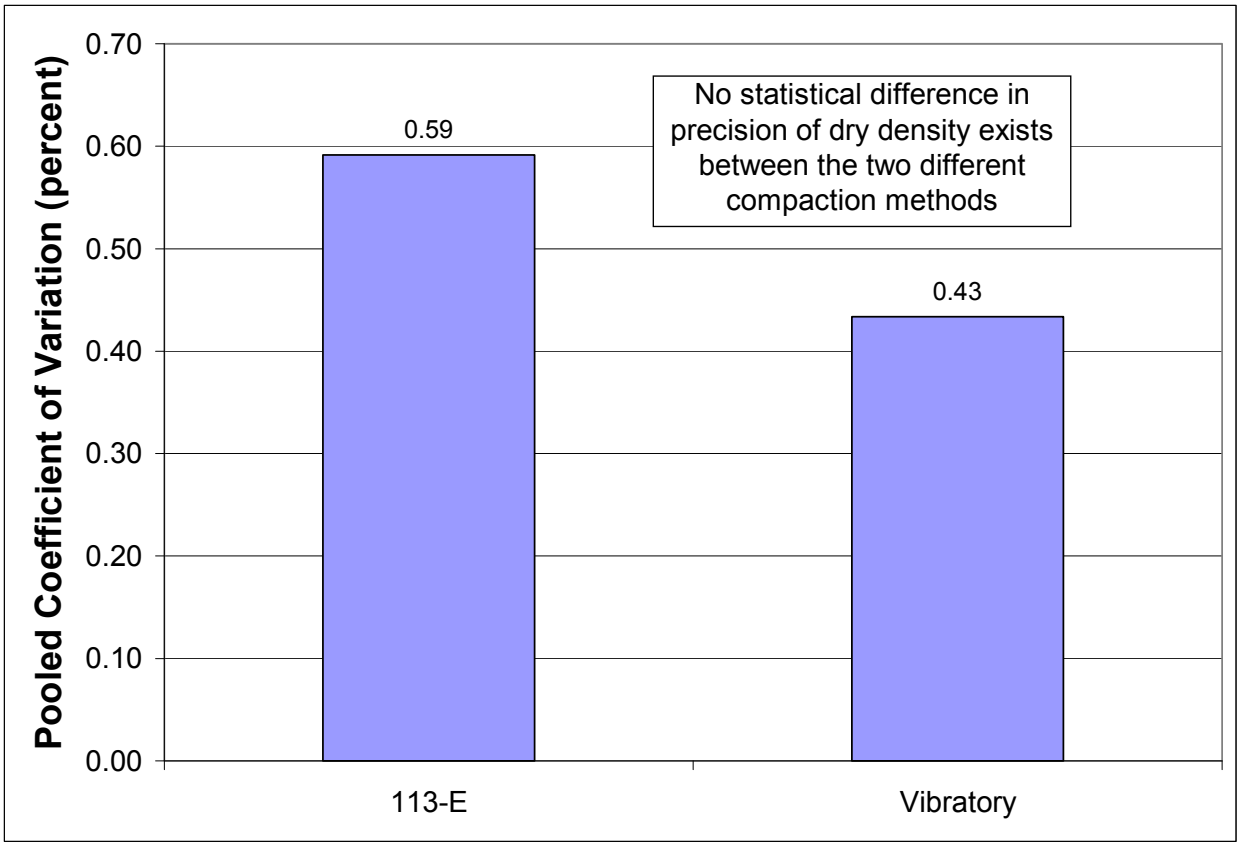

Figure 3.19. Pooled Coefficient of Variation of Specimen Dry Density for Tex-113-E and Vibratory Lab Compaction.

CHAPTER 4

INVESTIGATION OF SOIL FABRIC

SUMMARY

Soil fabric, the arrangement of particles within a soil, can have dramatic impact on the properties of the soil. This project sought to evaluate the fabric produced by different compaction methods for soils and bases. Limited success was achieved because numerous techniques attempted did not produce useable specimens for the cohesive soils investigated. With the bases, laboratory samples were investigated with CT scanning but no field specimen for comparison purposes was able to be obtained. No consistent trends were observed in the results obtained from the lab-molded base specimens.

RESULTS FROM SOILS TESTING

As discussed in Chapter 3, the soil fabric can significantly influence the engineering properties of materials. As part of this project, the research team sought to investigate the soil fabric of both field and laboratory specimens to evaluate which lab technique best matches the field. This analysis first requires epoxy impregnation of the specimens to fix the particle orientations. The researchers tried several techniques of epoxy impregnation on Vertisols. Vertisols were chosen because they are the most difficult soils to sample and prepare due to the shrink/swell properties. The procedures outlined in the soils literature call for drying the soil in an oven at 95ºC to facilitate water removal. The researchers did not want to dry at that high of a temperature, so different epoxies were tried at lower temperatures.

LR White resin was tried initially because it has a very low viscosity and can be cured at low temperatures. The first samples were placed in a vacuum oven and cured overnight at 30ºC. Figure 4.1 shows a sample that was cured in this fashion. A lot of air bubbles were generated and the epoxy did not fully impregnate the clays.

The researchers then tried curing the LR White resin with ultraviolet radiation. It took several days for the UV light to cure the epoxy and it introduced artifacts into the samples. The samples also contained a sticky residue indicating inefficient hardening. Figure 4.2 shows one of these samples.

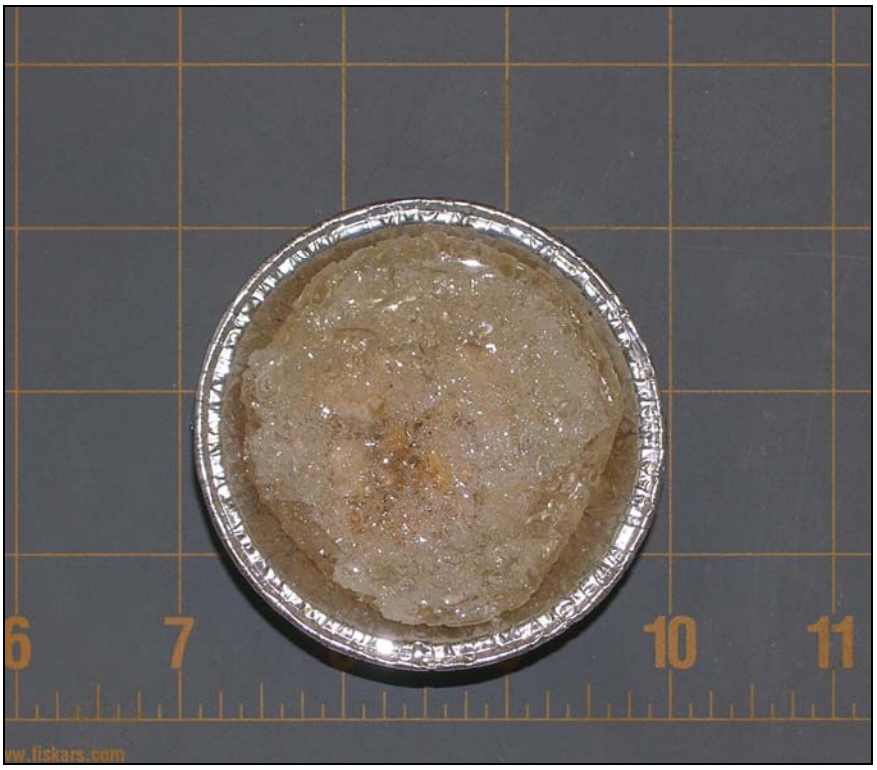

Figure 4.1. Sample Cured in a Vacuum Oven Using L R White Resin.

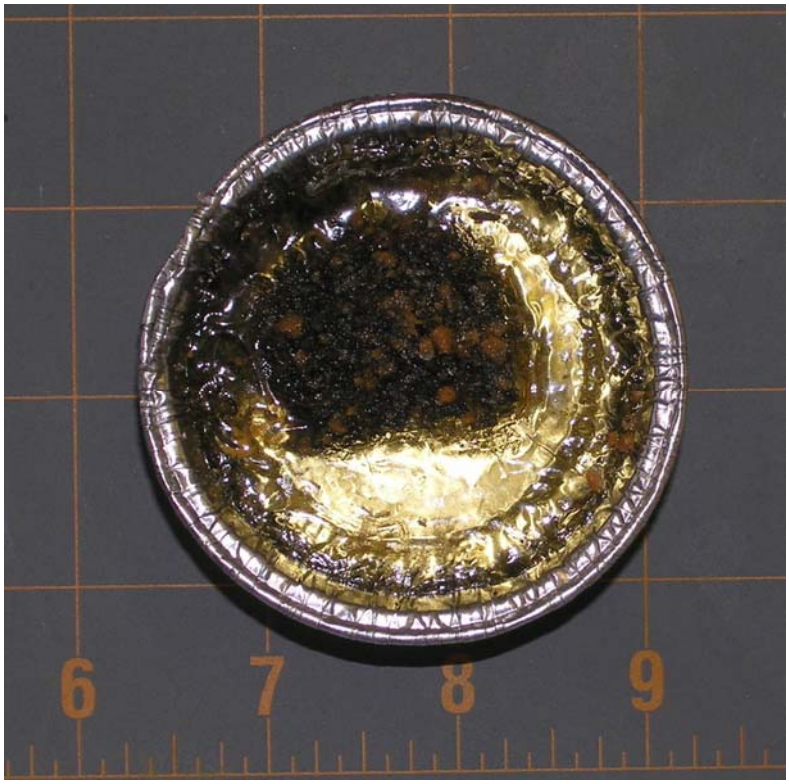

Figure 4.2. Sample Cured with UV Light Using L R White Resin.

The researchers then tried a new technique proposed by a researcher in Oceanography that required elaborate water replacement procedures using a low temperature vacuum microwave oven. Samples impregnated in this fashion are shown in Figure 4.3. This technique did not work well with the high pH stabilizers, and it could only be used on very small samples, which made it impractical for use on this project.

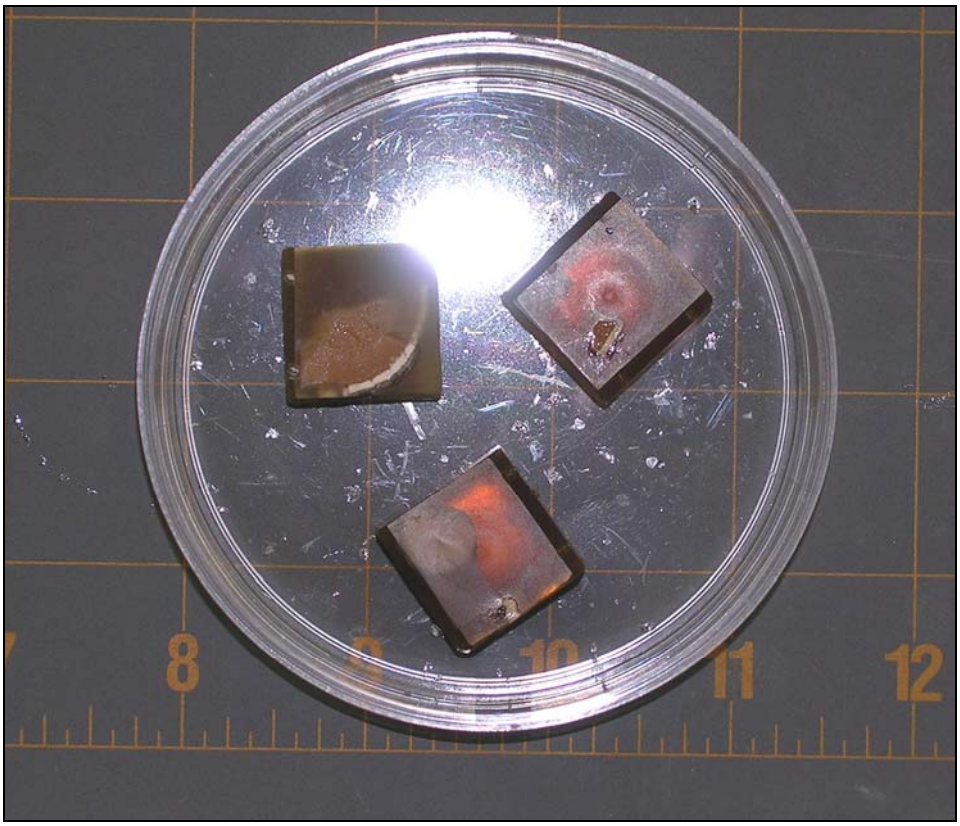

Figure 4.3. Three Samples Treated with a Biological Resin to Maintain Original Fabric.

The last impregnation technique that was used involved compacted sand samples. Low-viscosity Epofix epoxy was used with air dried compacted sand samples. As shown in Figure 4.4, the epoxy did not fully penetrate the sample, so a lot of the fabric was not preserved.

All of the techniques that the researchers tried for preserving the soil fabric had drawbacks. None of the sample preparation techniques tried to date was deemed adequate enough to provide quality data.

Figure 4.4. Partially Impregnated Compacted Sand Sample.

RESULTS FROM BASE MATERIALS

As described in Chapter 3, the research team compacted flex base samples in the laboratory using both impact hammer and vibratory compaction. The research team sought to determine if the orientation of the aggregate in lab specimens matched that from compacted bases in the field. Additionally, the research team sought to evaluate whether differences in the fabric existed between the two lab compaction methods. CT scanning was used to perform this analysis. Axial scans were collected at 0.5 mm spacing for the analysis.

To make a direct comparison with field molded base materials, the researchers needed to obtain an intact field specimen. An unstabilized base material is difficult to sample and maintain the original orientation of the aggregates. The researchers decided to pour a low viscosity epoxy onto the base and let the epoxy soak into the material by gravity. Figure 4.5 shows that, even with a low viscosity epoxy (Epofix), the base was too impermeable for the epoxy to permeate deep enough into the material. Instead, the epoxy ran out of the bucket along the top surface of the base without penetrating deep enough to take a core. Epoxies with lower viscosities were not tried because they required curing at high temperatures. The high temperature curing would make the other epoxies impractical in the field.

Figure 4.5. Epofix Epoxy with Fluorescent Dye Placed on Base Material.

Figures 4.6 through 4.8 show the CT results for the Spicewood laboratory samples, and Figures 4.9 through 4.11 show the results for the Groesbeck samples. The longitudinal images in Figure 4.6 and Figure 4.9 were generated by Dr. Ketchum at the University of Texas. Dr. Masad at Texas A&M conducted the data analysis to produce the graphs of the percent air voids and average pore size with depth.

With the Spicewood material, the results show vibratory compaction reduced the range to the extreme values for both air void content and pore size. In contrast, with the Groesbeck material vibratory compaction had a higher range and increased variability in air void and pore size values as compared to the impact hammer. The most noteworthy finding from the CT analysis may be from the Groesbeck material. With this base, the lower air void content and lower pore size at the bottom of the sample prepared with vibratory compaction may mean that there are fewer interconnected voids, which could help explain the reduction in dielectric value after Tex-144-E that was observed and documented in Chapter 3.

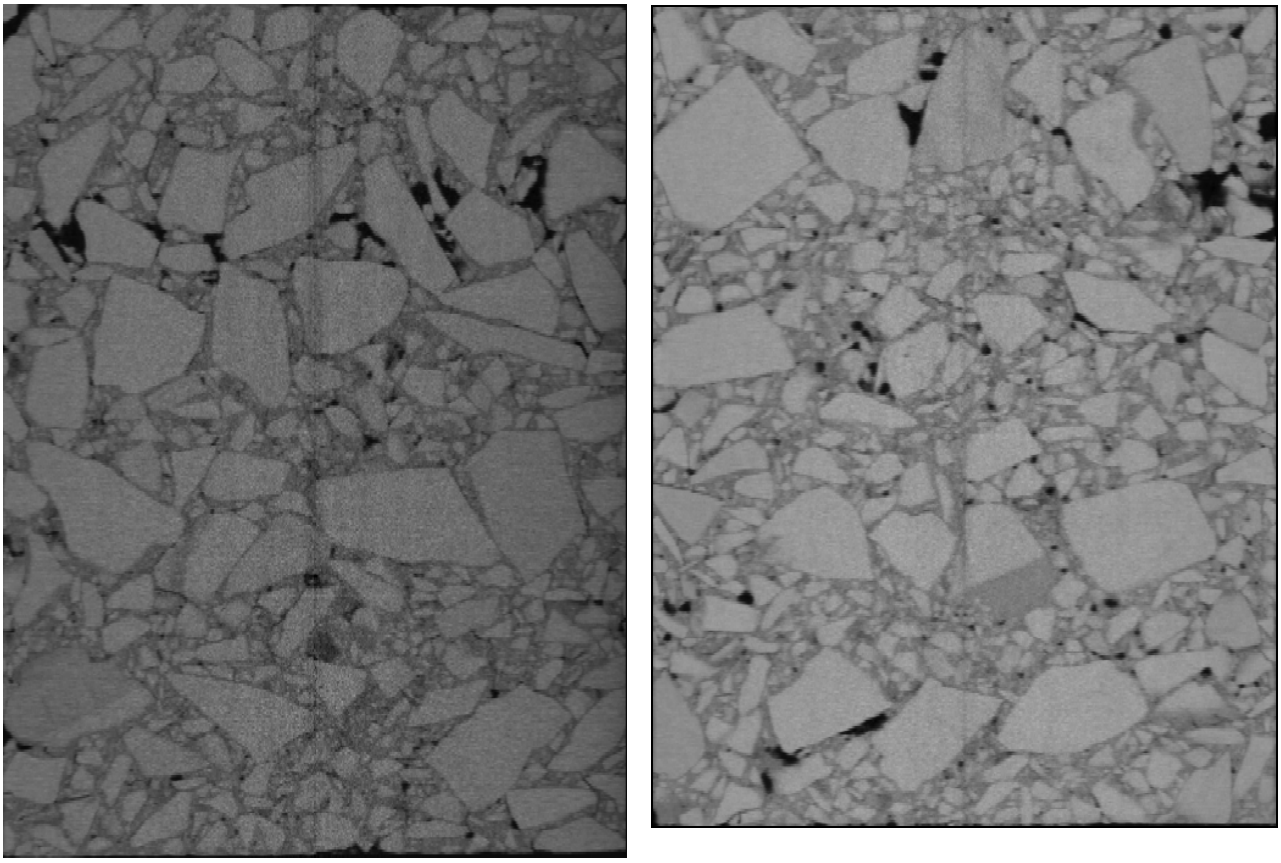

Impact Hammer Vibratory

Figure 4.6. Example Longitudinal Cross Sections from Spicewood Lab-Molded Samples.

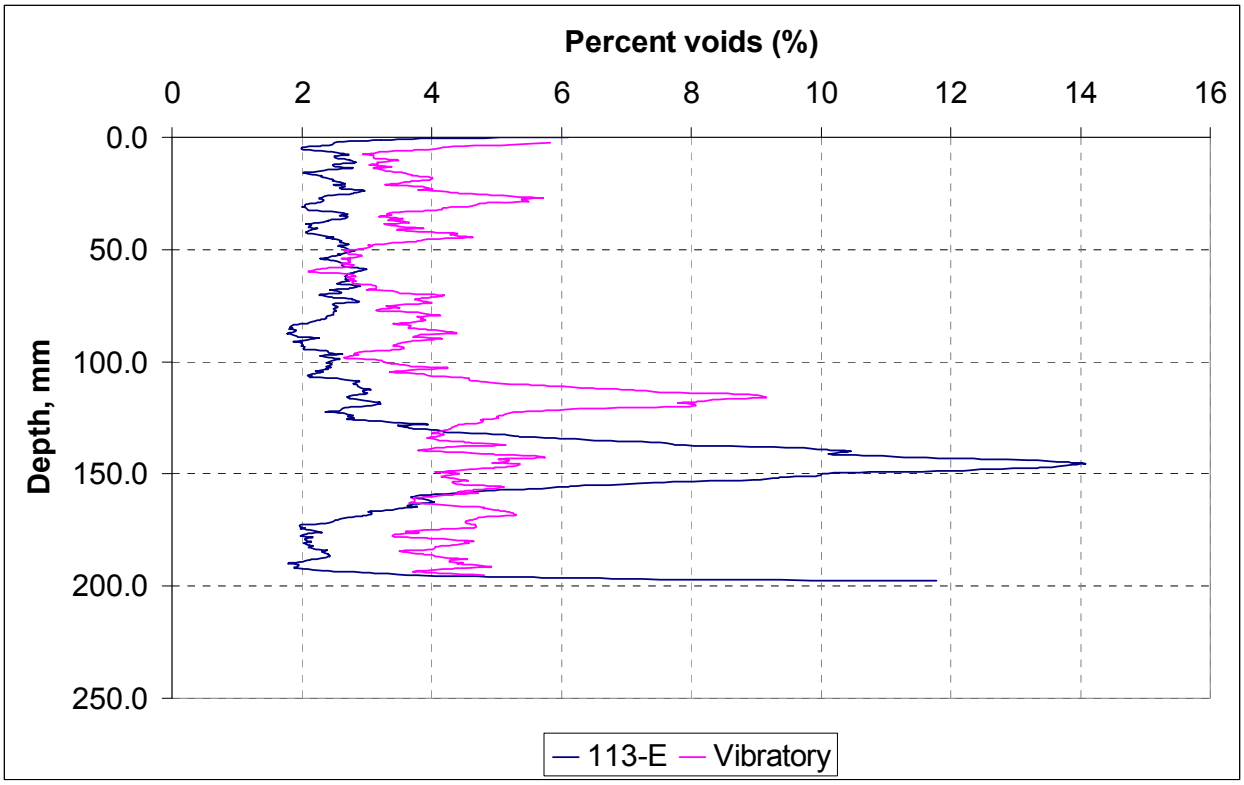

Figure 4.7. Voids with Depth for Spicewood CT Lab Samples.

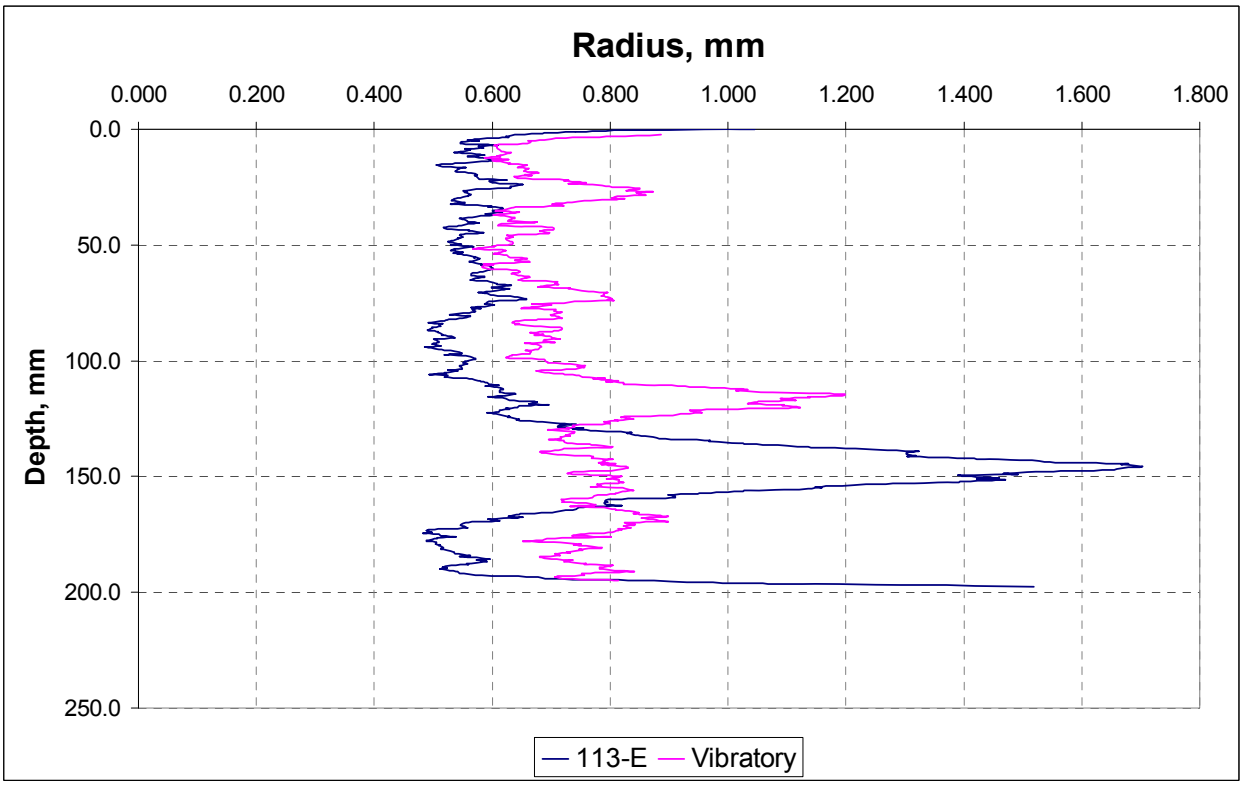

Figure 4.8. Pore Radius with Depth for Spicewood CT Lab Samples.

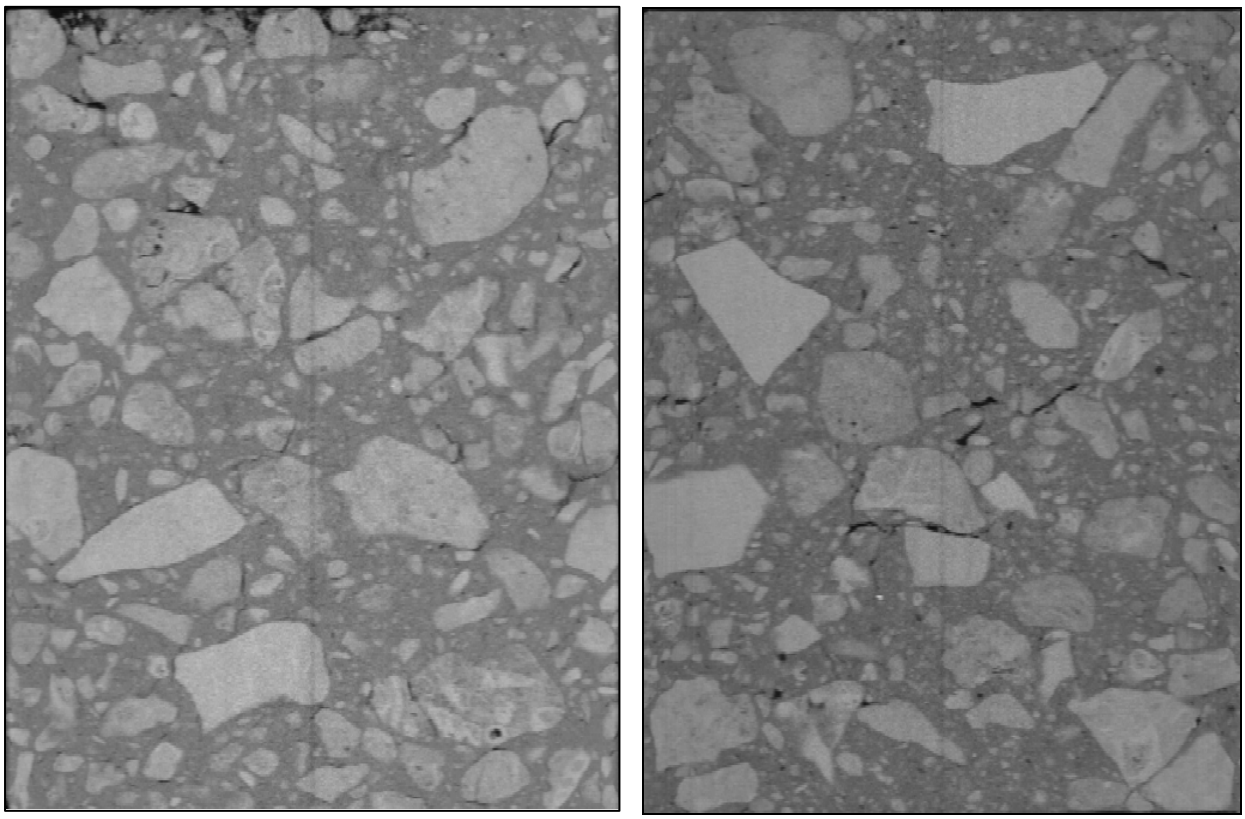

Impact Hammer Vibratory

Figure 4.9. Example Longitudinal Cross Sections from Groesbeck Lab-Molded Samples.

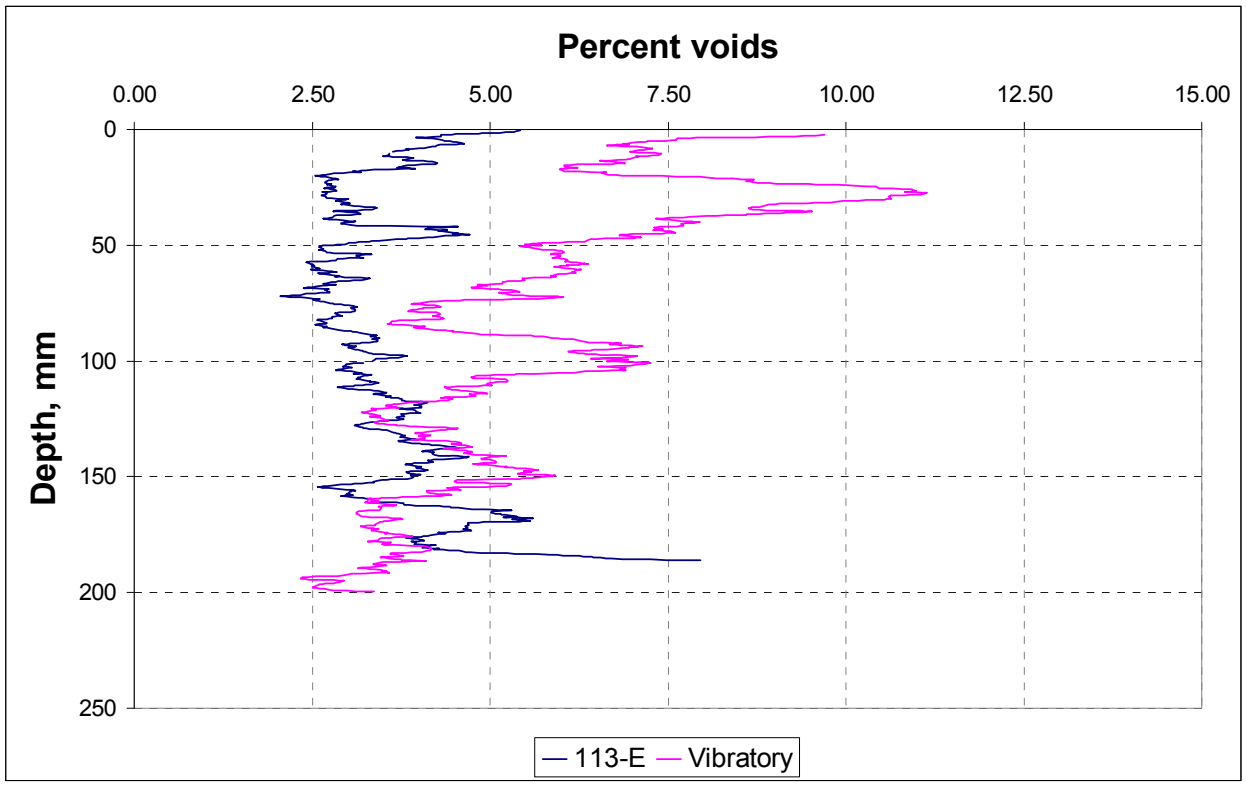

Figure 4.10. Voids with Depth for Groesbeck CT Lab Samples.

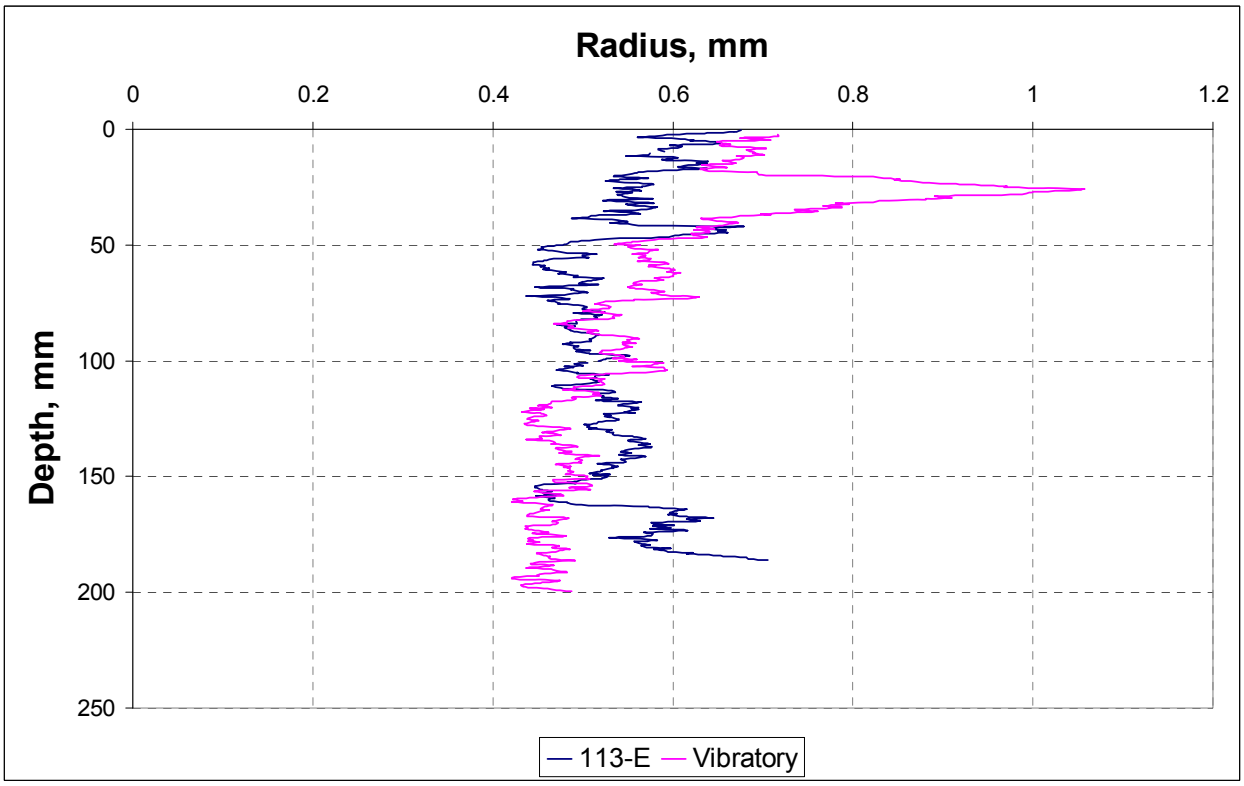

Figure 4.11. Pore Radius with Depth for Groesbeck CT Lab Samples.

CONCLUSIONS

While soil fabric is widely recognized as an important factor in the properties of materials, techniques to adequately study the fabric for purposes of this project proved elusive. The research team did not locate a suitable method to obtain satisfactory soil samples, and with the base materials no field sample could be obtained. Additionally, the results from the laboratory base materials do not show similar trends. With the Spicewood material, vibratory compaction appeared to reduce the range of extreme values in pore space parameters as compared to the impact hammer method of compaction. In contrast, with the Groesbeck material vibratory compaction appeared to increase variability. It must be noted, however, that these are observations from only a limited number of test specimens due to the costly nature of the CT testing.

CHAPTER 5

CONCLUSIONS AND RECOMMENDATIONS

SUMMARY

The results presented in this report from the Spicewood and Groesbeck base materials provided interesting pilot results that warrant further investigation. Highlights of findings from each phase of work are presented in the subsections below.

FINDINGS FROM INCREASED COMPACTIVE EFFORT ON BASE MATERIALS

In terms of strength and stiffness properties, lab results were mixed regarding improvements in measured properties by using Modified instead of Tex-113-E compaction. For the Spicewood Grade 1 base, Modified compaction did not result in improved mechanical properties. For the Groesbeck Grade 2 material, Modified compaction resulted in improved triaxial strength and improved seismic modulus. In Tex-144-E for evaluating moisture susceptibility, Modified compaction resulted in a poorer moisture susceptibility ranking for both materials.

FINDINGS FROM VIBRATORY LAB COMPACTION WITH BASE MATERIALS

For both bases evaluated, vibratory lab compaction resulted in improved triaxial strength properties as measured in Tex-117-E, improved moisture susceptibility rankings as measured by Tex-144-E, and improved rutting characteristics as measured with the VESYS pavement performance model. As compared to Tex-113-E compaction, vibratory compaction also resulted in higher measured seismic modulus values for both bases after the drying and after the moisture conditioning phases of Tex-144-E.

FINDINGS FROM SOIL FABRIC INVESTIGATIONS

These results were disappointing, as no suitable technique to prepare soil specimens was found, and CT results from the two bases investigated yielded mixed results. With the Spicewood material, the results show vibratory compaction reduced the range to the extreme values for both air void content and pore size. In contrast, with the Groesbeck material vibratory compaction had a higher range and increased variability in air void and pore size values as compared to the impact hammer.

RECOMMENDATIONS FOR FUTURE WORK

The phase of work investigating Modified compaction instead of Tex-113-E only indicated improvements in base properties with the Grade 2 material. Using vibratory compaction instead of Tex-113-E resulted in improved properties for each material tested. However, only two Texas base materials were evaluated in this program and therefore the

observations made in this phase of work should be validated with additional testing. A future phase of this project will evaluate four additional Texas base materials using Tex-113-E, Modified, and vibratory lab compaction. Additionally, the future work in this project will refine the impact hammer calibration apparatus into implementable form.

REFERENCES

Hoeg, K., Dyvik, R., and Sandbaekken, G., July 2000. Strength of Undisturbed versus Reconstituted Silt and Silty Sand Specimens. *ASCE Journal of Geotechnical and Geoenvironmental Engineering*, Vol. 126, Issue 7, pp. 583-673.

Holtz, R.D., and Kovacs, W.D., 1981. *An Introduction to Geotechnical Engineering*. Prentice Hall, Englewood Cliffs, New Jersey. 733 p.

Huang, Y.H., 1993. *Pavement Analysis and Design*. Prentice Hall, Upper Saddle River, New Jersey.

Kirkpatrick, W.M., and Rennie, I.A., 1973. Clay Structure in Laboratory Prepared Samples. In L. Barden and R. Pusch, (eds.) Proceedings of the international symposium on soil structure, Gothenburg, Sweden, p. 103-112.

Mitchell, J. K., 1993. *Fundamentals of Soil Behavior*. 2nd ed. John Wiley & Sons, Inc., New York. 437 p.

Sebesta, S., Guthrie, W.S., and Harris, J.P., 2004. Gyratory Compaction of Soils for Laboratory Swell Tests. Transportation Research Board 83rd Annual Meeting Compendium of Papers, January 11-15, 2004.

Weibiao, W., and Hoeg, K., 2002. Effects of Compaction Method on the Properties of Asphalt Concrete for Hydraulic Structures. In *International Journal on Hydropower and Dams*, Vol. 9, No. 6, pp. 63-71.

Witczak, M., January 2004. NCHRP Research Results Digest Number 285: Laboratory Determination of Resilient Modulus for Flexible Pavement Design. TRB, National Research Council, Washington, D.C.

Zhou, F. and Scullion, T., August 2004. Guidelines for Developing Input Parameters of Enhanced VESYS5 Program, Product 9-1502-01-P5, Texas Transportation Institute.